AD_____
(Leave blank)

Award Number:
W81XWH-07-1-0020

TITLE:
Dual-Modality Prostate Imaging with PET and Transrectal Ultrasound

PRINCIPAL INVESTIGATOR:
Jennifer S. Huber, Ph.D.

CONTRACTING ORGANIZATION:
University of California
Lawrence Berkeley National Laboratory
Berkeley, CA 94720

REPORT DATE:
April 2009

TYPE OF REPORT:
Annual

PREPARED FOR: U.S. Army Medical Research and Materiel Command
Fort Detrick, Maryland 21702-5012

DISTRIBUTION STATEMENT: (Check one)

X Approved for public release; distribution unlimited

☐ Distribution limited to U.S. Government agencies only; report contains proprietary information

REPORT DOCUMENTATION PAGE

Form Approved
OMB No. 0704-0188

1. REPORT DATE *(DD-MM-YYYY)*	**2. REPORT TYPE**	**3. DATES COVERED** *(From - To)*
04-14-2009	Annual	15 Mar 2008 – 14 Mar 2009

4. TITLE AND SUBTITLE
Dual-Modality Prostate Imaging with PET and Transrectal Ultrasound

5a. CONTRACT NUMBER
W81XWH-07-1-0020

5b. GRANT NUMBER

5c. PROGRAM ELEMENT NUMBER

6. AUTHOR(S)
Jennifer S. Huber, Ph.D.

5d. PROJECT NUMBER

5e. TASK NUMBER

5f. WORK UNIT NUMBER

7. PERFORMING ORGANIZATION NAME(S) AND ADDRESS(ES)

University of California
Lawrence Berkeley National Laboratory
1 Cyclotron Road
Berkeley, CA 94720

8. PERFORMING ORGANIZATION REPORT NUMBER

9. SPONSORING / MONITORING AGENCY NAME(S) AND ADDRESS(ES)
U.S.Army Med.Res.Aquis.Act. (USAMRAA)
ATTN: Cheryl Lowery
820 Chandler Street
Fort Detrick, MD 21702-5014

10. SPONSOR/MONITOR'S ACRONYM(S)

11. SPONSOR/MONITOR'S REPORT NUMBER(S)

12. DISTRIBUTION / AVAILABILITY STATEMENT

Distribution approved for public release.

13. SUPPLEMENTARY NOTES

14. ABSTRACT
We developed the hardware and software tools needed for dual Positron Emission Tomography-Transrectal Ultrasound (PET-TRUS) imaging of the prostate. We acquired and modified the necessary TRUS equipment to work when mounted on a patient table in conjunction with the prostate-optimized PET scanner or the EXACT HR PET scanner. We developed software to: determine the location of two point sources and calculate the corresponding location of the TRUS probe tip (both in PET coordinates), reconstruct PET data, reslice PET imaging data sets into TRUS coordinates, and display fused PET-TRUS images. We validated methods for positioning a patient's prostate in the center of the PET scanner (with 1 mm accuracy). We also constructed and imaged one-of-a-kind PET-TRUS prostate phantoms, using these phantoms to evaluate our dual PET-TRUS imaging techniques. We estimate our PET-TRUS image co-registration error to be 2 mm based on this preliminary phantom imaging, but we will perform further validation in Year 3 using a newly designed PET-TRUS phantom. Finally, we have updated IRB approval for patient studies.

15. SUBJECT TERMS
None listed.

16. SECURITY CLASSIFICATION OF:			**17. LIMITATION OF ABSTRACT**	**18. NUMBER OF PAGES**	**19a. NAME OF RESPONSIBLE PERSON**
a. REPORT	**b. ABSTRACT**	**c. THIS PAGE**			USAMRMC
U	U	U	UU	75	**19b. TELEPHONE NUMBER** *(include area code)*

Table of Contents

Introduction

The overall goal of this project is to develop dual Positron Emission Tomography–Transrectal Ultrasound (PET-TRUS) imaging of the prostate and validate the technology with 10 "proof of principle" patient studies. Newly developed PET radiopharmaceuticals (e.g., [^{11}C] choline) have recently demonstrated outstanding results in the sensitive detection of prostate cancer, detecting malignant tumors in the prostate region and determining tumor "aggressiveness" based on metabolic uptake levels. However, the relative uptake in a tumor is so great that few other anatomical landmarks are visible in the PET images. PET imaging would therefore be greatly enhanced if its functional information could be accurately fused with anatomical information. Transrectal ultrasound imaging of the prostate is a standard imaging technique widely used for prostate cancer diagnosis, biopsy, treatment planning and brachytherapy seed placement. Transrectal ultrasound imaging provides high resolution anatomical detail in the prostate region that can be accurately co-registered with the sensitive functional information from PET imaging, if the PET and TRUS prostate imaging are performed sequentially during the same patient imaging session. Hence, dual PET-TRUS prostate imaging will help determine the location of cancer within the prostate region. This novel dual-modality prostate imaging should help confirm initial diagnosis, guide biopsy, guide treatment decisions, monitor response to therapy, and detect local reoccurrence. Ultimately it should help provide better detection and treatment of prostate cancer. The goals of this research focus on developing the hardware and software tools needed for a validated dual PET-TRUS prostate imaging system. These tools are necessary for future clinical research.

Body

The development of dual PET-TRUS prostate imaging is focused on three research tasks: (1) develop methods to position a patient's prostate near the center of the PET scanner, (2) develop methods to accurately co-register PET and TRUS images, and (3) validate our ability to position patients in the PET scanner and to acquire co-registered PET and TRUS images with 10 "proof of principle" patient studies.

Task 1: Develop methods for positioning the prostate at the center of the prostate-optimized PET scanner

Task 1a) Mount transrectal ultrasound stabilizer arm to patient table, and mount transrectal ultrasound probe-stepper onto stabilizer arm.

During Year 1, we acquired all the necessary transrectal ultrasound equipment – ultrasound probe (Hitachi EUP-U533 endocavity ultrasound probe), stabilizer arm (Accucare micro-touch LP rightside table mount 610-912), and linear stepper (Accucare classic stepper 644-064). In agreement with the proposed budget, the rest of the ultrasound system (Hitachi Hi-Vision 5500 digital system) is borrowed as needed from UCSF Radiation Oncology Department in accordance with the UCSF sub-contract. As established in Year 2, the LBNL transportation group is used to transport the transrectal ultrasound system between LBNL and UCSF at an hourly cost to the project.

During Year 1, we made the modifications needed to mount the TRUS equipment onto the patient table of the prostate-optimized PET scanner. The heavy weight of the stabilizer arm required strong mechanical support for mounting the stabilizer arm onto the patient table, as well as a new support system for the patient table to help keep it level. Finally, a custom aluminum plate was designed, built and added beneath the commercial linear stepper to extend the motion of the TRUS probe-stepper to reach beyond the center of the PET scanner. Figure 1 shows the TRUS system mounted onto the patient table of the prostate-optimized PET scanner.

In Year 2 we decided that it will be necessary to utilize the EXACT HR PET scanner for initial patient studies, as discussed in detail below (see Tasks 2c and 2e). As a result, we designed and built a new mechanical support in order to mount the TRUS equipment onto the patient table of the EXACT HR PET scanner. The whole mechanical support had to be redesigned to accommodate a different table profile and attachment scheme, and this took longer than expected due to manpower conflicts. Figure 2a shows the completed PET-TRUS system with the new mechanical support and the EXACT HR PET scanner. Hence, task 1a has been completed for both available PET scanners.

Task 1b) Attach two 511 keV ^{68}Ge point sources to TRUS stepper (to define axial line of probe).

We acquired two 511 keV PET point sources (Isotope Products Laboratories Ge-68 spot marker MMS01-068, 175 μCi) during Year 1 and a third one this year. During Year 1, a custom point source holder was designed, built and mounted onto the TRUS stepper, as shown in figures 1 and 2. The holder is an acrylic bar with two machined cylindrical cavities that hold the two ^{68}Ge point sources (at the same height and 60.0 mm apart). The bar mounts on top of the TRUS stepper with positioning pins and screws, accurately aligning two ^{68}Ge point sources along the axial line of the TRUS probe at a known distance from the TRUS probe tip. The point source holder was completed in Year 1 and required no modifications in Year 2.

Task 1c) Mount low-powered lasers on PET gantry along minor and major axes.

During Year 1, two low-powered lasers were mounted along the minor and major axes of the prostate-optimized PET scanner. These lasers are used to visually position objects, such as the two point sources, near the center of the PET scanner (i.e., PET-center). We did not have to mount additional lasers in Year 2, since the EXACT HR PET scanner already had positioning lasers.

(a) (b)

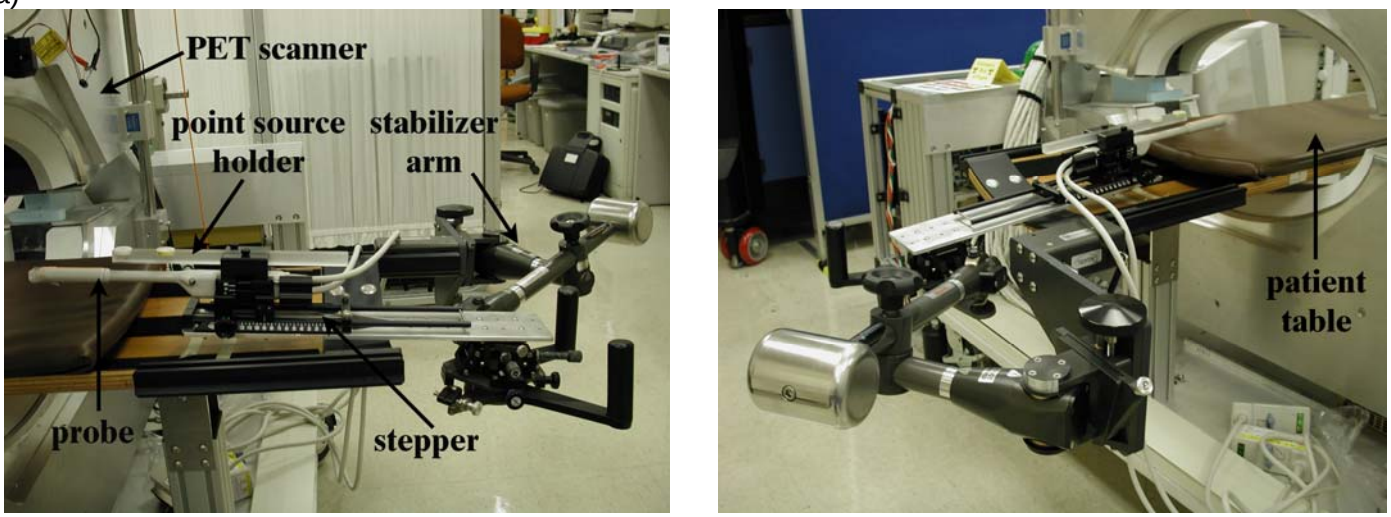

Figure 1. (a) Photograph (left side view) of the dual PET-TRUS system including prostate-optimized PET scanner, patient table, TRUS stabilizer arm, TRUS modified stepper, TRUS ultrasound probe, and point source holder. (b) Photograph (right side view) of dual PET-TRUS system with the prostate-specific PET scanner, focusing on the heavy counter-weight of the TRUS stabilizer arm.

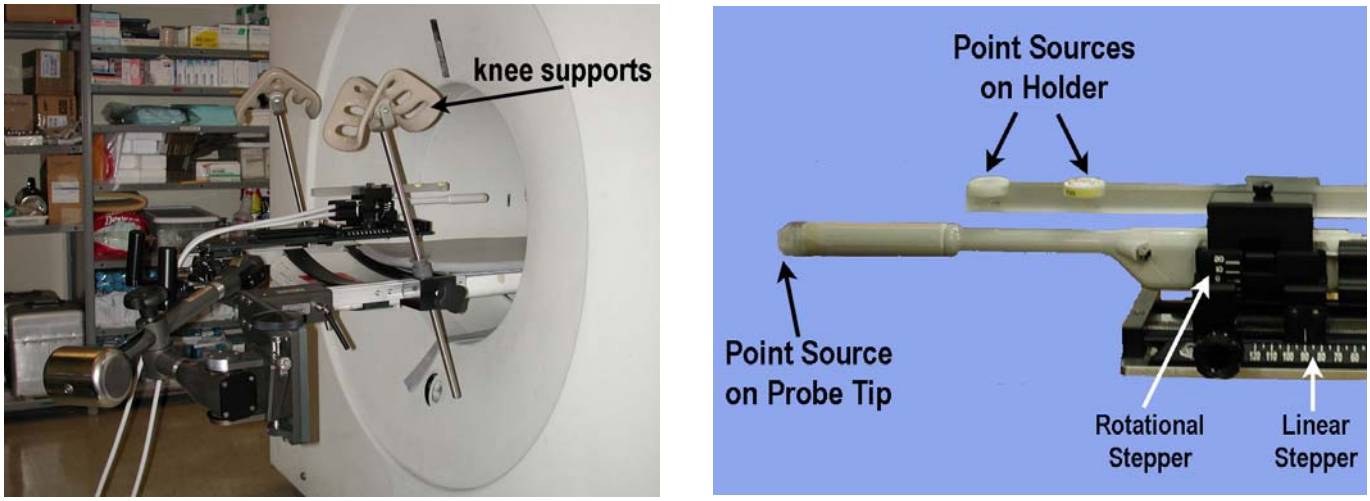

Figure 2. (a) Photograph of the dual PET-TRUS system using the EXACT HR PET scanner, including the patient's knee supports. (b) Photograph close-up of the TRUS ultrasound probe and point source holder. Two ^{68}Ge point sources are mounted on the holder, which are used to measure the position of the axial line of the TRUS probe. A third PET point source is taped to the TRUS probe tip, which is used for validation measurements (see Task 1e).

Task 1d) Develop software to rebin PET data into a single 2D sinogram and determine point source locations.

During Year 1, software was developed to quickly analyze point source PET data and determine the point source locations. An alternate technique was chosen over our originally proposed method (of rebinning the PET data into a single 2D sinogram). We acquired 1-5 minutes of PET data with ^{68}Ge point sources in the PET scanner and quickly reconstructed the data with a two-iteration expectation-maximum algorithm (with a simplified model of the PET scanner geometry). The resulting PET images were then quickly processed to determine the point source locations in PET coordinates, using modified ImageJ software to determine the brightness-weighted average (over all pixels in the image planes) for each point source in the 3D volumetric PET imaging data set.

During Year 2, the same two-iteration expectation-maximum algorithm was used to reconstruct the point source PET data. Initially, modified ImageJ software was used to determine the brightness-weighted average (over only a selected region of interest) for each point source in the 3D volumetric PET imaging data. However, the software used to determine the point source locations was then replaced with a more streamlined Matlab program based on more statistically rigorous methods. We now use an iterative Powell search method to perform 2D Gaussian fitting, in order to determine the projection of the point sources in each PET image slice. We then find the axial z coordinate of the point sources using a 1D Gaussian fit of the signal amplitude parameter. We find the transaxial x and y coordinates of the point sources using a 1D linear interpolation fit. The (x,y,z) PET coordinate of the two point sources are then used to calculate the position of the TRUS probe tip (in PET coordinates). This software is used for all tasks related to point source imaging (e.g., see Task 2b).

Task 1e) Validate prostate positioning by PET imaging a 511 keV point source attached to the TRUS probe tip.

In Year 1 we developed a method to position a prostate near the PET-center, and this method was also used for phantom imaging in Year 2. The TRUS probe is rigidly attached to the TRUS stepper that allows calibrated linear displacement along its axis. The point source holder, with two ^{68}Ge point sources (see Task 1b), is attached to the TRUS stepper. The TRUS probe-stepper-point source holder unit is mounted onto the moveable TRUS stabilizer arm that is rigidly attached to the patient table. The stabilizer arm moves to allow correct positioning of the TRUS probe in a patient (or phantom), then its position is fixed by tightening a single knob. Once the TRUS probe is inserted and positioned inside a patient (or phantom) at the prostate and the stabilizer arm is fixed, a series of 2D TRUS images in the transverse plane (i.e., perpendicular to the TRUS probe axis) are acquired from base to apex using the linear stepper. After the TRUS imaging is complete, the TRUS probe tip is positioned at the center of the prostate using the stepper. The patient table is then moved so the two ^{68}Ge point sources are visually positioned near the PET-center using visible low-powered lasers (see Task 1c). PET data are acquired for 1-5 minutes, quickly reconstructed, and the location of the point sources determined in PET coordinates (see Task 1d). Since the two ^{68}Ge point sources are placed along the axial line of the TRUS probe at a known location from the TRUS probe tip, the two point source locations are represented by two position vectors and vector algebra is used to calculate the actual location of the TRUS probe tip (in PET coordinates). The patient table is then moved to axially position the TRUS probe tip (i.e., prostate) at the PET-center. After the prostate is positioned in the PET scanner, the point source holder can be removed for the remainder of the study or the point sources can be left in place (since they are outside the PET imaging volume and have such low activity that patient dose is trivial). PET data of the prostate region is then acquired.

Our ability to position a prostate in the PET scanner was validated in Year 1 by imaging a point source that represents the prostate location. As figure 2b shows, we attached a third 511 keV ^{68}Ge point source on the TRUS probe tip. We positioned the TRUS probe tip using the procedure described above, acquired (for 5 minutes) and reconstructed PET data of this third point source, and determined the third point source location in PET coordinates (see Task 1d). This procedure was repeated several times for each TRUS probe position, and two very different probe angles were measured. As predicted, we were able to reproducibly position the TRUS probe tip within 1 mm from the PET-center in the axial direction (i.e., direction of patient table motion). Specifically, the third point source location on average was -0.64 $\pm$ 0.08 mm from the PET-center in the axial direction. The location of the third point source in the transaxial plane was different for the two measured probe angles, but the transaxial locations were measured to be reproducible with a sigma of less than 1 mm. A patient's prostate only needs to be positioned within the optimum central field of view of the scanner – 3 cm from the PET-center in the transaxial plane and 1 cm from the PET-center in the axial plane. Hence, we

achieved greater accuracy than required for patient positioning in Year 1, and no work was required in Year 2 on this task. However, it should be noted that this task is not sensitive to patient table motion that is not level, since the "prostate" point source is repeatedly measured at the same patient table position. This issue will be discussed below (see Task 2e).

Task 1f) Modify a commercial TRUS phantom to include a 511 keV point source on the "prostate" and validate prostate positioning by PET imaging the point source.

As detailed in Year 1's report, this second validation technique was deemed unnecessary and was not performed. It would only provide redundant information (to Task 1e) at additional cost.

Task 2: Develop methods for co-registering PET and TRUS images.

Task 2a) Construct TRUS-PET prostate phantom

PET-US Phantom:

In Year 1, we constructed a simple PET-ultrasound prostate phantom, as proof of principle, with structures that roughly simulate the acoustical properties for ultrasound and 511 keV ^{18}F activity concentrations for PET. We demonstrated our ability to construct and image a custom PET-ultrasound phantom (see figure 3). However, the phantom's mechanical and ultrasound properties did not have long-term stability especially at room temperature. For instance, this phantom (without preservative) was invaded by fungus and bacteria within a month even when stored in a refrigerator. So we needed to develop a different phantom construction process.

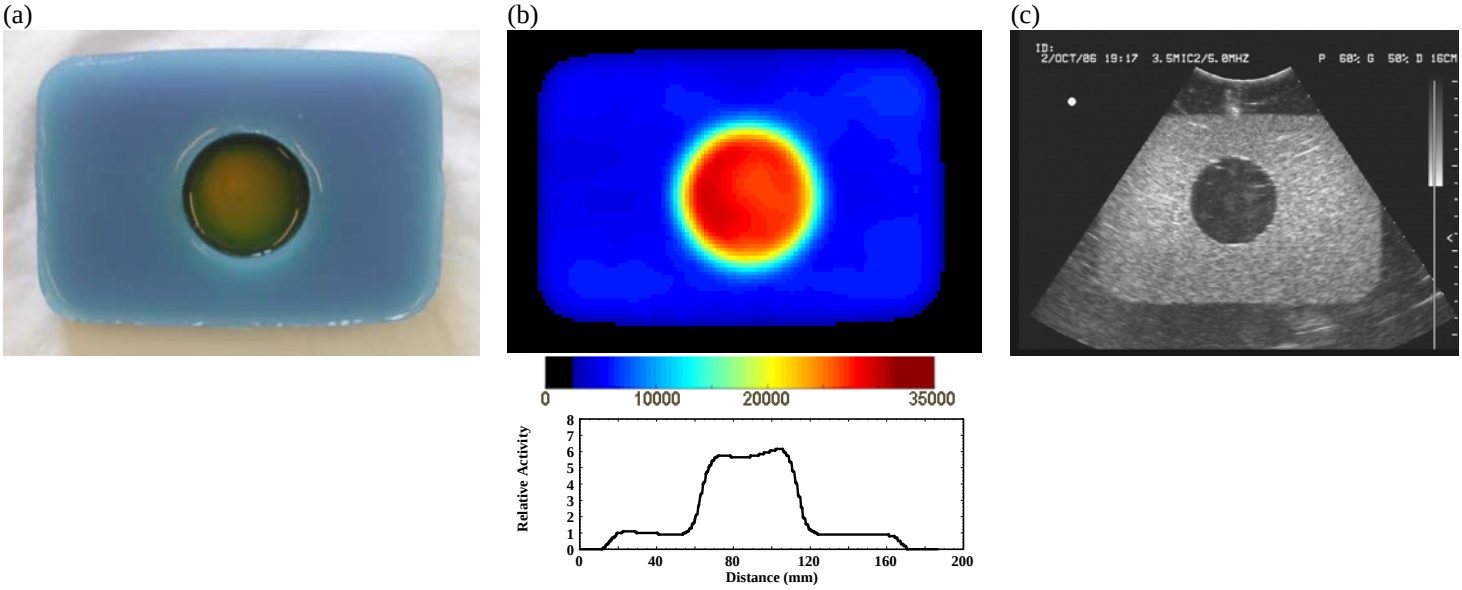

Figure 3. (a) Photograph of a simple PET-ultrasound phantom. The blue-colored agarose has outer dimensions of 16 cm x 11 cm x 3.5 cm. The yellow-colored gelatin cylinder has a 5 cm diameter and 2.5 cm depth. (b) Reconstructed coronal PET image of the PET-ultrasound phantom. The red-yellow circle shows the high ^{18}F activity concentration in the "prostate" region (1.07 μCi/ml), and the blue rectangle shows the low ^{18}F activity concentration in the background "pelvis" region (0.17 μCi/ml). Image represents 636 M counts (*i.e.,* 20 minutes of data). The voxel size is 1.47 mm x 1.47 mm x 3.13 mm. Horizontal profile through the "prostate" center is also shown. The ^{18}F activity is uniformly concentrated, with the expected 6 ("prostate") to 1 ("pelvis") relative activity. (c) Ultrasound image of the same phantom using a 5MHz external ultrasound probe. The dark gray circle shows the low-scatter gelatin "prostate," and the surrounding light gray background shows the high-scatter agarose "pelvis."

PET-TRUS-CT-MRI Phantoms:

In Year 1, we performed initial development of a multi-modality PET-US-CT-MRI phantom [1]. In Year 2, we constructed multi-modality PET-TRUS-CT-MRI phantoms using a finalized selection of tissue mimicking materials and phantom construction procedures. We use tissue mimicking mixtures of agar, gelatin, $CuCl_2$-$2H_2O$, EDTA-tetra Na Hydrate, NaCl, HCHO, Germall-Plus^{TM}, glass beads, $BaSO_4$, deionized water, and 511 keV radioactive solutions. Although only PET and TRUS properties are required for this project, we developed this tissue mimicking mixture because similar agar-gelatin mixtures were proven to have long-term mechanical, ultrasound and MRI properties for at least one year [2]. As a result, our novel multi-modality phantom has

many applications beyond this project. A more complete description of this phantom development is provided in the Appendices [2], including a summary of the primary role for each TMM ingredient.

When developing the procedures for the agar-gelatin-based phantom construction, we used (1) non-radioactive water and then (2) short-lived ^{18}F radioactive (110 minutes half-life) water with a small amount of non-radioactive 0.5M HCl. Once the phantom construction procedures were finalized, we used long-lived $^{68}GeCl_4$ radioactivity (271 day half-life) in a 0.5M HCl to allow repeated PET imaging of the same phantom. The main purpose of this phantom is to develop radioactive TMMs that both approximate the acoustical properties of patients more accurately and have improved long-term stability at room temperature than those developed previously (e.g., see PET-US Phantom above).

We constructed two-region PET-TRUS-CT-MRI phantoms with a "prostate" tapered cylinder within a "pelvis" rectangular cuboid. The "pelvis" has outer dimensions of 15 cm x 15 cm x 7.5 cm. The "prostate" is 7 cm deep with a tapering diameter ranging from 5 to 3 cm. We first filled the "pelvis" cubic container with the "Pelvis TMM" (Table I), creating two voids with petrolatum-coated plastic rods. A small 2.5 cm diameter cylindrical rod was used to create a hole for the TRUS imaging probe. A larger rod with a tapered end was used to create a void for the "prostate." Once the "pelvis" hardened, we removed both rods. We then filled the tapered cylindrical void with a "Prostate TMM" (Table I), having different multi-modality properties and ^{18}F or ^{68}Ge radioactivity concentrations than the "pelvis." Both TMMs were hardened at room temperature. These PET-TRUS-CT-MRI phantoms are stored with a thin layer of safflower oil on top to minimize dehydration and shrinkage. Figure 4a shows a photograph of the custom PET-TRUS-CT-MRI phantom made using ^{18}F-water in only the "prostate" (due to the time required for gel hardening and short ^{18}F half-life).

	Agar	Gelatin	$CuCl_2$-$2H_2O$	EDTA	NaCl	HCHO	Germall-Plus	Glass Beads	$BaSO_4$
Pelvis TMM	1.17	5.52	0.11	0.33	0.77	0.24	1.45	4.4	0.50
Prostate TMM	3.64	5.70	0.12	0.34	0.80	0.25	1.50	0	0

Table I. Dry-weight percents of the various components in the PET-TRUS-CT-MRI custom phantom. The remaining weight percent is deionized water.

The custom PET-TRUS-CT-MRI phantom with ^{18}F–water (in only the "prostate") was imaged with PET, CT and MRI. Using an EXACT HR PET scanner, PET data were acquired with a 60 minute emission scan in 3D mode and 10 minute transmission scan. At the start of the emission scan, the ^{18}F activity density was 0.33 μCi/ml in the prostate. Image reconstruction was performed with attenuation and scatter correction. Figure 4b shows a reconstructed coronal PET image of the phantom with uniform ^{18}F activity in the "prostate." A horizontal profile through the "prostate" center is also shown in figure 4b.

The phantom was imaged with a Nucletron KV ConeBeam CT scanner (100 keV; 16 mAmps) after the ^{18}F decayed. Reconstruction was performed with a proprietary SmartScatter algorithm using a Cone-Beam CT wedge filter. Figure 4c shows a reconstructed coronal CT image of the phantom with increased radiographic attenuation in the "pelvis" due to the $BaSO_4$.

After the ^{18}F decayed, the phantom was also imaged with an 1.5 T Avanto Siemens MRI scanner using a head coil with a T_1-weighted 2D spin echo pulse sequence (TE = 7.8 msec; TR = 500 msec; field of view = 230 mm x 230 mm x 3 mm; voxel size = 0.4 mm x 0.4 mm x 3 mm). Figure 4d shows a reconstructed T_1-weighted MRI image with a darker "prostate" representing a longer T_1 compared to the "pelvis." The glass beads (used for ultrasound imaging) shortened the T_1 in the "pelvis" despite having a lower agar concentration. The phantom was also imaged with a T_2-weighted 2D turbo spin echo pulse sequence (TE = 89 msec; TR = 5590 msec; field of view = 230 mm x 230 mm x 3 mm; voxel size = 0.4 mm x 0.4 mm x 3 mm). Figure 4e shows a reconstructed T_2-weighted MRI image with a darker "prostate" representing a shorter T_2 compared to the "pelvis."

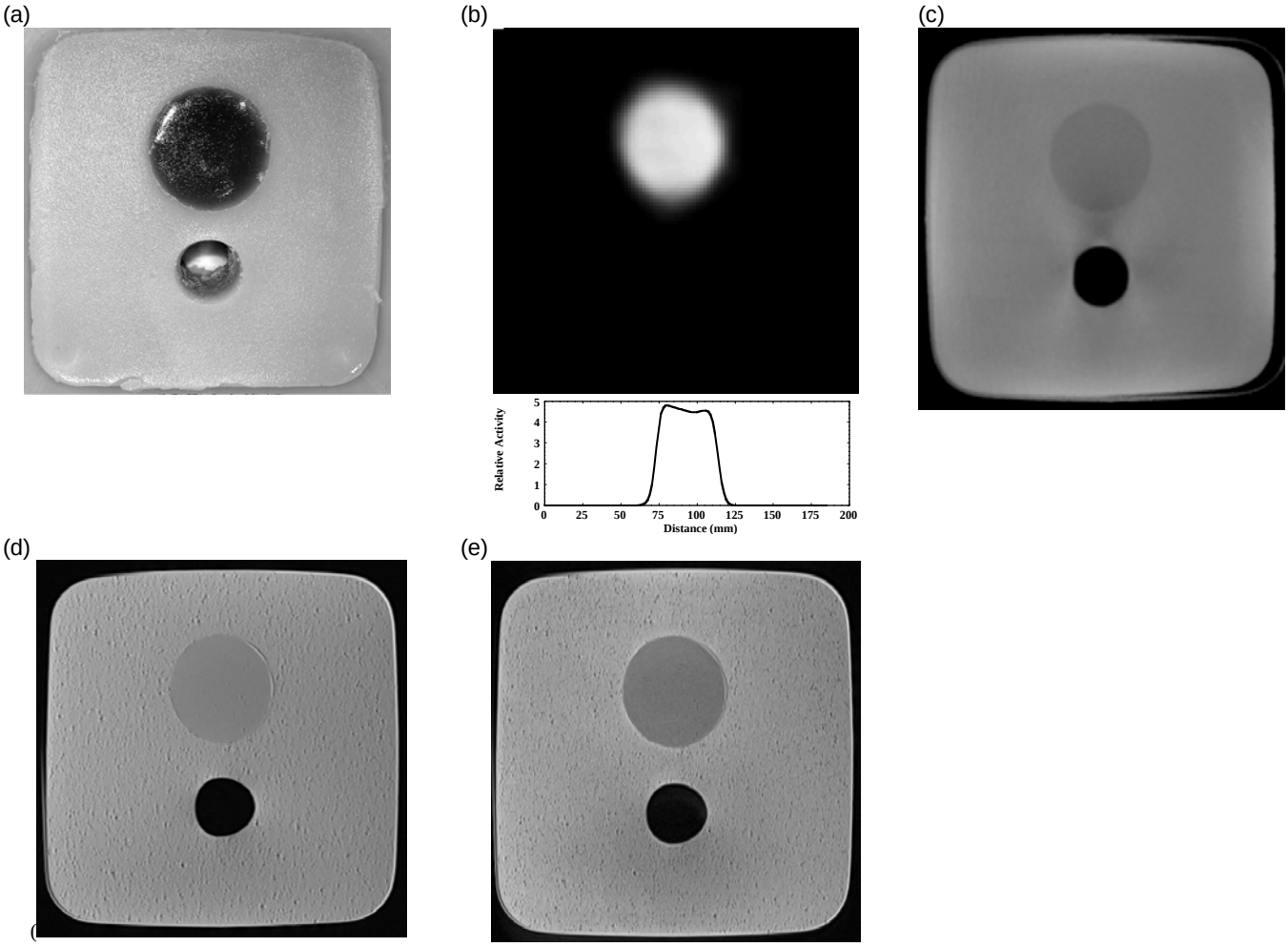

Figure 4. (a) Photograph of a custom PET-TRUS-CT-MRI phantom. The square "pelvis" has outer dimensions of 15 cm x 15 cm. The tapered cylindrical "prostate" is seen as a 5 cm diameter dark circle (the diameter of the cylinder tapers, decreasing from 5 cm to 3 cm towards the container bottom). The hole for transrectal ultrasound imaging (seen directly below the dark "prostate" circle) has a diameter of 2.5 cm. (b) Reconstructed coronal PET image of a custom PET-TRUS-CT-MRI phantom using ^{18}F (in the "prostate" only). The white circle shows the uniform ^{18}F activity in the "prostate." The ^{18}F initial activity density was 0.33 μCi/ml. Voxel size is 1.47 mm x 1.47 mm x 3.125 mm. Horizontal profile through the "prostate" center is also shown. (c) Reconstructed coronal x-ray CT image of the phantom with 1 mm axial thick slices. The pixel size is 0.5 mm x 0.5 mm x 1 mm. The dark gray circle shows lower radiographic attenuation in the "prostate" compared with the surrounding light gray higher-attenuation "pelvis." The black circle shows the hole used for the TRUS imaging probe. (d) Reconstructed coronal MRI T_1–weighted image of the custom PET-TRUS-CT-MRI phantom, representing 60 minutes of data. Voxel size is 0.4 mm x 0.4 mm x 3 mm. The dark gray circle shows the longer T_1 "prostate" surrounded by the shorter T_1 "pelvis." The black circle shows the hole used for the TRUS imaging probe. (e) Reconstructed coronal MRI T_2–weighted image of the phantom, representing 50 minutes of data. Voxel size is 0.4 mm x 0.4 mm x 3 mm. The black circle shows the hole used for the TRUS imaging probe.

A final custom PET-TRUS-CT-MRI phantom using $^{68}GeCl_4$ was then constructed and imaged. The phantom gel is inside a plastic cubic box with a lid that has a hole for TRUS imaging access. In order to prevent ^{68}Ge-gel pieces from escaping during TRUS imaging, a condom is used to seal the hole. The condom base is fixed around a centering ring on top of the container lid. The condom is held in place using a small washer inside the condom tip and a magnet outside the bottom of the plastic container. At the time of the phantom construction, the ^{68}Ge activity density was 0.73 μCi/ml in the "prostate" and 0.12 μCi/ml in the "pelvis."

This final custom PET-TRUS-CT-MRI phantom was imaged using an EXACT HR PET scanner 30 hours after phantom construction. PET data were acquired with a 3D emission scan followed by a 10 minute transmission scan. Iterative image reconstruction was performed with attenuation and scatter correction. Figure 5a shows a reconstructed coronal PET image of the phantom, as well as a horizontal profile through the "prostate" center. The initial ^{68}Ge activity density was six times higher in the "prostate" than the "pelvis." The ^{68}Ge activity in the "prostate" is clearly visible within the "pelvis" background. However, the "prostate" radioactivity in the PET image has a blurrier edge in this case (*e.g.*, compared to Fig. 3b), and the relative activity shown in the profile is only 4.8 ("prostate") to 1 ("pelvis") instead of the expected 6 to 1. This is probably due to the initial migration

of the ^{68}Ge tetrachloride molecules (see below for further discussion). This assumption is supported by the uniform radioactivity seen in the PET image of the previously discussed PET-TRUS-CT-MRI phantom constructed with ^{18}F-water (Figure 4b).

The phantom was also imaged with a Hitachi Hi-Vision 5500 digital ultrasound system, using a B mode bi-plane TRUS probe in a linear stepper. Figure 6b shows a transrectal ultrasound image of the phantom with a lower-scatter "prostate" surrounded by a higher-scatter "pelvis."

We intended to use this custom PET-TRUS-CT-MRI phantom repeatedly over a year. However, the ^{68}Ge tetrachloride molecules in the "prostate" migrated into the "pelvis" to become roughly uniformly distributed throughout the phantom in less than 57 days. Figure 5c shows a reconstructed coronal PET image of the phantom performed 57 days after construction, as well as a horizontal profile through the "prostate" center. We believe that the ^{68}Ge tetrachloride molecules were small enough to penetrate the gel pores, slowly reaching an equilibrium in radioactive concentration throughout the "prostate" and "pelvis." We should be able to prevent this $^{68}GeCl_4$ migration by using a barrier, such as a female latex condom, between the "prostate" and "pelvis" so the radioactivity instead reaches an uniform equilibrium within the "prostate" and "pelvis" separately. Based on repeated imaging results, these phantoms appear to have long-term stability otherwise (*i.e.*, except for the $^{68}GeCl_4$ migration). The mechanical properties also appear stable and there are no signs of bacterial or fungal invasion, when stored at room temperature for over six months. However, due to the safety issue of handling the long-lived ^{68}Ge radioactivity, we have decided to build a different kind of TRUS-PET phantom (that does not require ^{68}Ge handling). This new phantom is discussed below in the Custom PET-TRUS Phantom with Tubing section.

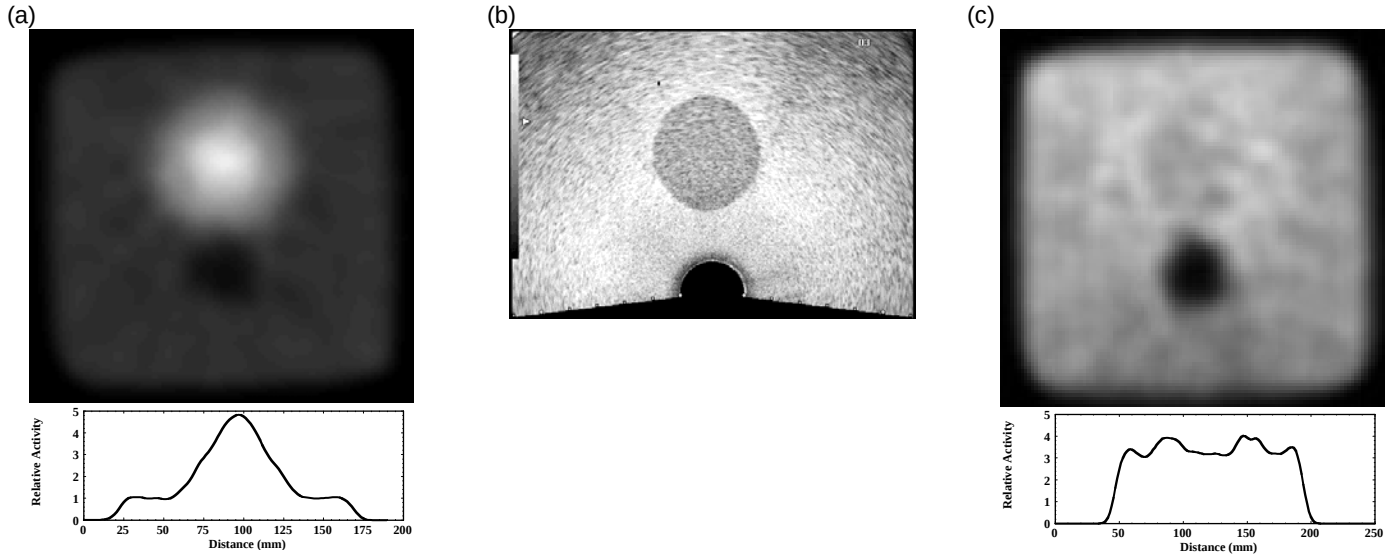

Figure 5. (a) Reconstructed coronal PET image of a custom PET-TRUS-CT-MRI phantom with ^{68}Ge; imaged using the EXACT HR PET scanner 30 hours after phantom construction. The white circle shows the higher ^{68}Ge activity in the "prostate" within the dark gray low ^{68}Ge activity in the "pelvis." The small black circle (below the larger white "prostate" circle) represents the TRUS probe position. Voxel size is 1.47 mm x 1.47 mm x 3.125 mm. Horizontal profile through the "prostate" center is also shown. (b) Ultrasound image of the phantom. The dark gray circle shows the lower-scatter "prostate," directly above the black circular hole used for the TRUS probe. The surrounding light gray background shows the higher-scatter "pelvis." (c) Reconstructed coronal PET image of the phantom, when PET imaging was performed with the EXACT HR PET scanner 57 days after phantom construction. The ^{68}Ge radioactivity is seen to be nearly uniform throughout the entire phantom.

Commercial TRUS Phantom with Tubing:

In Year 2, we also modified a commercial TRUS phantom (CIRS Model 58) that is normally used for TRUS-guided brachytherapy seed implantation training. This commercial phantom has tissue mimicking materials that simulate anatomical structures of the prostate region for transrectal ultrasound imaging, as shown in figure 6a. We modified this commercial TRUS phantom by adding a fillable silicon tube through the phantom. This tube can be filled with ^{18}F-water, allowing for PET and TRUS imaging of the same phantom. (Imaging results with this phantom are discussed below in the Tasks 2d and 2e sections). However, the commercial TRUS phantom was old and the gels inside were dried out and significantly compressed (see figure 6b). In addition, the gels were damaged when the tubing was pulled through. Overall the ultrasound images are very noisy for this old

phantom. These commercial TRUS phantoms are costly, so we did not purchase a new one. We need to image multiple line sources at various angles, in order to adequately validate our ability to acquire accurately co-registered PET and TRUS images, and it is unlikely that we will be able to pull tubing through the commercial soft gels without damaging them. Instead, we are making a Custom PET-TRUS Phantom with Tubing.

(a) (b)

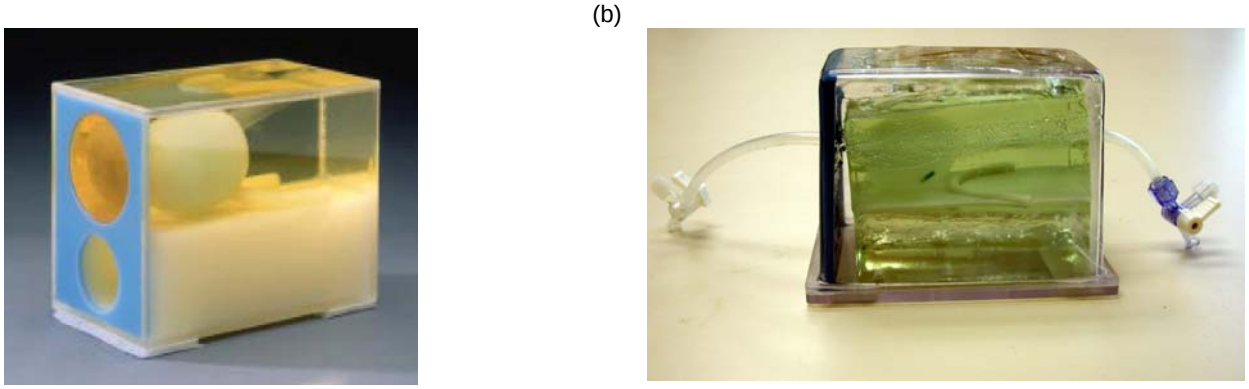

Figure 6. (a) CIRS Model 58 TRUS prostate training phantom, which is a clear acrylic box with structures simulating the prostate, rectal wall, seminal vesicles, urethra and perineal membrane for transrectal ultrasound imaging. (b) The older model CIRS TRUS prostate training phantom that we own, with gel that has dehydrated and shrunk. A silicone tube for ^{18}F-water was added to this phantom, which caused additional damage to the phantom gels.

Custom PET-TRUS Phantom with Tubing:

In Year 2, we designed a new Custom PET-TRUS Phantom with Tubing, which will be constructed and used in Year 3. The previously described PET-US and PET-TRUS-CT-MRI phantoms had "prostate" and "pelvis" structures that simulated 511 keV (^{18}F or ^{68}Ge) radioactivity concentrations for PET. However, our phantom does not need to have radioactive anatomical structures, because its only purpose is to validate image co-registration for PET and TRUS imaging. Hence, we have instead designed a phantom with tubing that winds through a non-radioactive ultrasound tissue mimicking gel. The tubing is distinguishable from the gel using ultrasound imaging, and the tubing will be filled with ^{18}F-water for PET imaging. This will permit us to image the cross-section of several small diameter line sources (i.e., tubes) in the new phantom with both PET and TRUS, which will allow us to fully validate our acquisition of accurately co-registered PET and TRUS images.

(a) (b)

Figure 7. Design drawing of the Custom PET-TRUS Phantom with Tubing from (a) front view and (b) side view. The plastic container has dimensions 15 cm x 15 cm x 15 cm, with a 2.5 cm diameter hole to allow access for the probe for TRUS imaging. The three white-colored line sources are in the same horizontal plane in a N pattern, as seen in the front view. The fourth dark-colored line source is within a plane angled relative to the other three, as seen in the side view. The four line sources are embedded in a "Prostate TMM" gel.

The phantom will be constructed using a plastic container with dimensions 15 cm x 15 cm x 15 cm. A 2.5 cm diameter hole will be made in the box and "Prostate TMM" gel, to allow access for the probe for TRUS imaging. (This void in the TMM gel will be created with a petrolatum-coated rod, as described previously.) A single piece of tubing will be accurately placed through the box to create four line sources that can be filled with a single injection of ^{18}F-water. Three of the line sources will be in a single horizontal plane in a "N" pattern. The fourth

line source will be within a plane angled relative to the other three line sources. Figure 7 shows the design drawing of the Custom PET-TRUS Phantom with Tubing. We have chosen to use Tygon 3350 silicone tubing (with a inner diameter of 5/32 inches and outer diameter of 7/32 inches), which should allow us to image the tubing cross-section with transrectal ultrasound when the tubing is filled with water and placed within the ultrasound TMM. Once the tubing is positioned, we will fill the container with non-radioactive "Prostate TMM" (previously described above in the PET-TRUS-CT-MRI Phantom section). This new custom PET-TRUS phantom will be reusable for repeated testing, without requiring the handling of long-lived ^{68}Ge. We simply have to inject new ^{18}F-water into the tube prior to PET-TRUS imaging for each use.

Task 2b) Attach 511 keV point source onto rear of TRUS probe. Image and reconstruct 3 point sources using PET, then determine 3D location of TRUS probe tip relative to PET-center.

In Year 1, we determined that we do not need the 511 keV point source attached to the rear of the TRUS probe. This point source was intended to track the TRUS probe's rotational motion. However, Dr. Hsu only plans to use the TRUS probe in the upright (*i.e.*, rotational angle of 0 degrees) position based on his extensive TRUS imaging experience. In the unlikely event that a rotational angle is needed for patient imaging, the probe angle is accurately known from the rotational component of the TRUS stepper (see figure 2b).

As described in Task 1d and 1e, the 3D location of the TRUS probe tip relative to the PET-center was determined in Year 1. In Year 2, a more streamlined Matlab program was developed for both Task 1 and 2. Thus the only real difference between these two tasks is the reconstruction algorithm used to analyze the point source PET data. Since patient positioning needs to be done quickly, Task 1 uses a fast 2-iteration expectation-maximum algorithm with a simplified model of the PET scanner geometry. Since greater accuracy is needed for Task 2 image co-registration and we have more time to reconstruct the same point source data, we instead use our optimized PET image reconstruction code (see Task 2c).

Task 2c) Optimize PET image reconstruction and develop image display algorithms.

PET Image Reconstruction:

In Years 1 and 2, we optimized the PET image reconstruction for the prostate-specific PET scanner. We developed a 3D iterative penalized maximum likelihood PET reconstruction algorithm that models our unusual prostate-optimized PET scanner geometry, with a pre-conditioned conjugate gradient optimization algorithm and an improved detector efficiency and randoms estimate technique. PET reconstruction is performed in a parallel processor mode to reduce PET reconstruction time to 2-3 hours for a patient study.

However, there are currently personnel issues concerning PET image reconstruction for the prostate-specific PET scanner. We are now dependent on one person to perform this PET reconstruction, and he has retired and works only part-time as a consultant. Until this manpower issue is addressed, we plan to proceed with this research using the EXACT HR PET scanner instead of the prostate-specific PET scanner. The development of dual PET-TRUS prostate imaging is not dependent on which PET scanner is used. As primary investigator, I was trained on how to use the EXACT HR PET scanner's commercially provided software for data acquisition and image reconstruction during Year 2. Hence, optimized PET image reconstruction software is available for this project for both available PET scanners.

Reslicing Software:

In Year 2, we developed software to reslice transrectal ultrasound imaging data into PET coordinates or reslice the 3D PET imaging data into TRUS coordinates. Either of these coordinate transformations are based on our measurement of the 3D location of the TRUS probe tip in PET coordinates (calculated from the two 511 keV point source data). Although the reslicing software allows us to reslice either PET or TRUS imaging data, we focused primarily on reslicing the PET imaging data (since this provided the best co-registered image display).

Functional PET image information is overlaid on anatomical TRUS images with use of the following image registration method. First, a preliminary reference position and orientation for the TRUS probe is measured while the probe is in the PET scanner. This is accomplished by using the PET scanner to image radioactive fiducial markers (i.e., two 511 keV point sources) attached to the TRUS probe at known positions relative to the probe tip. Given this preliminary probe position information, the patient table is then moved so that the TRUS

probe tip is centered in the axial field of view of the PET scanner; it is assumed that the table motion direction is parallel to the axis of the PET scanner. PET images acquired from a phantom (or patient) at this table position can now be registered with TRUS images acquired by the probe. The 3D geometric relationship between PET image pixels and TRUS image pixels is calculated based on the 511 keV point source images and the known amount of linear table motion. The 3D position in the PET coordinates is calculated for each TRUS pixel, and the PET image intensity at each TRUS pixel position is obtained via trilinear interpolation of the PET images. This yields registered sets of TRUS images and (resliced) PET images that have common pixel size and 3D pixel positions.

Image Display Software:

In Year 2, we developed the method for image display which will be used for co-registered PET and TRUS images. We first use ImageJ to convert a resliced 3D PET imaging volume data set into an acceptable raw data format (e.g. from 32-bit real to 16-bit integer). We can converted PET image data sets from both the prostate-optimized PET scanner and the EXACT HR PET scanner using this ImageJ software. The TRUS system provides the series of 2D images in an acceptable TIFF format directly. Once we have both the TRUS and resliced converted PET images, we use the OSIRIX software. This software allows us to import the resliced converted PET and TRUS images separately, then create a fused PET-TRUS image. We are able to translate (in real time) one image set relative to the other, allowing both linear translations and rotations, but such translations are not used.

We have chosen the OSIRIX software for data fusion in part because it is free software that is readily available without a license. In the unlikely event that OSIRIX doesn't work well for data fusion of the patient images, we have a number of commercial platforms (e.g., Occentra-MasterPlan, Nucletron, and RTT Coherence and Leonardo Workstation) and applications tools (e.g., Matlab) that could also be used for co-registered image display.

Task 2d) Acquire TRUS and PET "prostate" image of the custom phantom.

In Year 2 (after the final custom PET-TRUS-CT-MRI phantom was constructed with long-lived ^{68}Ge), we transferred the UCSF TRUS system to LBNL to perform this task in conjunction with the prostate-specific PET scanner. We acquired TRUS and PET data for a custom phantom during the same imaging session, using the data collection procedure outlined previously (see Task 1e). The two 511 keV point source PET data were reconstructed (with the optimized PET reconstruction software) and used to accurately determine the 3D location of the TRUS probe tip in PET coordinates (with the Matlab software). The optimized PET reconstruction software was also used to reconstruct a 3D PET imaging volume of the custom phantom. This reconstructed 3D PET imaging volume data set was resliced into TRUS coordinates and fused with the series of 2D TRUS images taken during the same phantom imaging session (see Task 2c).

Dual PET-TRUS data were acquired for two different custom phantoms in Year 2 – the PET-TRUS-CT-MRI phantom using $^{68}GeCl_4$ and the modified commercial TRUS phantom with tubing (see Task 2a). Figures 8 and 9 show the PET, TRUS and co-registered PET-TRUS images for these phantoms, as discussed below (see Task 2e).

In year 3, we will acquire TRUS, PET and co-registered PET-TRUS images for the new Custom PET-TRUS Phantom with Tubing using the EXACT HR PET scanner and TRUS system. We will use this data to more accurately validate our ability to acquire and co-register PET and TRUS images, prior to initiating patient studies.

Task 2e) Co-register the PET and TRUS phantom images, exploring how to present the dual-modality data.

In Year 2, we co-registered fully 3D TRUS and 3D PET imaging volume data sets of a custom phantom, using the reslicing and image display software described above in Task 2c. We determined that this is the best way to present the dual-modality co-registered images when evaluating the accuracy of co-registration of phantom images. We also contoured the series of 2D TRUS phantom images and co-registered these contours onto the corresponding PET image planes. We will further explore this second contouring display method for PET-TRUS images of patients in Year 3, if necessary.

We performed dual PET-TRUS imaging of the PET-TRUS-CT-MRI phantom with $^{68}GeCl_4$ seven days after the phantom was constructed. As discussed previously (Task 2a), the $^{68}GeCl_4$ molecules migrated through the gel pores prior to this imaging. Hence, we imaged a blurry diffused 511 keV radioactive region that extended beyond the prostate, using the prostate-specific PET scanner. Figure 8a shows the reconstructed coronal PET image of the phantom after the imaging data were resliced into TRUS coordinates. We see the white-colored higher ^{68}Ge radioactivity in the extended "prostate" region surrounded by the dark gray-colored low ^{68}Ge radioactivity in the "pelvis." Figure 8b shows the corresponding coronal TRUS image of the phantom with a dark gray lower-scatter "prostate" surrounded by a light gray higher-scatter "pelvis." The sharp boundaries seen between the regions in the TRUS image demonstrate that the "Prostate TMM" and "Pelvis TMM" are stable except for the $^{68}GeCl_4$ migration. Both the resliced PET and TRUS images show a black partial-circle in the bottom center of the image, where the TRUS probe is located. Figure 8c shows the corresponding co-registered coronal PET-TRUS image. In this co-registered image, the resliced PET image is shown in color overlaid onto a grayscale TRUS image. There appears to be a larger than desired co-registration error is this fused PET-TRUS image. However, it is difficult to truly determine the error, because it is complicated by the $^{68}GeCl_4$ migration. As a result, we performed dual PET-TRUS imaging on a second phantom.

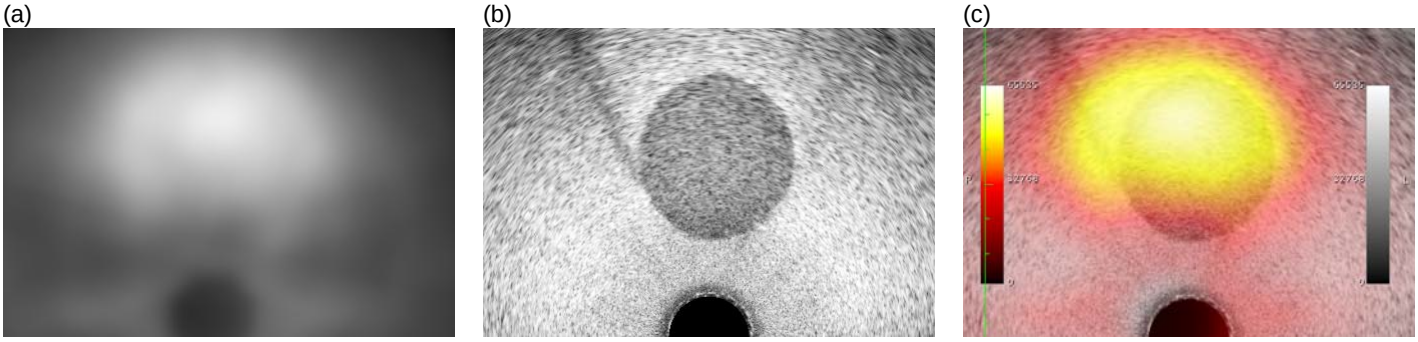

Figure 8. (a) Reconstructed resliced coronal PET image of a custom PET-TRUS-CT-MRI phantom with $^{68}GeCl_4$, which was imaged by the prostate-specific PET scanner and TRUS system during the same session 7 days after phantom construction. The white circle shows the higher ^{68}Ge activity in the extended "prostate" region within the dark gray lower ^{68}Ge activity in the "pelvis." The ^{68}Ge activity density was 0.73 μCi/ml in the "prostate" and 0.12 μCi/ml in the "pelvis" when initially constructed. The image also shows the black partial-circle of the TRUS probe at the bottom center. (b) Ultrasound image of the phantom. The dark gray circle shows the lower-scatter "prostate," directly above the black partial-circle representing the TRUS probe. The surrounding light gray background shows the higher-scatter "pelvis." (c) Coronal co-registered PET-TRUS image of the phantom. The PET image is shown in color overlaid onto the grayscale TRUS image (with proper co-registration).

We also performed dual PET-TRUS imaging of the modified commercial TRUS phantom that is shown in figure 6b. As discussed previously (see Task 2a), the TRUS images of this phantom are noisy since this commercial phantom is old and the gels have been damaged. The ultrasound images are also more difficult to read due to the more complicated anatomical TRUS structures (i.e., neighboring urethra tube) that overlay on the tubing that was added. However, we are able to see the tube filled with ^{18}F-water in both the PET and TRUS images. Figure 9a shows the reconstructed coronal PET image of the phantom, which was resliced into TRUS coordinates. We see a small white-colored circle from the ^{18}F radioactivity inside the tube. Figure 9b shows the corresponding coronal TRUS image of the phantom, with the urethra and ^{18}F tube both visible (and labeled). The TRUS image also shows a black partial-circle in the bottom center where the TRUS probe is located. Figure 9c shows the corresponding coronal co-registered PET-TRUS image. The resliced PET image is shown in color overlaid onto a grayscale TRUS image. The co-registration error is 2 mm. We plan to perform dual PET-TRUS imaging of the Custom PET-TRUS Phantom with Tubing (see Task 2a) to confirm this preliminary co-registration error estimate prior to initiating patient studies.

We believe that one source of error for co-registration is the patient table motion. As mentioned in Task 2c, it is assumed that the table motion direction is parallel to the axis of the PET scanner. However, the table motion of the prostate-specific PET scanner may not be level to the required precision. Namely, there is likely to be a very small physical displacement in the transaxial directions when the patient table is moved axially. This is an issue because the two point sources are imaged with the PET scanner at a different patient table position than the phantom (or patient), causing a small co-registration error. We expect the patient table motion of the EXACT HR PET scanner to be more precisely level for our Year 3 tests, because the patient table is designed to be more stable and we can easily provide additional table support(s) if necessary.

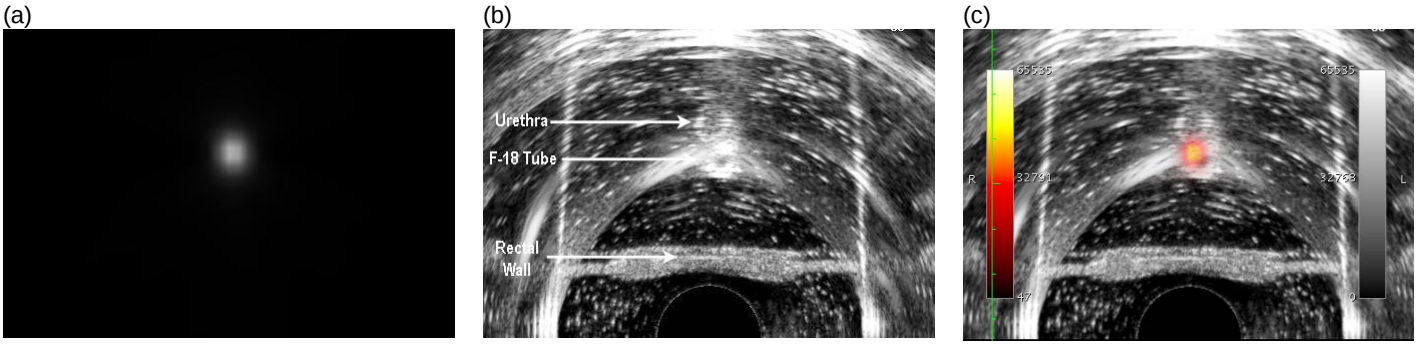

Figure 9. (a) Reconstructed resliced coronal PET image of a Commercial TRUS Phantom with Tubing, which was imaged by the prostate-specific PET scanner and TRUS system during the same imaging session. The small white circle shows the ^{18}F activity within the tube. The ^{18}F activity inside the entire tube length was 132 μCi, with 45 μCi within the field of view of the prostate-optimized PET scanner. (b) Ultrasound image of the phantom. The urethra, ^{18}F tube, rectal wall, and overall rectangular phantom shape are visible (and labeled) despite noise streaks in the image. The urethra tube is above the ^{18}F tube in this phantom region. (c) Coronal co-registered PET-TRUS image of the phantom. The PET image is shown in color overplayed onto the grayscale TRUS image.

Task 3: Validate our ability to position patients in the PET scanner and to acquire co-registered PET and TRUS images.

Task 3a) Write human subjects protocol, and get approval from LBNL, UCSF and DOD.

Although this task was not scheduled to begin until proposal Year 2, we completed Task 3a ahead of schedule in Year 1. LBNL, UCB, UCSF and DOD gave IRB approval for our human subjects studies. This was a major accomplishment, in part because this project involves a novel radiopharmaceutical (i.e., ^{11}C-choline) and novel device (i.e., LBNL prostate-optimized PET scanner).

In Year 2, modifications to the human subjects documentation were made primarily to (1) add personnel to the project (due to the retirement of a non-key person) and (2) allow use of either the EXACT HR PET scanner or the prostate-specific PET scanner. We are currently approved to perform human subjects studies through January 2010 with either available PET scanner. We expect IRB approval to be renewed annually without issue.

Task 3b) Recruit 10 patients with confirmed prostate cancer.

This task has not started yet. Recruitment materials are approved and ready to be distributed when appropriate.

Task 3c) Perform patient studies with TRUS system and PET scanner (using ^{11}C choline) during the same exam.

Patient studies have not started yet.

Task 3d) Reconstruct PET images, identify 3D contours from TRUS images, and co-register.

Patient studies have not started yet.

Task 3e) Optimize image co-registration.

Patient studies have not started yet.

Key Research Accomplishments

Our key research accomplishments in this year are summarized as follows:

Task 1: We have completed the mechanical setup of the dual PET-TRUS imaging system, including modifications to the TRUS equipment and patient table, to allow use of the EXACT HR PET scanner.

We have also developed improved streamlined Matlab software to more accurately determine the two ^{68}Ge point source locations, as well as automatically calculate the location of the TRUS probe tip in PET coordinates (based on these point source locations).

Task 2: We have successfully constructed and imaged custom PET-TRUS-CT-MRI phantoms using agar-gelatin based tissue mimicking materials mixed with 511 keV radioactive solutions. These custom phantoms approximate a patient's acoustical properties for TRUS imaging, 511 keV activity concentrations for PET imaging, nuclear magnetization for MRI imaging, and radiographic density for CT imaging.

We have optimized the PET image reconstruction software. In addition, we have developed reslicing and image display software for PET and TRUS image co-registration.

We performed dual PET-TRUS imaging of the final PET-TRUS-CT-MRI phantom constructed with $^{68}GeCl_4$, reconstructed and resliced the 3D PET imaging volume (into TRUS coordinates), and co-registered the resliced PET and TRUS images. However, the evaluation of this PET-TRUS co-registration was compromised by migration of the $^{68}GeCl_4$ molecules from the "Prostate TMM" to ultimately become uniformly distributed throughout the phantom.

We modified a commercial TRUS phantom by adding a fillable silicone tube that can be filled with ^{18}F-water. We performed dual PET-TRUS imaging of this phantom, reconstructed and resliced the 3D PET imaging volume, and co-registered the resliced PET and TRUS images. We estimate our preliminary co-registration error to be 2 mm based on these results.

We designed a custom "PET-TRUS Phantom with Tubing" consisting of a fillable (four line source) tube embedded in an ultrasound tissue mimicking gel.

Task 3: We have received updated IRB approval for our human subject studies.

Reportable Outcomes

- Oral presentation at the IEEE Medical Imaging and Nuclear Science Symposium Conference on "Dual-Modality Prostate Imaging with PET and Transrectal Ultrasound" (Dreseden Germany, October 2008).
- Manuscript: J. S. Huber, Q. Peng, and W. W. Moses, "Multi-Modality Phantom Development," submitted to *IEEE Trans. Nucl. Sci.* (March 2009).
- International patent application: Patent Application Ser. No. PCT/US2008/064160; Title "Co-registration for Dual PET-Transrectal Ultrasound (PET-TRUS) Prostate Imaging;" Inventors Jennifer S. Huber, William W. Moses, Jean Pouliot, I-Chow Hsu, Qiyu Peng, Ronald H. Huesman, and Thomas F. Budinger; File Date May 19, 2008.

Conclusions

We have completed the mechanical setup of the PET-TRUS system, independent of whether we use the prostate-specific PET scanner or the EXACT HR PET scanner for our dual-modality imaging studies. We have developed critical software to: (1) determine point source locations in PET coordinates and calculate the corresponding 3D location of the TRUS probe tip, (2) position a prostate at the PET-center, (3) reconstruct PET data, (4) reslice PET imaging data (into TRUS coordinates), and (4) display co-registered resliced PET - TRUS images.

We have also constructed a novel PET-TRUS-CT-MRI phantom and performed dual PET-TRUS imaging with this custom phantom. Unfortunately the evaluation of the co-registration error was compromised by migration of the $^{68}GeCl_4$ molecules inside the phantom. Although we should be able to prevent this migration by using a latex barrier between the "prostate" and "pelvis" regions, we have instead decided to build a different kind of

phantom that does not require handling of ^{68}Ge long-lived radioactivity. However, these multi-modality PET-TRUS-CT-MRI phantoms still have many potential applications beyond this project.

We have modified a commercial TRUS phantom by adding a fillable silicon tube (that can be filled with ^{18}F-water for PET imaging). We performed dual PET-TRUS imaging of this phantom and obtained co-registered resliced PET – TRUS images, with a co-registration error of only 2 mm. We plan to confirm this preliminary co-registration error estimate using a Custom PET-TRUS Phantom with Tubing, which we have designed to consist of four ^{18}F fillable line source tubes (at different known angles) embedded in an ultrasound tissue mimicking gel. We plan to construct and image this new custom phantom to further validate our dual PET-TRUS imaging techniques. Once validation with phantoms is complete, we are ready to initiate human subject studies. We have updated IRB approval for human subject studies.

Based on our results, our dual PET-TRUS imaging still appears to be a promising new technology for prostate imaging. Accurately co-registered PET and TRUS images should accurately guide subsequent diagnosis and treatment procedures. For instance, dual PET-TRUS prostate imaging could be used to: (1) increase the diagnostic accuracy of biopsy, (2) determine where higher dose is needed for external beam irradiation and brachytherapy treatment, and (3) detect early failure response to external beam irradiation, brachytherapy, prostatectomy, or androgen ablation.

References

[1] J. S. Huber, Q. Peng, and W. W. Moses, “Multi-Modality Phantom Development,” *Nuclear Science Symposium Conference Record*, vol. 4, pp. 2944-2948, 2007.

[2] E. L. Madsen, M. A. Hobson, S. Hairong, T. Varghese and G. R. Frank, “Tissue-mimicking agar/gelatin material for use in heterogeneous elastography phantoms,” *Phys. Med. Biol.*, vol. 50, pp. 5597-5618, 2005.

Appendices

- Abstract of oral presentation at the IEEE Medical Imaging and Nuclear Science Symposium Conference on “Dual-Modality Prostate Imaging with PET and Transrectal Ultrasound” (Dresden, Germany; October 2008).
- J. S. Huber, Q. Peng, and W. W. Moses, “Multi-Modality Phantom Development,” manuscript submitted to *IEEE Trans. Nucl. Sci.* (March 2009).
- International patent application: Patent Application Ser. No. PCT/US2008/064160; Title “Co-registration for Dual PET-Transrectal Ultrasound (PET-TRUS) Prostate Imaging;” Inventors Jennifer S. Huber, William W. Moses, Jean Pouliot, I-Chow Hsu, Qiyu Peng, Ronald H. Huesman, and Thomas F. Budinger; File Date May 19, 2008.

DUAL-MODALITY PROSTATE IMAGING WITH PET AND TRANSRECTAL ULTRASOUND

J.S. Huber, W.W. Moses, Q. Peng, R.H. Huesman, B.W. Reutter, D.S. Wilson, J. Pouliot, and I.C. Hsu
Lawrence Berkeley National Laboratory
University of California, San Francisco

We are developing a dual-modality positron emission tomograph (PET) and transrectal ultrasound (TRUS) prostate imaging system, which allows us to accurately co-register PET and TRUS images that are acquired sequentially during a single imaging session. Functional PET imaging with [^{11}C]choline detects malignant prostate tumors and determines a tumor's aggressiveness based on metabolic uptake level. However, the relative uptake in a prostate tumor can be so great that few other anatomical landmarks are visible in a PET image. Ultrasound imaging with a transrectal probe provides high-resolution anatomical detail in the prostate region that will be accurately co-registered with the sensitive functional information from the PET imaging. This dual-modality PET-TRUS imaging will help localize any cancer within the prostate region.

We have developed initial hardware and software tools for dual PET-TRUS prostate imaging. We have completed the mechanical setup, mechanically modifying the TRUS equipment to work when mounted onto a common patient table in conjunction with the LBNL prostate-optimized PET scanner. We have developed and validated methods for positioning a patient's prostate in the center of the PET scanner, reproducibly positioning the TRUS probe tip (which will be positioned axially at the prostate center) within 1 mm of the PET-center. This prostate positioning is important, since the prostate-optimized PET scanner has optimal resolution and sensitivity near the PET-center and a reduced axial extent. We have also improved the PET image reconstruction software and have developed preliminary image display software. Finally, we have constructed and imaged unique TRUS-PET prostate phantoms that are used to validate PET and TRUS image co-registration. Co-registered PET and TRUS phantom images acquired with this dual-modality system will be presented.

Address correspondence to:
Jennifer Huber
Lawrence Berkeley National Laboratory
1 Cyclotron Rd.
Mail Stop 55-121
Berkeley, CA 94720
(510) 486-6445
(510) 486-4768 (FAX)
jshuber@lbl.gov

Multi-Modality Phantom Development

J.S. Huber, *Member, IEEE,* Q. Peng, and W.W. Moses, *Fellow, IEEE*

***Abstract*–Multi-modality imaging has an increasing role in the diagnosis and treatment of a large number of diseases, particularly if both functional and anatomical information are acquired and accurately co-registered. Hence, there is a resulting need for multi-modality phantoms in order to validate image co-registration and calibrate the imaging systems. We present our PET-ultrasound phantom development, including PET and ultrasound images of a simple prostate phantom. We use agar and gelatin mixed with radioactive water. We also present our development of custom multi-modality phantoms that are compatible with PET, transrectal ultrasound (TRUS), MRI and CT imaging. We describe both our selection of tissue mimicking materials and phantom construction procedures. These custom PET-TRUS-CT-MRI prostate phantoms use agar-gelatin radioactive mixtures with additional contrast agents and preservatives. We show multi-modality images of these custom prostate phantoms, as well as discuss phantom construction alternatives. Although we are currently focused on prostate imaging, this phantom development is applicable to many multi-modality imaging applications.**

***Index Terms*—Positron Emission Tomography, Ultrasound, Magnetic Resonance Imaging, X-ray Computed Tomography**

I. Introduction

Multi-modality imaging plays an increasingly important role in the diagnosis and treatment of a large number of diseases. Combining modalities that provide both functional and structural information is particularly important. For instance, functional information can be acquired with single photon emission computed tomography (SPECT), positron emission tomography (PET) or functional magnetic resonance imaging (fMRI), whereas anatomical information can be acquired using x-ray computed tomography (CT), ultrasound (US) or magnetic resonance imaging (MRI).

Combining PET and CT has recently revolutionized the role of imaging in diagnosis and treatment planning for many kinds of cancer. As a result, there are commercially available PET-CT phantoms that are used for acceptance testing and routine quality evaluation of the PET-CT systems. For instance, these phantoms are used to determine how accurately the two image sets are aligned and how accurately the CT-based PET attenuation correction works. However, PET-CT imaging is not the preferred modality combination for all diseases or even all cancers. For instance, ultrasound imaging is an integral part of diagnosis and treatment procedures for many diseases, such as prostate cancer. Transrectal ultrasound (TRUS) provides good anatomical detail of the prostate region and accurately measures the prostate volume, whereas CT has poor contrast for soft-tissue (like the prostate) and it over-estimates prostate volume. Hence, phantoms for multi-modality imaging with ultrasound and PET or MRI are needed. Ultrasound phantoms are readily available commercially, but we are not aware of any commercially available US-PET or US-MRI phantoms.

We believe that imaging the prostate with ^{11}C-choline using a dual PET-TRUS system will help locate cancer within the prostate region. We envision that dual PET-TRUS prostate imaging could be used to guide biopsy, guide treatment procedures, and detect local recurrence earlier than is currently possible. Therefore, we are developing a dual imaging system that acquires PET and TRUS data sets during the same patient imaging session, using methods that allow us to accurately determine the 3D location of the TRUS probe tip relative to the PET scanner. As a result, co-registration of the PET and TRUS patient images will be simple and accurate. However, prior to our patient studies, we must validate our ability to image and accurately co-register PET and TRUS images using a PET-TRUS prostate phantom.

Since the phantom that we need is not commercially available, we have built a custom PET-TRUS prostate phantom with structures that simulate the acoustical properties for TRUS and 511 keV activity concentrations for PET. In addition, we have built custom PET-TRUS-CT-MRI phantoms with structures that also simulate the nuclear magnetization for MRI and radiographic density for CT. We present here our PET-ultrasound phantom and PET-TRUS-CT-MRI phantom development, including multi-modality images of phantoms. We also discuss alternative phantom construction options. This phantom development is applicable to many multi-modality applications.

II. PET-Ultrasound Phantom

We have constructed a simple PET-ultrasound prostate phantom as proof of principle. It was constructed with two basic tissue mimicking materials (TMMs). The “pelvis” was prepared as a high-scatter ultrasound TMM, using 4% agarose mixed with deionized water and heated to 62 °C (in a hot water bath on a hot plate and mixed continuously with a magnetic stir rod). The temperature of the agarose-water was kept below 70 °C to maintain the high-scatter ultrasound properties. The “prostate” was prepared as a low-scatter ultrasound TMM, using 8% gelatin mixed with deionized water and heated until the gelatin dissolved.

The PET-US phantom was constructed in two stages. We first filled a rectangular plastic box with the 4% agarose TMM, creating a void with a petrolatum-coated plastic rod in the center. As soon as the rectangular agarose “pelvis” hardened, the rod was removed and we filled the inner cylindrical “prostate” region with the 8% gelatin TMM. Fig.

Manuscript received March 20, 2009. This work was supported in part by the Director, Office of Science, Office of Biological and Environmental Research, Medical Science Division of the U.S. Deparment of Energy under Contract No. DE-AC02-05CH11231, and in part by Department of Defense grant number W81XWH-07-1-0020.

J.S. Huber, Q. Peng, and W.W. Moses are with Lawrence Berkeley National Laboratory, Berkeley, CA 94720 USA (e-mail: jshuber@lbl.gov).

1a shows a photograph of the PET-US phantom. At each stage, the TMM was mixed with radioactive ^{18}F-water (mixed with a drop of food coloring) before placing it in a refrigerator to harden. We used short-lived ^{18}F radioactive (110 minutes half-life) water, since ^{18}F is readily available from our in-house cyclotron and no long-lived radioactive waste were generated by the tests. As a result, the gel hardening time was important due to the ^{18}F half-life. The "pelvis" gel hardened in 52 minutes (using an ice bath within the refrigerator) and the "prostate" hardened in 31 minutes (without ice bath). The resulting phantom had six times higher 511 keV activity density in the inner cylindrical "prostate" than in the outer rectangular "pelvis."

(a)

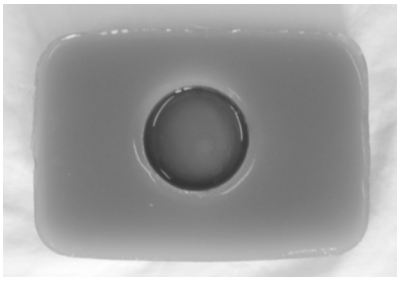

(b)

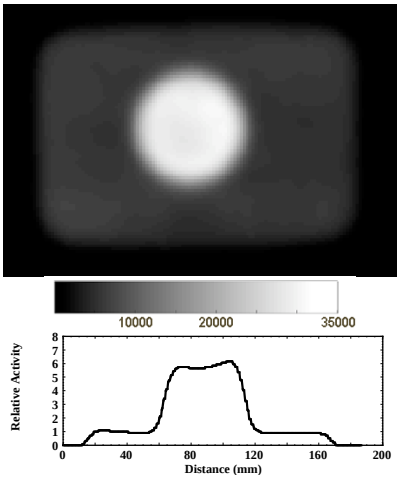

(c)

Fig. 1. (a) Photograph of a PET-ultrasound prostate phantom. The agarose "pelvis" has outer dimensions of 16 cm x 11 cm x 3.5 cm. The cylindrical gelatin "prostate" has a 5 cm diameter and 2.5 cm depth. (b) Reconstructed coronal PET image of the phantom. The white circle shows the high ^{18}F activity density in the "prostate," and the dark gray rectangle shows the low ^{18}F activity density in the background "pelvis." Image represents 636 M counts (*i.e.*, 20 minutes of data). The voxel size is 1.47 mm x 1.47 mm x 3.125 mm. Horizontal profile through the "prostate" center is also shown. (c) Ultrasound image of the same phantom using a 5MHz external ultrasound probe. The dark gray circle shows the low-scatter gelatin "prostate," and the surrounding light gray background shows the high-scatter agarose "pelvis."

The phantom was roughly centered in an EXACT HR PET scanner, and PET data were acquired with a 20 minute emission scan in 3D mode and 10 minute transmission scan. At the start of the emission scan, the ^{18}F activity density was 1.07 μCi/ml in the cylindrical "prostate" gelatin and 0.17 μCi/ml in the rectangular "pelvis" agarose. Image reconstruction was performed with attenuation and scatter correction. Fig. 1b shows a reconstructed coronal PET image of the phantom, as well as a horizontal profile through the "prostate" center. The ^{18}F activity uniformly concentrated in the cylindrical "prostate" gelatin is clearly visible within the rectangular "pelvis" background activity, with the expected 6 ("prostate") to 1 ("pelvis") relative activity.

The phantom was then imaged using a 5 MHz external Elektra ultrasound system, as shown in Fig. 1c. The ultrasound image clearly shows the low-scatter cylindrical "prostate" gelatin, which is surrounded by the high-scatter "pelvis" agarose. Thus, we have demonstrated our ability to construct and image a custom PET-ultrasound phantom. However, the phantom's mechanical and ultrasound properties did not have long-term stability, especially at room temperature. For instance, this phantom (without preservative) was invaded by fungus and bacteria within about a month even when stored in a refrigerator.

III. PET-TRUS-CT-MRI PHANTOMS

Methods for ultrasound phantom construction are well represented in literature [1-5]. Since the phantom described in Section II did not have long-term stability at room temperature, we needed to develop a different phantom construction process. We therefore constructed a multi-modality phantom using tissue mimicking mixtures of agar, gelatin, $CuCl_2$-$2H_2O$, EDTA-tetra Na Hydrate, NaCl, HCHO, Germall-Plus^{TM}, glass beads, $BaSO_4$, and deionized water (Table I). Similar agar-gelatin mixtures were proven to have stable mechanical, ultrasound and MRI properties for at least one year [5]. These agar-gelatin-based tissue mimicking materials were mixed with radioactive solutions (with a drop of food coloring). When developing the procedures for this phantom construction, we used short-lived radioactive ^{18}F-water and a small amount of non-radioactive 0.5M HCl. Once the phantom construction procedures were finalized, we used long-lived $^{68}GeCl_4$ radioactivity (271 day half-life) in a 0.5M HCl solution to allow repeated PET imaging of the same phantom. The main purpose of these custom PET-TRUS-CT-MRI phantoms are to develop radioactive TMMs that both approximate the acoustical properties of patients more accurately and have improved long-term stability at room temperature than those developed in Section II.

We constructed two-region PET-TRUS-CT-MRI phantoms with a "prostate" tapered cylinder within a "pelvis" rectangular cuboid. The "pelvis" has outer dimensions of 15 cm x 15 cm x 7.5 cm. The "prostate" is 7 cm deep with a tapering diameter ranging from 5 to 3 cm. We first filled the

"pelvis" cubic container with the "Pelvis TMM" (Table I), creating two voids with petrolatum-coated plastic rods. A small 2.5 cm diameter cylindrical rod was used to create a hole for the TRUS imaging probe. A larger rod with a tapered end was used to create a void for the "prostate." Once the "pelvis" hardened, we removed both rods. We then filled the tapered cylindrical void with a "Prostate TMM" (Table I), having different multi-modality properties and ^{18}F or ^{68}Ge activity concentrations than the "pelvis." Both TMMs were hardened at room temperature. Theses phantoms are stored with a thin layer of safflower oil on top to minimize dehydration and shrinkage. Fig. 2 shows a photograph of a custom PET-TRUS-CT-MRI phantom.

	Agar	Gelatin	$CuCl_2$-$2H_2O$	EDTA	NaCl	HCHO	Germall-Plus	Glass Beads	$BaSO_4$
Pelvis TMM	1.17	5.52	0.11	0.33	0.77	0.24	1.45	4.4	0.50
Prostate TMM	3.64	5.70	0.12	0.34	0.80	0.25	1.50	0	0

Table I. Dry-weight percents of the various components in the PET-TRUS-CT-MRI custom phantom. The remaining weight percent is deionized water.

Table I outlines the dry-weight percentages of the materials used to construct the "Prostate TMM" and "Pelvis TMM" of the custom PET-TRUS-CT-MRI phantoms. For initial tests, only the "Prostate TMM" was mixed with ^{18}F-water due to the time required for gel hardening. For the final phantom, both TMM regions were mixed with $^{68}GeCl_4$ solution. The primary role of each ingredient is summarized below:

- *Agar*: concentration set to achieve tissue-like ultrasound properties, such as ultrasound propagation speed. Higher agar concentration also produces shorter longitudinal (T_1) and transverse (T_2) MRI relaxation times.
- *Gelatin*: concentration set for tissue-like ultrasound properties, such as ultrasound propagation speed. Concentration must be roughly the same for "prostate" and "pelvis" regions to avoid changes in volumes due to osmosis.
- *$CuCl_2$-$2H_2O$* and *EDTA-tetra Na Hydrate*: EDTA forms chelate with the Cu^{2+} ions to allow Cu^{2+} to remain mobile, allowing controlled lowering of the T_1 MRI relaxation time.
- *NaCl*: anti-bacterial agent that also produces tissue-like MRI coil loading.
- *HCHO* (37% formaldehyde): cross-links the gelatin, raising the melting point to 78 °C where the agar component melts.
- *Germall-Plus*^{TM}: preservative to prevent fungal and bacterial invasion.
- *Glass Beads* (20 μm average diameter): increases ultrasound attenuation and backscatter to tissue-like levels. Also shortens T_1 and T_2 MRI relaxation times.
- *$BaSO_4$*: increases radiographic attenuation for CT imaging.
- *^{18}F-water or $^{68}GeCl_4$*: 511 keV radioactivity for PET imaging.

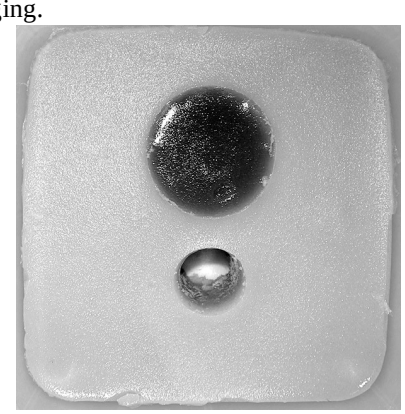

Fig. 2. Photograph of a custom PET-TRUS-CT-MRI phantom. The square "pelvis" has outer dimensions of 15 cm x 15 cm. The tapered cylindrical "prostate" is seen as a 5 cm diameter dark circle (the diameter of the cylinder tapers, decreasing from 5 cm to 3 cm towards the container bottom). The hole for transrectal ultrasound imaging (seen directly below the dark "prostate" circle) has a diameter of 2.5 cm.

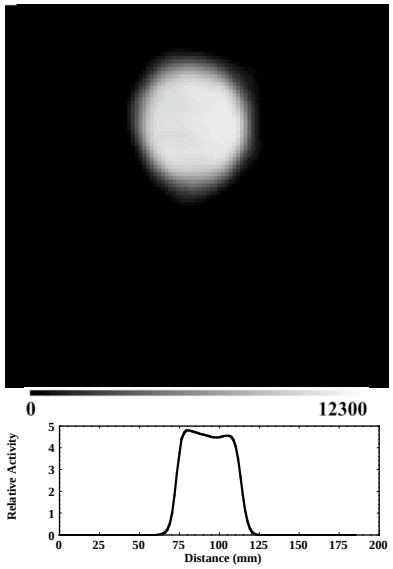

Fig. 3. Reconstructed coronal PET image of a custom PET-TRUS-CT-MRI phantom using ^{18}F (in the "prostate" only). The white circle shows the uniform ^{18}F activity in the "prostate." The ^{18}F initial activity density was 0.33 μCi/ml. Voxel size is 1.47 mm x 1.47 mm x 3.125 mm. Horizontal profile through the "prostate" center is also shown.

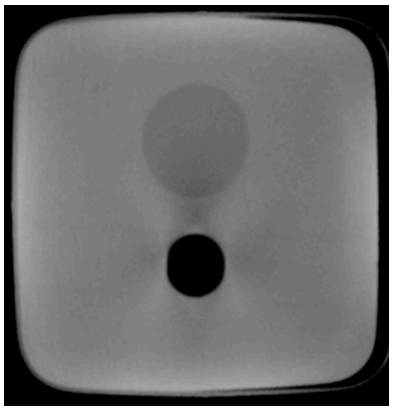

Fig. 4. Reconstructed coronal x-ray CT image of the phantom with 1 mm axial thick slices. The pixel size is 0.5 mm x 0.5 mm x 1 mm. The dark gray

circle shows lower radiographic attenuation in the "prostate" compared with the surrounding light gray higher-attenuation "pelvis." The black circle shows a hole used for the TRUS imaging probe.

(a)

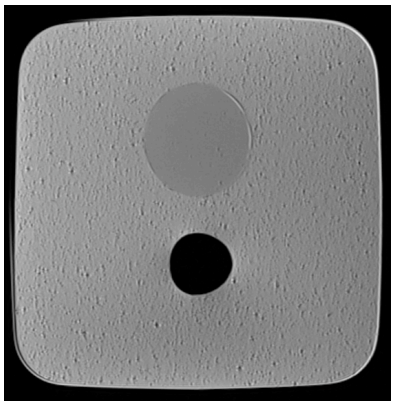

(b)

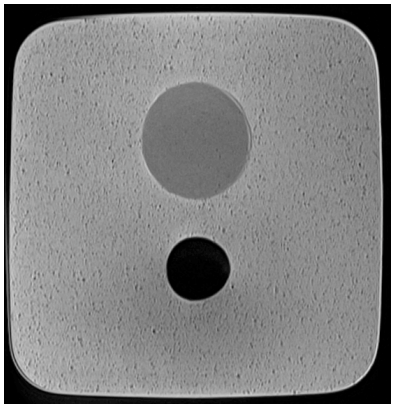

Fig. 5. (a) Reconstructed coronal MRI T_1–weighted image of the custom PET-TRUS-CT-MRI phantom, representing 60 minutes of data. Voxel size is 0.4 mm x 0.4 mm x 3 mm. The dark gray circle shows the longer T_1 "prostate" surrounded by the shorter T_1 "pelvis." (b) Reconstructed coronal MRI T_2–weighted image of the phantom, representing 50 minutes of data. Voxel size is 0.4 mm x 0.4 mm x 3 mm.

The expected ultrasound properties include a propagation speed of about 1534 m/s, a density of about 1.04 g/ml, and an attenuation coefficient divided by frequency of about 0.14 dB/cm/MHz for the "Prostate TMM" and 0.38 dB/cm/MHz for the "Pelvis TMM." The MRI T_1 relaxation times are expected to be about 494 ms for the "Prostate TMM" and 423 ms for the "Pelvis TMM." The MRI T_2 relaxation times are expected to be approximately 58 ms [5]. The CT number is expected to be about 50 HU for the "Prostate TMM" and about 140 HU for the "Pelvis TMM."

A custom PET-TRUS-CT-MRI phantom, using ^{18}F–water in only the "prostate," was imaged with PET, CT and MRI. Using an EXACT HR PET scanner, PET data were acquired with a 60 minute emission scan in 3D mode and 10 minute transmission scan. At the start of the emission scan, the ^{18}F activity density was 0.33 μCi/ml in the prostate. Image reconstruction was performed with attenuation and scatter correction. Fig. 3 shows a reconstructed coronal PET image of the phantom with uniform ^{18}F activity in the "prostate," as well as a horizontal profile through the "prostate" center.

The phantom was imaged with a Nucletron KV ConeBeam CT scanner (100 keV; 16 mAmps) after the ^{18}F decayed. Reconstruction was performed with a proprietary SmartScatter algorithm using a Cone-Beam CT wedge filter. Fig. 4 shows a reconstructed coronal CT image of the phantom with increased radiographic attenuation in the "pelvis" due to the $BaSO_4$.

After the ^{18}F decayed, the phantom was also imaged with an 1.5 T Avanto Siemens MRI scanner using a head coil with a T_1-weighted 2D spin echo pulse sequence (TE = 7.8 msec; TR = 500 msec; field of view = 230 mm x 230 mm x 3 mm; voxel size = 0.4 mm x 0.4 mm x 3 mm). Fig. 5a shows a reconstructed T_1-weighted MRI image with a darker "prostate" representing a longer T_1 compared to the "pelvis." The glass beads (used for ultrasound imaging) shortened the T_1 in the "pelvis" despite having a lower agar concentration. The phantom was also imaged with a T_2-weighted 2D turbo spin echo pulse sequence (TE = 89 msec; TR = 5590 msec; field of view = 230 mm x 230 mm x 3 mm; voxel size = 0.4 mm x 0.4 mm x 3 mm). Fig. 5b shows a reconstructed T_2-weighted MRI image with a darker "prostate" representing a shorter T_2 compared to the "pelvis."

(a)

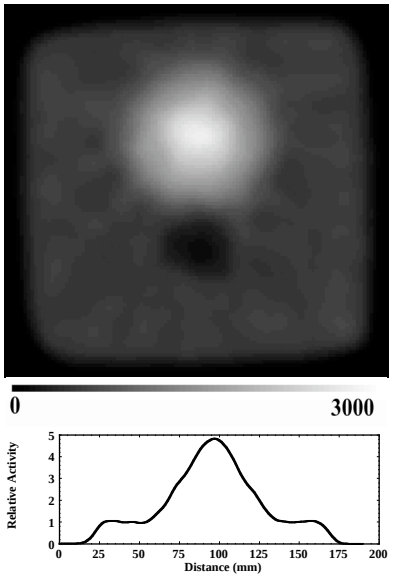

(b)

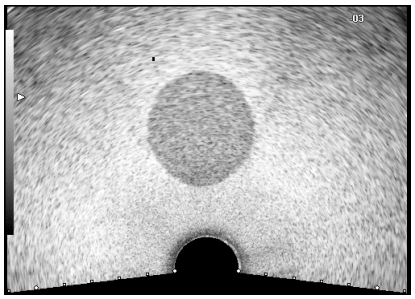

Fig. 6. (a) Reconstructed coronal PET image of a custom PET-TRUS-CT-MRI phantom using ^{68}Ge. The white circle shows the higher ^{68}Ge activity in the "prostate" within the dark gray low ^{68}Ge activity in the "pelvis." The ^{68}Ge activity density was 0.73 μCi/ml in the "prostate" and 0.12 μCi/ml in the "pelvis" during initial construction. Voxel size is 1.47 mm x 1.47 mm x 3.125 mm. Horizontal profile through the "prostate" center is also shown. (b) Ultrasound image of the phantom. The dark gray circle shows the lower-scatter "prostate," directly above the black circular hole used for the TRUS probe. The surrounding light gray background shows the higher-scatter "pelvis."

A custom PET-TRUS-CT-MRI phantom using $^{68}GeCl_4$ in a 0.5M HCl solution was also constructed. The phantom gel is inside a plastic cubic box with a lid that has a hole for TRUS imaging access. In order to prevent ^{68}Ge-gel pieces from escaping during TRUS imaging, a condom is used to seal the hole. (The condom base is fixed around a centering ring on top of the container lid. The condom is held in place using a small washer inside the condom tip and a magnet outside the bottom of the plastic container.) At the time of the phantom construction, the ^{68}Ge activity density was 0.73 μCi/ml in the "prostate" and 0.12 μCi/ml in the "pelvis."

This custom phantom was imaged using an EXACT HR PET scanner 30 hours after phantom construction. PET data were acquired with a 3D emission scan followed by a 10 minute transmission scan. Iterative image reconstruction was performed with attenuation and scatter correction. Fig. 6a shows a reconstructed coronal PET image of the phantom, as well as a horizontal profile through the "prostate" center. The ^{68}Ge activity density was six times higher in the "prostate" than the "pelvis." The ^{68}Ge activity in the "prostate" is clearly visible within the "pelvis" background. However, the "prostate" radioactivity in the PET image has a blurrier edge in this case (*e.g.*, compared to Fig. 1b), and the relative activity shown in the profile is only 4.8 ("prostate") to 1 ("pelvis"). This is probably due to the initial migration of the ^{68}Ge tetrachloride molecules, which is discussed in detail in Section IV. This assumption is supported by the uniform radioactivity seen in the PET image of the previously discussed PET-TRUS-CT-MRI phantom constructed with ^{18}F-water (Fig. 3).

The phantom was also imaged with a Hitachi Hi-Vision 5500 digital ultrasound system, using a B mode bi-plane TRUS probe in a linear stepper. Fig. 6b shows a transrectal ultrasound image of the phantom with a lower-scatter "prostate" surrounded by a higher-scatter "pelvis."

IV. Discussion

We intended to use this custom PET-TRUS-CT-MRI phantom repeatedly over a year. However, the ^{68}Ge tetrachloride molecules in the "prostate" migrated into the "pelvis" to become roughly uniformly distributed throughout the phantom in less than 57 days. We believe that the ^{68}Ge tetrachloride molecules were small enough to penetrate the gel pores, slowly reaching an equilibrium in radioactive concentration throughout the "prostate" and "pelvis." We should be able to prevent this $^{68}GeCl_4$ migration by using a barrier, such as a female latex condom, between the "prostate" and "pelvis" so the radioactivity instead reaches an uniform equilibrium within the "prostate" and "pelvis" separately.

Other tissue mimicking materials could also be used for PET-US phantom construction. Typical ultrasound TMMs include agar, Zerdine™, urethanes, epoxies, liquids and natural materials. There are three ultrasound TMMs commercially available: Zerdine™ from CIRs Inc., condensed-milk-based gel from Gammax RMI, and urethane-rubber-based material from ATS Labs. Alternative PET-US phantom construction could utilize radioactive water in condensed milk-agar-based mixtures [2] or poly(vinyl alcohol) cryogels [4]. However, $^{68}GeCl_4$ migration is still expected for these alternative TMMs (due to the relative size of the $^{68}GeCl_4$ molecule), so a mechanical barrier would still be necessary.

We investigated the construction of a PET-TRUS-CT-MRI prostate phantom with a more realistic geometry, using the agar-gelatin mixtures from Section III. The phantom would have structures simulating the prostate, rectal wall and urethra in a background gel with an opening for the TRUS probe (Fig. 7). The urethra is routinely simulated by filling a tube with ultrasound gel with some air bubbles. Since this PET-TRUS prostate phantom would be used only to validate image co-registration, the phantom would not have to exactly mimic the PET and TRUS properties of the prostate region.

(a) Top View:

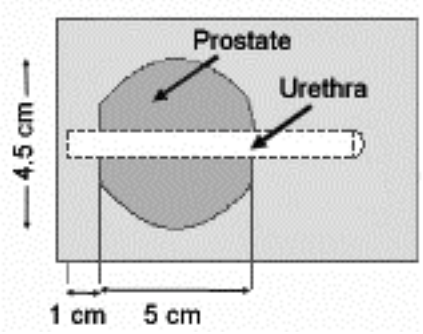

(b) Side View:

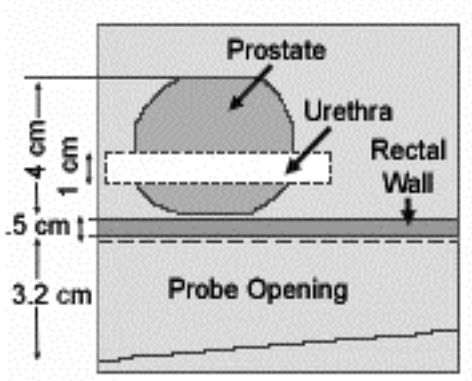

Fig. 7. Design drawing of a PET-TRUS-CT-MRI prostate phantom with more realistic geometry. The phantom structures simulate the prostate, rectal wall and urethra in a background gel with an opening for the TRUS probe.

V. Conclusions

We have successfully developed multi-modality phantoms, including PET-TRUS-CT-MRI phantoms with two regions distinguishable by all four imaging modalities and long-term stability at room temperature. These phantoms had a relatively simple geometry, as their main purpose was to validate image co-registration for PET and TRUS prostate imaging. Long-lived ^{68}Ge was used to allow repeated imaging, but the long-term use of the phantom for PET imaging was unsuccessful due to migration of the $^{68}GeCl_4$ molecules; thus a mechanical barrier between the "prostate" and "pelvis" is required. Based on repeated imaging results, these phantoms appear to have long-term stability otherwise (*i.e.*, except for the $^{68}GeCl_4$ migration). The mechanical properties also appear stable and

there are no signs of bacterial or fungal invasion, when stored at room temperature for over six months.

VI. References

[1] C. L. de Korte, E. I. Cespedes, A. F. W. van der Steen, B. Norder and K. Te Nijenhuis, "Elastic and Acoustic Properties of Vessel Mimicking Material for Elasticity Imaging," *Ultrason. Imaging*, vol. 19, pp. 112-126, 1997.

[2] W. D. D'Souza, E. L. Madsen, O. Unal, K. V. Vigen, G. R. Frank, et al., "Tissue mimicking materials for a multi-imaging modality prostate phantom," *Med. Phys.*, vol. 28, pp. 688-700, 2001.

[3] J. E. Browne, K. V. Ramnarine, A. J. Watson and P. R. Hoskins, "Assessment of the acoustic properties of common tissue-mimicking test phantoms," *Ultrasound Med. Biol.*, vol. 29, pp. 1053-1060, 2003.

[4] K. J. M. Surry, H. J. B. Austin, A. Fenster and T. M. Peters, "Poly(vinyl alcohol) cryogel phantoms for use in ultrasound and MR imaging," *Phys Med Biol*, vol. 49, pp. 5529-5546, 2004.

[5] E. L. Madsen, M. A. Hobson, S. Hairong, T. Varghese and G. R. Frank, "Tissue-mimicking agar/gelatin material for use in heterogeneous elastography phantoms," *Phys. Med. Biol.*, vol. 50, pp. 5597-5618, 2005.

Co-registration for Dual PET-Transrectal Ultrasound (PET-TRUS) Prostate Imaging

Inventors: J. S. Huber, W. W. Moses, J. Pouliot, I-Chow Hsu, Qiyu Peng, Ronald H. Huesman and Thomas F. Budinger

CROSS REFERENCE TO RELATED APPLICATIONS

[001] This application claims priority to U.S. Provisional Patent Application No. 60/939,051, filed on May 19, 2008, herein incorporated by reference in its entirety.

STATEMENT OF GOVERNMENTAL SUPPORT

[002] This invention was made during work supported in part under Contract No. DE-AC02-05CH11231 awarded by the Office of Biological and Environmental Research, Medical Science Division, U.S. Department of Energy, in part under grant numbers DAMD17-02-1-0081 and W81XWH-07-1-0020 awarded by the Department of Defense, in part under grant numbers R01-EB-00194 and R01-HL-071253 awarded by the National Institute for Biomedical Imaging and Bioengineering,. The government has certain rights in this invention.

BACKGROUND OF THE INVENTION

FIELD OF THE INVENTION

[003] The present invention relates to multi-modality positron emission tomograph-ultrasound imaging for prostate cancer detection and therapy.

RELATED ART

[004] More than half of all malignant prostate tumors detected today are not palpable, and prostate specific antigen and digital rectal exam screenings have high false-positive rates in general clinical practice. In addition, the diagnostic accuracy of biopsy is problematic. A new imaging technology is needed for sensitive detection of prostate cancer to confirm diagnosis, guide biopsy and help guide treatment decisions. Administration of multiple courses of a therapy is often needed before a clear indication of response or progression can be determined, so an improved prostate imaging technique is also needed to monitor response to therapy, assess the efficacy of new treatments and detect local recurrence sooner.

[005] We believe that positron emission tomography (PET) can meet many of these needs, because newly developed PET radiopharmaceuticals (such as [^{11}C]choline) have demonstrated outstanding results in the sensitive detection of prostate cancer. Functional PET imaging with [^{11}C]choline detects malignant tumors and helps determine the tumor "aggressiveness," but few other anatomical features are visible in the PET images.

[006] Prostate cancer imaging with radiopharmaceuticals has used three types of instruments: (1) gamma camera scanning using ^{99m}Tc bone agents, (2) single photon emission tomography (SPECT) using ^{111}In-labeled monoclonal antibodies or ^{99m}Tc-labeled peptides, and (3) positron emission tomography (PET) using [^{18}F]fluorodeoxyglucose (FDG), [^{11}C]methionine, [^{11}C]choline, [^{11}C]acetate, or [^{18}F]fluorocholine. ProstaScint™ is an ^{111}In-labeled murine monoclonal antibody directed against prostate specific membrane antigen. The acquisition and interpretation of the ProstaScint™ images are technically demanding due to radiopharmaceutical uptake by background organs. The reported sensitivity and specificity of ProstaScint™ imaging for detection of pelvic lymph node metastases is only 62% and 72%, respectively [M. K. Haseman, "Capromab pendetide imaging of occult lymph node metastases," *J Nucl Med*, vol. 39, pp. 653, 1998]. Despite these problems, ProstaScint™ imaging is superior to PET imaging with FDG in predicting the presence of prostate cancer [M. K. Haseman, N. L. Reed, and S. A. Rosenthal, "Monoclonal antibody imaging of occult prostate cancer in patients with elevated prostate-specific antigen. Positron emission tomography and biopsy correlation," *Clin Nucl Med*, vol. 21, pp. 704-13, 1996], particularly for less aggressive disease [P. F. Faulhaber, D. B. Sodee, E. Echt and J. K. O'Donnell, "Staging of Prostate Adenocarcinoma, comparison of FDG Dedicated PET and In-111 Capromab Pendetide," *J Nucl Med*, vol. 41, pp. 116 (abstract), 2000]. While PET has higher sensitivity and spatial resolution than SPECT, FDG is not very prostate specific and bladder accumulation of radioactivity often obscures prostate tumors [E. R. Sigurdson and A. M. Cohen, "Commentary on the applications of PET in clinical oncology," *J. Nucl. Med.*, vol. 32, pp. 649-650, 1991]. Fortunately, newly developed PET radiopharmaceuticals have recently demonstrated outstanding results in the sensitive detection of prostate cancer. Hara and co-workers find that: [^{11}C]choline clears the blood quickly; its uptake in prostate tumors provides excellent tumor/normal contrast; and bladder accumulation is minimal [T. Hara, N. Kosaka, and H. Kishi, "PET imaging of prostate cancer using carbon-11-choline," *J Nucl Med*, vol. 39, pp. 990-5, 1998]. Therefore, [^{11}C]choline is an extremely

attractive PET tracer for imaging prostate tumors [See for example, M. Picchio, C. Messa, C. Landoni, L. Gianolli, S. Sironi, et al., "Value of [11C]choline-positron emission tomography for re-staging prostate cancer: a comparison with [18F]fluorodeoxyglucose-positron emission tomography," *J Urol.*, vol. 169, pp. 1337-1340, 2003]. Figure 2 shows a [^{11}C]choline image of prostate cancer before and after therapy, demonstrating the ability to detect prostate carcinoma and follow therapy efficacy using [^{11}C]choline. Several other radiopharmaceuticals are also currently under investigation for prostate cancer imaging, including [^{11}C]acetate [E. Fricke, S. Machtens, M. Hofmann, J. Van Den Hoff, S. Bergh, et al., "Positron emission tomography with 11C-acetate and 18F-FDG in prostate cancer patients," *Eur J Nucl Med Mol Imaging*, vol. 30, pp. 607-610, 2003], [^{11}C]methionine [G. Toth, Z. Lengyel, L. Balkay, M. A. Salah, L. Tron, et al., "Detection of prostate cancer with 11C-methionine positron emission tomography," *J. Urol.*, vol. 173(1), pp. 66-69, 2005], and [^{18}F]fluorocholine [T. R. Degrado, R. E. Coleman, S. Wang, S. W. Baldwin, M. D. Orr, et al., "Synthesis and Evaluation of F18-labeled Choline as an Oncologic Tracer for Positron Emission Tomography: Initial Findings in Prostate Cancer," *Cancer Research*, vol. 61(1), pp. 110-117, 2001, T. R. Degrado, S. W. Baldwin, S. Wang, M. D. Orr, R. P. Liao, et al., "Synthesis and Evaluation of F18-Labeled Choline Analogs as Oncologic PET Tracers," *J. Nuc. Med.*, vol. 42, pp. 1805-1814, 2001].

[007] Transrectal ultrasound (TRUS) imaging identifies lesions but some are not cancerous. By accurately co-registering the sensitive functional information from PET imaging with the high resolution anatomical detail from TRUS imaging, dual PET-TRUS prostate imaging can accurately localize prostate cancer. The co-registered PET and TRUS images can then accurately guide subsequent diagnosis and treatment procedures. We discussed the possibility of combining PET and TRUS previously in Huber, J.S.; Moses, W.W.; Pouliot, J.; Hsu, I.C.; Dual-modality PET/ultrasound imaging of the prostate, *Nuclear Science Symposium Conference Record, 2005, IEEE*, Volume 4, 23-29 Oct. 2005 Page(s):2187 – 2190, herein incorporated by reference. Herein, we describe the methods and tools for acquiring accurately co-registered PET and TRUS images, as well as the construction and use of PET-TRUS prostate phantoms.

BRIEF SUMMARY OF THE INVENTION

[008] The present invention provides a method for accurate co-registration for dual-modality positron emission tomography (PET) and transrectal ultrasound (TRUS) imaging for prostate cancer, comprising the steps of: (1) providing a PET-TRUS system comprising a PET

scanner having a patient table with a TRUS probe attached to the table through a TRUS calibrated linear stepper-arm assembly (with a holder with 511 keV point sources mounted onto the TRUS stepper); (2) inserting the rectal probe into the patient; (3) acquiring TRUS image data of the prostate stepwise from base to apex; (4) positioning axially the TRUS probe tip at the prostate center using the TRUS stepper; (5) moving the patient bed to position the 511 keV point sources near the PET-center, (6) acquiring PET point source data and analyzing it; (7) moving the patient table to position the prostate of a patient near the PET-center; (8) injecting a 511 keV radiopharmaceutical into the patient; (9) acquiring PET image patient data; (10) 2D contouring the TRUS data and reconstructing a 3D TRUS image of the prostate region; (11) 3D reconstructing the PET data; and (12) accurately superimposing the PET and TRUS images; thus resulting in PET-TRUS images of the patient's prostate region showing anatomical and functional detail for precise localization of any prostate cancer.

[009] In a preferred embodiment, a point source holder, mounted onto the TRUS stepper, places two 511 keV ^{68}Ge (<50 μCi) point sources along the axial line of the TRUS probe at a known location from the TRUS probe tip. In a preferred embodiment, the radiopharmaceutical injected in the patient is [^{11}C]choline.

[010] A multi-modality prostate phantom comprising a rigid container comprising a structure simulating an inner cylindrical and spherical prostate region within an outer rectangular pelvic region, said structure comprised of tissue mimicking mixtures and deionized radioactive water. In one embodiment, the tissue mimicking mixture as set forth in Table I.

[011] In another embodiment, the multi-modality prostate phantom structures simulating the rectum, rectal wall and urethra in a background gel with an opening for the TRUS probe. The urethra can be simulated by filling a tube with ultrasound gel and air bubbles.

BRIEF DESCRIPTION OF THE DRAWINGS

[012] **Figure 1.** Outline of current and future plans for dual PET-TRUS imaging. We acquire and co-register PET and TRUS images that are taken during the same patient exam. A simulated "merged PET-TRUS image" (shown in the center) represents the goal for each patient imaged. In the future, these co-registered PET and TRUS images will be used to guide subsequent diagnosis and treatment procedures.

[013] **Figure 2.** [^{11}C]choline image of prostate cancer before and after treatment. These color images indicate a high (red) uptake in the prostate cancer compared to a low (blue) uptake elsewhere**.** Images provided by Hara and co-workers [*J Nucl Med*, vol. 39, pp. 990-5, 1998].

[014] **Figure 3.** (a) Photograph of a partially-assembled prostate-optimized PET scanner with the lead shielding on one side removed and a single axial row of detector modules visible. The individual detector modules are angled to point towards the center of the scanner (where the prostate will be positioned). (b) Photograph of the completed scanner with a person in position on the patient table. The detector banks can be tilted to accommodate a patient′s bent knees if necessary.

[015] **Figure 4.** Transrectal ultrasound system with the probe inserted in a patient, a 2D TRUS image with grid, and contours from a 3D TRUS reconstruction.

[016] **Figure 5.** (a) Drawing of a modified TRUS probe-stepper-point source unit. The two point sources on the TRUS stepper are used for patient positioning. All three point sources are used for image co-registration. (b) Photograph of the dual PET-TRUS system including prostate-optimized PET scanner, patient table, TRUS stabilizer arm, TRUS modified stepper, TRUS ultrasound probe, and point source holder (with two ^{68}Ge point sources mounted parallel to the TRUS probe axis).

[017] **Figure 6.** (a) Ultrasound images of the prostate region taken for brachytherapy treatment planning. (b) 3D view of a prostate (yellow contours), penis bulb (burgundy), bladder (beige), rectum (pink) and urethra (yellow brown). The prostate and urethra contours were measured using TRUS, and the other contours were measured with CT. The turquoise area was defined by MR-spectroscopy as a dominant intraprostatic cancer lesion.

[018] **Figure 7.** CIRS Model 58 ultrasound prostate training phantom.

[019] **Figure 8.** Design drawing of a realistic custom TRUS-PET prostate phantom. Phantom has structures simulating the prostate, rectal wall and urethra in a background gel with an opening for the TRUS probe.

[020] **Figure 9.** (a) Reconstructed image of 37-line source phantom (each 5 cm in axial direction). In the transverse plane, single line sources are 2, 4, 6, and 8 cm from the central line. Clusters of four line sources are placed radially at 4 and 8 cm from the central line. The four line sources in each cluster are spaced 8, 6, 5, and 4 mm apart (clockwise from the 8 mm labeled clusters). Phantom was filled with ^{18}F at an initial activity of 0.8 mCi and imaged for 2 hours.

Phantom was centered in the PET scanner. Image represents 45 M counts. Voxel size equals 2 mm x 2 mm x 2 mm. (b) Modified NEMA ["Performance Measurements of Positron Emission Tomographs," National Electrical Manufacturers Association (NEMA) Report No., 2001] body phantom. Six spheres are placed on a 12 cm diameter in the transaxial plane (37, 28, 22, 17, 13, and 10 mm sphere diameters), and a 28 mm diameter sphere is placed in the center. All seven spheres have a common axial center line. (c) Reconstructed images (central slices) of the modified body phantom, which was centered in the PET scanner. Initial ^{18}F activity density was 1.1 μCi/ml in five spheres (shown in white) and 0.12 μCi/ml in background torso.

[021] **Figure 10.** (a) Photograph of a simple PET-ultrasound phantom. The blue-colored agarose has outer dimensions of 16 cm x 11 cm x 3.5 cm. The yellow-colored gelatin cylinder has a 5 cm diameter. (b) Reconstructed coronal PET image of the PET-ultrasound phantom. The circle shows the high uniform ^{18}F activity concentration in the prostate region, and the rectangle shows the low uniform ^{18}F activity concentration in the background pelvis region. Image represents 636 M counts (*i.e.,* 20 minutes of data). The voxel size is 1.47 mm x 1.47 mm x 3.13 mm. (c) Ultrasound image of the same phantom using an external 5MHz ultrasound probe. The dark gray circle shows the lower-scatter gelatin prostate, and the surrounding light gray background shows the high-scatter agarose pelvis.

Figure 11. (a) Photograph of a custom PET-US-CT-MRI phantom. The aqua-colored rectangular pelvis has outer dimensions of 16 cm x 11 cm x 3.5 cm. The dark green-colored cylindrical prostate has a 5 cm diameter and 2.5 cm depth (*i.e.* inner cylinder does not go all the way through). (b) Reconstructed coronal PET image of the custom PET-US-CT-MRI phantom. The colored circle shows the ^{18}F activity in the prostate region; the ^{18}F activity density was 0.8 μCi/ml in the prostate at the start of the 60 minute emission scan. Voxel size is 3.6 mm x 3.6 mm x 4 mm. (c) Ultrasound image of the phantom using a 5 MHz external ultrasound probe. The dark gray circle shows the lower-scatter prostate, and the surrounding gray background shows the higher-scatter pelvis. (d) Reconstructed coronal x-ray CT image of the phantom with 1 cm axial thick slices. The pixel size is 1 mm x 1 mm x 10 mm. The dark gray circle shows lower radiographic attenuation in the prostate compared with the surrounding light gray higher-attenuation pelvis. (e) Reconstructed coronal MRI T_1–weighted image of the custom PET-US-CT-MRI phantom, representing 60 minutes of data. Voxel size is 0.4 mm x 0.4 mm x 3 mm. The dark gray circle shows the longer T_1 prostate surrounded by the shorter T1 pelvis. (f)

Reconstructed coronal MRI T_2–weighted image of the phantom, representing 60 minutes of data. Voxel size is 0.4 mm x 0.4 mm x 3 mm. (g) Fused PET (color) and TRUS (grayscale) coronal image.

DETAILED DESCRIPTION OF THE PREFERRED EMBODIMENT

[022] Multi-modality imaging has an increasing role in the diagnosis and treatment of a large number of diseases, particularly if both functional and anatomical information is acquired and accurately co-registered. Although PET-CT has recently revolutionized the role of imaging in diagnosis and treatment for many kinds of cancer, ultrasound is the preferred imaging technology for many diseases such as prostate cancer. Since transrectal ultrasound imaging is an integral part of diagnosis and treatment for prostate cancer, we describe a dual imaging system that will acquire PET and TRUS data during the same patient imaging session and accurately co-register the images. To validate our methods, we also describe the construction and use of novel custom PET-TRUS prostate phantoms.

[023] Dual PET-TRUS prostate imaging acquires PET images (to provide sensitive functional information) and transrectal ultrasound images (to give high resolution, 3D volumetric anatomical detail) sequentially during the same patient imaging session, using methods that allow the PET and TRUS images to be accurately co-registered. This combined PET-TRUS system with a single patient table for sequential acquisition of PET and TRUS images helps overcome alignment problems due to internal organ movement, variations in patient table profile, and positioning of the patient for the scan. Dual PET-TRUS imaging will help locate increased metabolic activity (i.e., cancer) within the prostate region. This dual prostate imaging should help confirm initial diagnosis, guide biopsy, guide treatment decisions, monitor response to therapy, and detect local reoccurrence. Ultimately it should provide better detection and treatment of prostate cancer. Figure 1 shows the general motivation behind dual PET-TRUS imaging. A simulated “merged PET-TRUS image” (shown in the center) represents the goal for each patient imaged. Figure 1 also outlines some possible applications for dual PET-TRUS imaging. Dual positron emission tomography and transrectal ultrasound prostate imaging has not been done previously.

[024] PET is fundamentally different than most imaging technologies commonly used for prostate cancer detection, because PET is based on function (*e.g.*, whether or not a

radiopharmaceutical is taken up by the prostate tumors) rather than anatomical structure (*e.g.*, whether or not a tumor mass is observed using X-ray computed tomography or transrectal ultrasound). Our dual PET-TRUS prostate imaging tools and methods may be applied to whole-body PET scanners using positron-emitting tracers, including but not limited to, PET radiopharmaceuticals such as, [^{11}C]choline, [^{18}F]fluorodeoxyglucose (FDG), [^{11}C]methionine, [^{11}C]choline, [^{11}C]acetate, or [^{18}F]fluorocholine.

[025] PET imaging is especially useful for prostate imaging because functional PET imaging will detect malignant tumors in the prostate region, as well as help determine tumor "aggressiveness" based on metabolic uptake levels. Although some scanners are not optimized to detect distant metastatic disease, in a preferred embodiment, the PET scanner used should also be able to image local spread beyond the prostate bed. Figure 2 shows a [^{11}C]choline image of prostate cancer before and after therapy, demonstrating the ability to detect prostate carcinoma and follow therapy efficacy using choline.

[026] However, Figure 2 also shows that the relative uptake in a tumor can be so great that few other anatomical landmarks are visible in the PET images. PET imaging is therefore greatly enhanced if its functional information is fused with anatomical information. Transrectal ultrasound imaging provides high resolution anatomical detail in the prostate region that can be co-registered with the sensitive functional information from PET imaging. TRUS imaging can also be used to help align the patient (with the prostate near the center of the PET scanner), which is important due to the limited axial extent of some PET scanners. Transrectal ultrasound imaging of the prostate is a standard imaging technique widely used for prostate cancer diagnosis, biopsy, treatment planning and brachytherapy seed placement. A TRUS probe is relatively small and the procedure is generally well tolerated by patients. We have chosen transrectal ultrasound over CT to provide localization and anatomical imaging because TRUS is cheaper, does not expose the patient to radiation, and provides outstanding prostate image quality.

[027] It is important to acquire the PET and TRUS data sets during the same imaging session. If PET and TRUS images are taken independently (at different times), the co-registration of the images needs to be based on image features such as body contour. This registration method is difficult and inaccurate, since PET images do not show detailed anatomical features. Acquiring the PET and TRUS prostate images during the same exam is

necessary for the following main reasons: (1) The TRUS probe distorts the soft-tissue anatomy, so the rectal probe needs to be in place during the PET scan; (2) PET prostate images do not show detailed anatomical landmarks and the TRUS probe position is patient dependent, so the position of the TRUS probe (relative to the center of the PET scanner) needs to be determined for each patient; (3) PET scanners have a limited axial extent, so image resolution may be improved if transrectal ultrasound is used to help locate and position the patient's prostate near the center of the PET scanner; (4) It is easier for the patient to have both procedures done together in one appointment. In short, patient positioning and accurate image co-registration require the PET and TRUS images to be sequentially acquired during the same imaging session.

[028] In order to take full advantage of new prostate cancer radiopharmaceuticals, in a preferred embodiment, a prostate-optimized PET scanner is used to image the prostate, such as the high performance positron emission tomograph scanner optimized to image the prostate and described in J. S. Huber, S. E. Derenzo, J. Qi, W. W. Moses, R. H. Huesman, et al., "Conceptual Design of a Compact Positron Tomograph for Prostate Imaging," *IEEE Trans Nucl Sci*, vol. NS-48, pp. 1506-1511, 2001 and J. S. Huber, W. S. Choong, W. W. Moses, J. Qi, J. Hu, et al., "Initial Results of a Positron Tomograph for Prostate Imaging," *IEEE Trans Nucl Sci*, NS-53, pp. 2653-2659 (2006), hereby incorporated by reference and also described in Example 1. Compared with a standard whole-body PET scanner (*e.g.,* the CTI EXACT HR or HR+ and GE Advance), a prostate-optimized PET scanner has comparable sensitivity and resolution, less background, and a lower cost. Performance of the prostate-optimized PET scanner is described in detail in a recent paper, J. S. Huber, W. S. Choong, W. W. Moses, J. Qi, J. Hu, G.C. Wang, D. Wilson, S. Oh, R.H. Huesman, S.E. Derenzo, and T.F. Budinger, "Initial Results of a Positron Tomograph for Prostate Imaging, " IEEE Trans. Nucl. Sci, NS-53, pp. 2653-2659, 2006, herein incorporated by reference .

[029] In other preferred embodiments, known and commercially available PET or PET/CT scanners can be used to carry out dual modality PET-TRUS prostate imaging. Such scanners include but are not limited to those commercially sold by Siemens (e.g., Biograph, ECAT ACCEL, or ECAT EXACT HR+), GE Healthcare (e.g., Discovery PET/CT), and Philips (e.g., CPET, Gemini, or Allegro).

[030] The transrectal ultrasound imaging probe used for the dual PET-TRUS imaging can be acquired commercially. Some commonly used TRUS probes include Hitachi Medical Systems

EUP-U533, Aloka UST-672-5/7.5 and UST-678, and B-K Medical model 8808 and 8658. In one embodiment, the transrectal ultrasound imaging system is a commercially available system, such as the Hitachi Hi Vision 5500. In another embodiment, the TRUS stepper and stabilizer arm assembly is a commercially available stepper and arm assembly, such as the Accucare EXII stepper with micro-touch stabilizer arm. However, modifications to the TRUS stepper-arm assembly are likely required to work in conjunction with a PET scanner and would be appreciated by one having skill in the art.

[031] We first describe a method for positioning a patient's prostate near the center of the PET scanner ("PET-center"). As used herein, by the term, "PET-center," it is meant the center of the imaging volume of a PET scanner. This prostate positioning is particularly important for the prostate-optimized PET scanner, since it has a limited axial extent of 8 cm. In a preferred embodiment, the transrectal ultrasound probe will be rigidly attached to a calibrated linear stepper that allows linear displacement along its axis, as shown in Figure 4. In one embodiment, the calibrated linear stepper that allows displacement along its axis is motorized and the stepper is controlled by computer means. In another embodiment, the linear stepper is controlled manually. In a preferred embodiment, the stepper also has calibrated control (manual or motorized) of the TRUS probe rotational motion. The TRUS equipment is commercially available and may be used in the present invention. For example, the TRUS system used in the present Examples is a Hitachi Hi Vision 5500 with a EUP-U533 bi-plane transrectal transducer probe, Accucare EXII stepper, and micro-touch stabilizer arm, or equivalent.

[032] The TRUS probe is rigidly mounted in a TRUS calibrated linear stepper. This TRUS probe-stepper unit is mounted onto a moveable TRUS stabilizer arm that is rigidly attached to the patient table. The arm moves to allow correct positioning of the TRUS probe in a patient or phantom, then its position is fixed typically using the locking mechanism(s) provided with the commercial TRUS arm or through a fastening means. In a preferred embodiment, the TRUS stabilizer arm position is fixed by tightening a single knob locking mechanism. The patient table is equipped with means of supporting the patient's torso, abdomen, legs and/or feet to prevent movement after the probe has been inserted and positioned.

[033] In one embodiment, three point sources are used to determine the TRUS probe location relative to the PET-center. Two 511 keV PET point sources are placed in a holder that is attached to the TRUS stepper. The two point sources are accurately placed along the axial line of

the TRUS probe at a known location from the TRUS probe tip (Figure 5a). Only these two point sources are needed for prostate positioning. In a preferred embodiment, the point sources are <50μCi ^{68}Ge point sources. A third non-collinear 511 keV PET point source is placed on the rear of the probe to define the probe rotation, and all three point source locations are used for image co-registration. The point sources can be purchased from a commercial vendor (*e.g.*, Isotope Products Laboratories model MMS01).

[034] In another embodiment, an alternate technique is to mechanically restrict one or more dimensions of the TRUS probe-stepper assembly after the probe is inserted into the patient, thus eliminating the need for one of the PET point sources during patient studies. For instance, in the preferred embodiment, the rotation of the TRUS probe is always set to the specific angle of zero rotation using the calibrated rotational control of the TRUS stepper (which is available in addition to the linear stepper control); thus eliminating the need for the third point source on the rear of the TRUS probe.

[035] Another alternate technique would be to develop a TRUS probe assembly that utilizes an articulated arm with multiple angular encoders on it, allowing the absolute spatial resolution of the ultrasound images to be known. This arm would also be used to identify the PET-center in the same coordinates.

[036] In a preferred embodiment, the TRUS probe is attached to a calibrated stepper and a series of 2D TRUS images in the transverse plane (*i.e.,* perpendicular to the probe axis) are taken as the probe is moved in steps past the prostate. The TRUS images are acquired every 2-5 mm from base to apex. The 2D images are then reconstructed to visualize a single 3D volumetric image of the prostate, urethra and rectum wall. Such 3D TRUS images are currently used to determine the prostate volume and calculate dose for brachytherapy planning. In one embodiment, a physical puncture attachment for radiotherapeutic seed implantation is also attached to the TRUS stepper. A virtual grid position, corresponding to the projection of the puncture attachment holes, is projected on the TRUS image to provide localization. Figure 4 shows a drawing of the TRUS unit with the probe inserted in a patient, as well as a 2D transverse ultrasound image with grid and the contours from a 3D reconstruction. In one embodiment, the probe is controlled step-wise using the motorized and computer means. The movement of the probe from base to apex of the prostate can be automated to occur in stepwise distance and timed increments coinciding with the acquisition of a 2D ultrasound image. It is estimated that a

brachytherapist or skilled or trained technician should be able to position the probe in the patient in about 2 minutes, and acquire 10-30 2D ultrasound images (or "slices") in about 3 minutes. No anesthesia is required.

[037] The present TRUS system should provide 3D volumetric images of the prostate. Figure 6a shows TRUS images of the prostate region which were taken for brachytherapy planning to determine the optimal dose and seed distribution. The top left image shows the axial view of an ultrasound image of the prostate, urethra and anterior section of the rectum. The top center and right images show the prostate and urethra which are contoured on each plane from base to apex. The bottom plots show the dose distribution superimposed on an ultrasound image to present the dose delivered to the prostate. Figure 6b shows a 3D reconstructed TRUS image. The prostate and urethra contours were reconstructed from TRUS transverse contours, and the other contours were measured using CT.

[038] In another embodiment, the longitudinal transducer on the TRUS probe is used instead of the transverse transducer. The stepper may have two modes: (1) step linearly along the probe axis or (2) step rotationally around the probe axis. In this case, the TRUS probe is not stepped in the linear direction. Instead, the biplane transrectal ultrasound probe is positioned (to view the entire length of the prostate at once) and rotated in steps, in order to acquire TRUS image data for the entire prostate region. Contouring can still be performed to create a 3D volumetric TRUS image.

[039] Once the TRUS probe is inserted and positioned in the patient (or phantom), the stabilizer arm position is fixed, and the TRUS image data are acquired, then the TRUS probe tip is positioned axially at the center of the prostate using the linear stepper. The patient table is then moved so the point sources are visually positioned near the PET-center with the aid of visible low-powered lasers mounted on the gantry along the minor and major axis of the PET scanner. PET point source data are then acquired for 1-5 minutes, analyzed, and the location of the point sources determined in PET coordinates (i.e., relative to the PET-center). In a preferred embodiment, the data analysis uses a two-iteration expectation-maximization algorithm, with a simplified model of the PET scanner geometry, to quickly reconstruct the data in less than 5 minutes. The resulting PET images are then quickly processed to determine the point source locations in PET coordinates, by determining the brightness-weighted average for each point source in the 3D volumetric PET images. In another embodiment, the data analysis is performed

by rebinning the data into a single 2D sinogram, and determining the point source locations using the sinogram data; no image reconstruction of the point sources is needed for patient positioning for this embodiment.

[040] Once the point source locations are determined in PET coordinates, these locations are represented by two position vectors and vector algebra is used to calculate the location of the TRUS probe tip. Finally, the patient table is then moved to position the TRUS probe tip (i.e., prostate) at the PET-center and patient (or phantom) PET data is acquired. After the prostate is positioned, the point sources can be removed for the remainder of the study or they can be left in place (since they are outside the PET imaging volume and have such low activity that patient dose is trivial).

[041] Thus, in the general method, the probe is inserted into the patient, the TRUS imaging is done, the patient table is moved to acquire and analyze point source PET data, the patient table is moved to locate the patient's prostate near the PET-center, then PET imaging of the patient is performed. In a preferred embodiment, a method for accurate co-registration for dual-modality positron emission tomography and transrectal ultrasound imaging for prostate cancer, comprises the steps of: providing a PET-TRUS system comprising a PET scanner having a patient table with a TRUS probe attached to the table through a TRUS calibrated linear stepper-arm assembly (with a holder with 511 keV point sources mounted onto the TRUS stepper); inserting the rectal probe into the patient; acquiring TRUS image data of the prostate stepwise from base to apex; positioning axially the TRUS probe tip at the prostate center using the TRUS stepper; moving the patient bed to position the 511 keV point sources near the PET-center, acquiring PET data and analyzing it; moving the patient table to position a patient’s prostate near the PET-center; injecting a 511 keV PET radiopharmaceutical into the patient; acquiring PET image patient data; 2D contouring the TRUS data and reconstructing a 3D TRUS image of the prostate region; 3D reconstructing the PET data; and accurately superimposing the PET and TRUS images; thus resulting in PET-TRUS images of the patient’s prostate region showing anatomical and functional detail for precise localization of any prostate cancer.

[042] The TRUS probe will remain in the patient during the PET imaging to minimize organ motion. The TRUS prostate images will be exported (e.g. in BMP or TIFF format) to one of many different platforms to create contours such as in Figure 4. In one embodiment, the contours are specified by points in xyz coordinate space, and a simple text file is exported to the

PET reconstruction computer where the TRUS prostate contours are superimposed with the PET prostate images using methods and software described in and adapted from G. J. Klein, X. Teng, W. J. Jagust, J. L. Eberling, A. Acharya, et al., "A methodology for specifying PET VOI's using multimodality techniques," *IEEE Trans Med Imag*, vol. 16, pp. 405-415, 1997, and R. H. Huesman, G. J. Klein, J. A. Kimdon, C. Kuo and S. Majumdar, "Deformable registration of multimodal data including rigid structures," *IEEE Trans Nucl Sci*, vol. 50, pp. 389-392, 2003, both of which are hereby incorporated by reference.

[043] In another embodiment, the PET prostate images can be combined with the TRUS reconstructed image and can be presented in a variety of ways, including 2D TRUS contours, 3D TRUS contours, or the TRUS images superimposed with the PET images. A large number of software packages or custom software can be used for image fusion, allowing the simultaneous display of PET images, ultrasound images and contours**.** Such commercial platforms to perform image fusion between any 2 DICOM format 3D image sets include but are not limited to Occentra-MasterPlan™, Nucletron, RTT Coherence™ and Leonardo™ Workstation, Siemens and also Pinnacle™ (Phillips). These applications can also display simultaneously 2D contours and points. We have also developed application tools (using Matlab and DICOM-convert) to translate any 3D data set from raw or other known format (Tiff, jpeg, etc.) into a DICOM format.

[044] The ability to position the prostate can be validated by imaging a point source that represents the prostate location. One embodiment is to verify prostate positioning by attaching a third 511 keV ^{68}Ge point source on the TRUS probe tip and positioning the probe tip at the PET-center using the previously described procedure. The positioning error is then determined by comparing the third point source location (from a 3D PET image) to its expected location (e.g., the PET-center). PET data are acquired, a 3D PET image of the point source at the probe tip is reconstructed, and the third point source location in PET coordinates is determined. This procedure is repeated several times. Although the spatial resolution of the PET scanner is 4 mm FWHM, the centroid of the profile can be more accurately determined. The TRUS probe tip should be positioned reproducibly (e.g., within 1 mm) from the PET-center. A patient's prostate only needs to be positioned within the optimum central field of view of the scanner near the PET-center. In a preferred embodiment, when using an prostate-optimized PET scanner, the patient's prostate should be positioned within 3 cm from the PET-center in the transaxial plane

and 1 cm from the PET-center in the axial plane. In another embodiment, the patient's prostate is positioned to within at 4 mm from the PET-center.

[045] In another embodiment, prostate positioning is validated using a 511 keV ^{68}Ge point source that is placed at a fixed known position on the prostate in a commercial TRUS prostate phantom (e.g., CIRS model 058), which is a clear acrylic box with structures simulating the prostate, rectal wall, seminal vesicles, urethra and perineal membrane (Figure 7). In another embodiment, validation is performed with a commercial TRUS prostate phantom that has tubing filled with a 511 keV radioactive solution (e.g., ^{18}F-water). The tubing is placed at a fixed known location through the prostate of the TRUS phantom. For either embodiment, the phantom is placed on the patient table and imaged with the TRUS probe in 2-5 mm steps from base to apex of the prostate. The patient table is then moved to center the prostate at the PET-center (using the previously described procedure), PET phantom data is acquire and reconstructed. If the PET images indicate that the PET (point or line) source is near the PET-center, then prostate positioning is successfully validated. This can be further validated by repeating the phantom imaging procedure several times to confirm that the prostate positioning is reproducible.

[046] The ability to accurately co-register PET and TRUS images can be validated by constructing and imaging a custom PET-TRUS prostate phantom. Methods on ultrasound phantom construction are described in literature [See W. D. D'Souza, E. L. Madsen, O. Unal, K. V. Vigen, G. R. Frank, et al., "Tissue mimicking materials for a multi-imaging modality prostate phantom," *Med. Phys.*, vol. 28, pp. 688-700, 2001; K. J. M. Surry, H. J. B. Austin, A. Fenster and T. M. Peters, "Poly(vinyl alcohol) cryogel phantoms for use in ultrasound and MR imaging," *Phys Med Biol*, vol. 49, pp. 5529-5546, 2004; and E. L. Madsen, M. A. Hobson, S. Hairong, T. Varghese and G. R. Frank, "Tissue-mimicking agar/gelatin material for use in heterogeneous elastography phantoms," *Phys. Med. Biol.*, vol. 50, pp. 5597-5618, 2005] with the exception of any discussion of the manufacturing of PET-ultrasound phantoms. The custom PET-TRUS prostate phantom has structures that simulate the acoustical properties for TRUS imaging and 511 keV activity concentrations for PET imaging. In one embodiment, the PET-TRUS phantom can be made of agar-gelatin-based tissue mimicking materials (TMMs) that are mixed with radioactive water solutions. The TMMs can be made compatible with MR imaging through the correct choice of materials. Since most commercial PET scanners now have CT capability, the

phantom can also be made CT compatible (e.g., by adding concentrations of iodine contrast agent or barium sulfate to the radioactive water solutions).

[047] A PET-TRUS phantom can be constructed using short-lived radioactivity, such as ^{18}F (110 minutes half-life). Short-lived radioactivity is readily available from in-house cyclotrons or commercial companies that deliver 18F-fluorodeoxyglucose. If long term repeated use of the phantom is desired, then the phantom needs to be constructed with a long-lived radioactivity, such as ^{68}Ge radioactivity (271 days half-life).

[048] In one embodiment, a PET-TRUS prostate phantom with a simple geometry is used for validation. In one embodiment, the multi-modality prostate phantom comprising a rigid container comprising a structure simulating an inner cylindrical prostate region within an outer rectangular pelvic region. The phantom is comprised of a cylinder or spherical prostate with 511 keV radioactivity concentrated uniformly, and an outer background pelvis with a different uniform concentration of 511 keV radioactivity. For instance the 511 keV activity density could be three times higher in the prostate compared to the pelvis.

[049] The phantom can be constructed with ultrasound agar-gelatin-based TMMs with different ultrasound scatter properties for the prostate and pelvis, using a tissue-mimicking mixture. Similar agar-gelatin mixtures were proven to have long-term stability at room temperature for at least one year by Madsen, *et al*. [E. L. Madsen, M. A. Hobson, S. Hairong, T. Varghese and G. R. Frank, "Tissue-mimicking agar/gelatin material for use in heterogeneous elastography phantoms," *Phys. Med. Biol.*, vol. 50, pp. 5597-5618, 2005]. In one embodiment, the structure simulating an inner cylindrical or spherical prostate region within an outer rectangular pelvic region is comprised of tissue mimicking mixtures of agar, gelatin, $CuCl_2$-$2H_2O$, EDTA-tetra Na Hydrate, NaCl, HCHO, anti-bacterial and/or anti-fungal preservative, glass beads, $BaSO_4$, and deionized radioactive water as set forth in Table I. [J.S. Huber, Q. Peng, and W.W. Moses, "Multi-Modality Phantom Development," IEEE Nuclear Science Symposium Conference Record 2007, vol. 4, pp. 2944-2948, (Edited by B. Yu), Honolulu, Hawaii, 2007].

[050] The simple phantom is produced in two stages. First the outer pelvis is filled, creating an inclusion with a petrolatum-coated rod in the center. This rod is removed, then the inner prostate is filled with a TMM with different acoustical properties and activity concentration. Similarly, a second rod can be used to create an inclusion for the TRUS probe to allow TRUS

imaging. In a preferred embodiment, a membrane-sealed hole is created in the radioactive pelvis gel for the TRUS probe.

[051] In a preferred embodiment, a TRUS-PET prostate phantom with realistic anatomy can be used for validation. For instance, the phantom having structures simulating the prostate, rectal wall and urethra in a background gel with an opening for the TRUS probe, as shown in Figure 8. If this TRUS-PET prostate phantom is only used to validate image co-registration, the phantom does not have to exactly mimic tissue or anatomy of the pelvis region. It can be constructed using a variety of tissue mimicking materials, such as the one described above and shown in Figure 8.

[052] In another embodiment, tissue mimicking materials could be used other than agar-gelatin mixtures. Typical TMMs include agar, Zerdine™, urethanes, epoxies, liquids and natural materials. There are three TMMs commercially available: Zerdine™ from CIRS Inc., condensed-milk-based gel from Gammax RMI, and urethane-rubber-based material from ATS Labs. Alternative phantom construction using radioactive water in condensed milk-agar-based mixtures [W. D. D'Souza, E. L. Madsen, O. Unal, K. V. Vigen, G. R. Frank, et al., "Tissue mimicking materials for a multi-imaging modality prostate phantom," *Med. Phys.*, vol. 28, pp. 688-700, 2001] or poly(vinyl alcohol) cryogels [K. J. M. Surry, H. J. B. Austin, A. Fenster and T. M. Peters, "Poly(vinyl alcohol) cryogel phantoms for use in ultrasound and MR imaging," *Phys Med Biol*, vol. 49, pp. 5529-5546, 2004] can be used. The urethra could also be simulated by filling a tube with ultrasound gel with some air bubbles.

[053] In another embodiment, image co-registration can be validated using a PET-TRUS phantom similar to the methods described above. Namely, tubing is added through a commercial TRUS prostate phantom (such as CIRS model 058) and filled with 511 keV radioactive solution. The tubing is placed at a fixed known location through the prostate of the TRUS phantom. The tubing material is chosen for clear ultrasound imaging (e.g., the entire tube outline cross-section should be visible in coronal ultrasound images) and appropriate dimensions (e.g., large enough inner volume for the necessary 511 keV radioactive solution).

[054] In order to validate our co-registration methods, the custom PET-TRUS prostate phantom is placed on the patient table, TRUS and PET prostate images are acquired and reconstructed, and the images co-registered (using the method described above). The dual-modality imaging phantom and patient data can be presented in a variety of ways, including 2D

TRUS contours, 3D TRUS contours, or the TRUS images superimposed with the PET images. A large number of software packages or custom software can be used for image fusion, allowing the simultaneous display of PET images, ultrasound images and contours.

[055] In a preferred embodiment, a prostate-optimized PET scanner is used and PET images are reconstructed using a 3D iterative penalized maximum likelihood algorithm as described in J. S. Huber, S. E. Derenzo, J. Qi, W. W. Moses, R. H. Huesman, et al., "Conceptual Design of a Compact Positron Tomograph for Prostate Imaging," *IEEE Trans Nucl Sci*, vol. NS-48, pp. 1506-1511, 2001; R. H. Huesman, G. J. Klein, W. W. Moses, J. Qi, B. W. Reutter, et al., "List mode maximum likelihood reconstruction applied to positron emission mammography with irregular sampling.," *IEEE Trans Med Imag*, vol. 19, pp. 532-537, 2000; and J. Hu, J. Qi, J. S. Huber, W. W. Moses and R. H. Huesman, "MAP image reconstruction for arbitrary geometry PET systems with application to a prostate-specific scanner." Proceedings of The International Meeting on Fully Three-Dimensional Image Reconstruction in Radiology and Nuclear Medicine, pp. 416-420, Salt Lake City, Utah, 2005, hereby incorporated by reference (although use of other reconstruction algorithms are also possible). The attenuation correction factors are calculated based on body contours and a uniform attenuation coefficient. Anatomical boundaries are obtained from the outer edges of emission sinograms acquired from transverse sections [C. Michel, A. Bol, A. G. DeVolder and A. M. Goffinet, "Online brain attenuation correction in PET: towards a fully automated data handling in a clinical environment," *Euro J Nucl Med*, vol. 15, pp. 712-718, 1989]. Heterogeneous attenuation coefficients could also be used, by identifying tissue types (*e.g.,* soft tissue, bone, and air) based on the TRUS ultrasound images. In another embodiment, a commercially available PET scanner is used with the provided reconstruction software, and transmission scan data is typically used for attenuation correction. In either embodiment, attenuation correction is made for the TRUS probe (which is left in place at a known location during the PET scan) and the patient table.

[056] In another embodiment, further validation of the co-registration of these images is made by taking transversal and sagittal TRUS images during the PET procedure to measure the extent of prostate motion during PET imaging. Motion correction algorithms can be used on the patient PET data if necessary [See G. J. Klein, B. W. Reutter, and R. H. Huesman, "Four-dimensional affine registration models for respiratory-gated PET," *IEEE TNS Nucl Sci*, vol. 48, pp. 756-760, 2001, and G. J. Klein and R. H. Huesman, "Four-dimensional processing of

deformable cardiac PET data," *Med Imag Anal*, vol. 6, pp. 29-46, 2002]. As the data can be acquired in listmode, they lend themselves to retrospective motion correction.

[057] In another embodiment, dual PET-TRUS can be validated by initial patient studies. Radiopharmaceutical uptake in a patient's prostate should be visible with the PET scanner after injection if the patient is positioned properly. The patient positioning technique is successfully validated if the prostate has been positioned within the optimum central field of view of the PET scanner as evidenced by PET imaging. If no radiopharmaceutical uptake is seen in the field of view of the PET scanner, then there is some uncertainty. This patient may not have enhanced radiopharmaceutical uptake in his prostate or he may not have been properly positioned in the PET scanner. PET data can be acquired at the neighboring regions to eliminate potential uncertainty. For instance, the patient table could be moved ±7 cm from the initial position and PET data acquired for at each position. If the patient has no enhanced radiopharmaceutical uptake in either of these neighboring regions, then the patient positioning is considered valid.

[058] In one embodiment, once co-registered PET and TRUS images have been acquired and have localized prostate cancerous tumors, these PET and TRUS images can accurately guide subsequent diagnosis and treatment procedures. For instance, dual PET-TRUS prostate imaging could be used to guide biopsy. Clinical staging and treatment decisions are largely based on biopsy confirmation of prostate cancer, with the Gleason histologic grading recognized as the best indicator of prognosis currently available. However, the diagnostic accuracy of biopsy is problematic, mainly due to sampling effects caused by tumor heterogeneity and to interpretational bias [D. Gleason, "Histologic grading of prostate cancer: A perspective," *Hum Pathol*, vol. 23, pp. 273-279, 1992]. There is up to a 1-in-3 chance that the underlying pathologic Gleason grade is higher than the Gleason grading from sextant prostate biopsies [C. R. King, J. E. McNeal, H. Gill and J. C. Presti, "Extended Prostate Biopsy Scheme Improves Reliability of Gleason Grading: Implications For Radiotherapy Patients," *Int. J. Radiation Oncology Biol. Phys.*, vol. 59, pp. 386-391, 2004]. For the sub-population of men with rising PSA levels and non-diagnostic biopsies or TRUS techniques, dual PET-TRUS prostate imaging could help target the area to biopsy. It has been shown that a 10-core peripheral zone biopsy scheme (compared to sextant biopsies) improves the Gleason grade reliability. An even higher degree of sampling with image-directed cores could yield even better agreement between biopsy and surgical grade, carrying important implications for management decisions [C. R. King, J. E. McNeal, H. Gill

and J. C. Presti, "Extended Prostate Biopsy Scheme Improves Reliability of Gleason Grading: Implications For Radiotherapy Patients," *Int. J. Radiation Oncology Biol. Phys.*, vol. 59, pp. 386-391, 2004]. Biopsy is used for initial diagnosis, guiding treatment decisions, and detecting local recurrence after therapy. Using dual PET-TRUS prostate imaging to increase the diagnostic accuracy of biopsy could have a major clinical impact at several stages of disease management.

[059] In another embodiment, dual PET-TRUS prostate imaging could be used to guide treatment decisions. For example, dual PET-TRUS prostate imaging could aid in treatment planning of external beam irradiation and brachytherapy. Dual PET-TRUS prostate imaging should help determine which part of the prostate and/or prostate table needs higher treatment dose by identifying the location and aggressiveness of the prostate cancer. This improvement could reduce the dosage to surrounding normal tissue, which could reduce treatment side effects.

[060] In another embodiment, dual PET-TRUS prostate imaging could be used to monitor response to therapy. Current means of assessing treatment response in prostate cancer are imprecise because changes in tumor size may be difficult to document, and changes in serum PSA do not always correlate well with clinical outcomes. Transrectal ultrasound is used to identify lesions but some of the detected lesions are not cancerous, so transrectal guided biopsy is needed to follow a patient. The administration of multiple courses of a therapy is often necessary before a clear indication of response or progression can be determined. For the sub-population of patients post-therapy with an increasing PSA level and no definitive recurrence evident, dual PET-TRUS prostate imaging could detect an early failure response to therapy. Currently, it typically takes six months to a year to determine treatment failure, largely due to the high false-positive rate of PSA testing, and approximately 20-50% of patients have local recurrence (J. A. Connolly, K. Shinohara, J. C. Presti and P. R. Carroll, "Local Recurrence after Radical Prostatectomy: Characteristics In Size, Location, and Relationthip to Prostate-Specific Antigen and Surgical Margins," Urology, vol. 47, pp. 225-231, 1996; S. E. Lerner, M. L. Blute, E. J. Bergstralh, D. G. Bostwick, J. T. Eickholt, et al., "Analysis of risk factors for progression in patients with pathologically confined prostate cancers after radical retropubic prostatectomy," J Urol., vol. 156, pp. 137-143, 1996; D. A. Kuban, H. D. Thames, L. B. Levy and et. al., "Long-term multi-institutional analysis of stage T1-T2 prostate cancer treated with radiotherapy in the PSA era," Int J Radiat Oncol Biol Phys, vol. 57, pp. 915-928, 2003; J. Crook, S. Malone, G. Perry, Y. Bahadur, S. Robertson, et al., "Postradiotherapy prostate biopsies: What do they really

mean? Results for 498 patients.," Int J Radiat Oncol Biol Phys, vol. 48, pp. 355-367, 2000; and A. L. Zietman, M. L. DeSilvio, J. D. Slater and et. al., "Comparison of conventiona-dose vs. high-dose conformal radiation therapy in clinically localized adenocarcinoma of the prostate: a randomized controlled trial.," Jama., vol. 294, pp. 1233-1239, 2005). PET imaging with radiopharmaceuticals, such as [^{11}C]choline, has the potential to effectively detect prostate cancer about a month after therapy once the initial healing has occurred. This represents a large potential improvement in therapy monitoring that would have a significant clinical impact

[061] In another embodiment, the TRUS images (from dual PET-TRUS) can be used to accurately co-register the PET images (from dual PET-TRUS) to other high-resolution anatomical images of the prostate, such as CT, MRI, or TRUS images taken on different days. This would provide improved subsequent co-registration with the PET images than if the PET images were co-registered directly, since PET images of the prostate do not contain high-resolution anatomical detail. TRUS images from a biopsy, volume study, and brachytherapy seed placement are routinely co-registered with 1-2 mm accuracy. TRUS images are fused with subsequent TRUS, CT, and MRI images for diagnosis and treatment planning. This clinical work would be greatly enhanced if preceded by dual PET-TRUS exams that identified and localized the prostate cancerous tumors, rather than relying on only anatomical information.

EXAMPLE 1: PET-TRUS PROSTATE SCANNER AND IMAGING

LBNL Prostate-Optimized PET Scanner

[062] LBNL has built a high performance positron emission tomograph optimized to image the prostate [32-34]. Coincidence imaging of positron emitters is achieved using a pair of external curved detector banks with the patient centered between them. The two banks form an incomplete elliptical ring of detectors with a 45 cm minor axis and a 70 cm major axis, which reduces the distance between the detectors and patient. Figure 3 shows the transaxial and sagittal views of the scanner. Each bank consists of two axial rows of 20 ECAT HR+ PET block detector modules for a total of 80 detectors per scanner; thus the scanner uses about one-quarter the number of detectors as an EXACT HR or HR+ scanner. The ECAT HR+ block detectors are three attenuation lengths thick for good detection efficiency with narrow detector elements (*i.e.*, 8 x 8 arrays of 4.4 x 4.1 x 30 mm^3 BGO crystals) to achieve good spatial resolution. The individual detector modules are angled to point towards the scanner center (where the prostate

will be positioned), thus reducing penetration effects for annihilation photons originating in the prostate region. We use modified front end, coincidence, and readout electronics originally developed by CTI Inc. for the HRRT PET scanner. Inter-module septa that extend 5 cm beyond the scintillator crystals reduce the background events from random coincidences and from photons that Compton scatter in the patient [J. Qi, J. S. Huber, R. H. Huesman, W. W. Moses, S. E. Derenzo, et al., "Septa Design for a Prostate Specific PET Camera," *IEEE Trans Nucl Sci*, vol. NS-52, pp. 107-113, 2004.]. The scanner has a reduced axial extent (8 cm) and thus better shielding than a conventional whole body PET scanner, which reduces the number of scatter and random events. Hence, we achieve lower backgrounds and improved detection efficiency in the central imaging volume at a lower cost.

[063] We use a 3D iterative penalized maximum likelihood reconstruction algorithm that is very flexible in modeling arbitrary scanner geometry [J. S. Huber, et al., *IEEE Trans Nucl Sci*, vol. NS-48, pp. 1506-1511, 2001; R. H. Huesman, et al., *IEEE Trans Med Imag*, vol. 19, pp. 532-537, 2000; and J. Hu, et al., Proceedings of The International Meeting on Fully Three-Dimensional Image Reconstruction in Radiology and Nuclear Medicine, pp. 416-420, Salt Lake City, Utah, 2005, hereby incorporated by reference]. We have characterized the completed scanner in 3D mode (*i.e.*, without septa). The sensitivity of a point source in the center is 946 cps/μCi (2.6%). Using a 19 cm diameter cylinder phantom, the maximum total count rate is 528 kHz at 1.5 μCi/ml and the trues+scatter events cross the randoms at 0.41 μCi/ml. We have reconstructed images of line sources, and the spatial resolution is 4 mm full width at half maximum (FWHM) in the central region. We have also successfully reconstructed extended simple prostate and NEMA body phantoms [J. S. Huber, W. S. Choong, W. W. Moses, J. Qi, J. Hu, et al., "Initial Results of a Positron Tomograph for Prostate Imaging," *IEEE Trans Nucl Sci*, NS-53, pp. 2653-2659 (2006)], as shown in Figure 9.

Transrectal Ultrasound

[064] Transrectal ultrasound imaging of the prostate is a standard imaging technique widely used for prostate cancer diagnosis, biopsy, treatment planning and brachytherapy seed placement. A volumetric 3D reconstructed image of the prostate can be generated using a series of 2D TRUS images. Such 3D images are currently used to determine the prostate volume and calculate dose for brachytherapy planning. The images are formed by mounting a transrectal probe to a fixture that is rigidly attached to the table through a calibrated linear stepper that

allows displacement along its axis. Ultrasound images in the transverse plane (*i.e.,* perpendicular to the probe axis) are acquired from base to apex. A complete 3D TRUS image of the prostate, urethra and rectum wall is then reconstructed using a series of 2D images taken in a step and shoot protocol. A physical puncture attachment for radiotherapeutic seed implantation is also attached to the probe fixture. A virtual grid position, corresponding to the projection of the puncture attachment holes, is projected on the image to provide localization. Figure 4 shows a drawing of the TRUS unit with the probe inserted in a patient, as well as a 2D transverse ultrasound image with grid and the contours from a 3D reconstruction. We determine the position of the TRUS probe relative to the PET scanner, allowing the PET and TRUS images to be accurately co-registered using a simple rigid-body transformation specified by the alignment of the two systems.

EXAMPLE 2: PET-TRUS PROSTATE POSITIONING

[065] We used the LBNL prostate-optimized PET scanner, shown in Figure 3, to acquire 3D volumetric PET images [J. S. Huber, W. S. Choong, W. W. Moses, J. Qi, J. Hu, et al., "Initial Results of a Positron Tomograph for Prostate Imaging," *IEEE Trans Nucl Sci*, NS-53, pp. 2653-2659 (2006)]. We also use a commercial TRUS imaging system to acquire a series of 2D TRUS images, then reconstruct them to visualize a 3D TRUS image of the prostate region (see Figure 4). We have mechanically modified this TRUS equipment to work when mounted onto a common patient table in conjunction with the PET scanner (see Figure 5b). The TRUS probe is rigidly attached to the modified TRUS stepper that allows calibrated linear displacement along its axis. A point source holder (with two ^{68}Ge point sources) is attached to the TRUS stepper. The TRUS probe-stepper-point source holder unit is mounted onto a moveable TRUS stabilizer arm that is rigidly attached to the patient table. The stabilizer arm moves to allow correct positioning of the TRUS probe in a patient (or phantom), then its position is fixed by tightening a single knob.

[066] Using this dual PET-TRUS system, we have developed a method to accurately position a prostate near the PET-center:

a. The TRUS probe is inserted inside a patient (or phantom), positioned at the prostate and the stabilizer arm is fixed.
b. A series of 2D TRUS prostate images in the transverse plane (i.e., perpendicular to the probe axis) is acquired from base to apex using the linear stepper.

c. The TRUS probe tip is positioned axially at the center of the prostate using the stepper.

d. The patient table is then moved so that two ^{68}Ge point sources are visually positioned near the PET-center with the aid of visible low-powered lasers. (These two ^{68}Ge point sources are placed in a holder, along the axial line of the TRUS probe, at a known location from the TRUS probe tip (Fig. 5b)).

e. PET data are acquired for 1-5 minutes, quickly reconstructed, and the location of the point sources determined in PET coordinates. We use a two-iteration expectation-maximization algorithm, with a simplified model of the PET scanner geometry, to quickly reconstruct the data in about 3 minutes. The resulting PET images are then quickly processed (within 1 minute) to determine the point source locations in PET coordinates, by determining the brightness-weighted average for each point source in the 3D volumetric PET image.

f. The two point source locations are represented by two position vectors and vector algebra is used to calculate the location of the TRUS probe tip (within 1 minute.)

g. The patient table is then moved to position the TRUS probe tip (i.e., prostate) at the PET-center.

[067] Both our patient positioning and PET-TRUS image co-registration depend on our ability to determine the 3D location of the TRUS probe tip in PET coordinates (i.e., relative to the PET-center) using the method outlined above. However, these two tasks require different levels of accuracy. For patient positioning, a patient's prostate only needs to be positioned within the optimum central field of view of the PET scanner – within 3 cm from the PET-center in the transaxial plane and within 1 cm from the PET-center in the axial plane.

[068] We have validated our ability to accurately determine the TRUS probe tip's 3D location in PET coordinates by imaging a point source that represents the prostate location. We attached a third 511 keV ^{68}Ge point source on the TRUS probe tip. We positioned the TRUS probe tip using the procedure described above, acquired (for 5 minutes) and reconstructed PET data, and determined the third point source location in PET coordinates. This procedure was repeated several times for each TRUS probe position. Two very different probe positions were measured – (1) with the probe roughly level to the patient table and pointing along the axial z-axis and (2) with the probe pointing down 11 degrees (i.e., at greater angle than expected for patients) and to the left 2 degrees. Although the spatial resolution for the PET scanner is 4 mm FWHM, the centroid of a point source profile can be more accurately determined. We were able

to reproducibly position the TRUS probe tip within 1 mm from the PET-center in the axial direction (i.e., direction of patient table motion). Specifically, the third point source location on average was -0.64 ± 0.08 mm from the PET-center in the axial direction. Thus, we have achieved greater accuracy than required for patient positioning.

[069] We can also validate prostate positioning using a modified commercial TRUS prostate phantom (e.g., CIRS model 058), which is a clear acrylic box with structures simulating the prostate, rectal wall, seminal vesicles, urethra and perineal membrane (Figure 7). Tubing is added at a fixed known location through the prostate of the TRUS phantom, and filled with 511 keV radioactive solution (e.g., ^{18}F or ^{68}Ge water). The tubing material is chosen for clear ultrasound imaging (e.g., so the entire tube cross-section is visible in coronal ultrasound images) and appropriate dimensions (e.g., a large enough inner volume for the necessary 511 keV radioactive solution). For instance, silicone tubing (e.g. Tygon #3350 sanitary silicone tubing) with a 5/32" inner diameter and 7/32" outer diameter can be used. The phantom is placed on the patient table and imaged with the TRUS probe in 2-5 mm steps from base to apex of the prostate. The patient table is then moved to center the prostate at the PET-center (using the previously described procedure), PET phantom data is acquire and reconstructed. If the PET images indicate that the line source is near the PET-center, then prostate positioning is successfully validated. This can be further validated by repeating the phantom imaging procedure several times to confirm that the prostate positioning is reproducible.

EXAMPLE 3: CO-REGISTRATION AND PET-TRUS PROSTATE PHANTOMS

Custom PET-US Phantom

[070] We have developed a method to co-register PET and TRUS images and validate this method using a custom TRUS-PET prostate phantom. We construct and use a TRUS-PET prostate phantom with structures that simulate the acoustical properties for TRUS and 511 keV activity concentrations for PET. We use agar-gelatin-based tissue mimicking materials (TMMs) that are mixed with radioactive water solutions [J.S. Huber, Q. Peng, and W.W. Moses, "Multi-Modality Phantom Development," IEEE Nuclear Science Symposium Conference Record 2007, vol. 4, pp. 2944-2948, (Edited by B. Yu), Honolulu, Hawaii, 2007]. When developing the procedures for the agar-gelatin-based phantom construction, we first used non-radioactive water to test ultrasound properties. We then used short-lived ^{18}F radioactive (110 minutes half-life) water solutions, since ^{18}F is readily available from our in-house cyclotron and no radioactive

waste is generated by these construction tests (since ^{18}F quickly decays away). We will also use long-lived ^{68}Ge radioactivity (271 days half-life) for phantom construction to allow repeated PET imaging of the same phantom over at least one year.

[071] We have constructed a simple PET-ultrasound prostate phantom as proof of principle. We are not aware of previous work on the manufacturing of PET-ultrasound phantoms. Our simple PET-ultrasound phantom was constructed in two stages. We first filled a rectangular plastic box with 4% agarose that was prepared as a high-scatter ultrasound tissue mimicking material (TMM), creating an inclusion with a petrolatum-coated plastic rod in the center. Once the "pelvis" agarose hardened, the rod was removed and we filled the inner cylindrical "prostate" region with a low-scatter 8% gelatin TMM. Figure 10a shows a photograph of the final phantom. At each stage, the TMM was mixed with ^{18}F radioactive (110 minute half-life) water solution before putting it into a refrigerator to harden. The phantom had six times higher 511 keV activity density in the inner cylinder "prostate" than in the outer "pelvis." It was roughly centered in an EXACT HR PET scanner, and PET data were acquired with a 10 minute transmission scan followed by a 20 minute emission scan in 3D mode. At the start of the emission scan, the ^{18}F activity density was 1.07 μCi/ml in the inner cylinder gelatin and 0.17 μCi/ml in the background agarose. Reconstruction was performed with attenuation and scatter correction. Figure 10b shows a reconstructed coronal PET image of the phantom. The ^{18}F activity uniformly concentrated in the cylindrical "prostate" gelatin is clearly visible within the "pelvis" background activity. The phantom was then imaged using a 5MHz external Elektra ultrasound system, as shown in Figure 10c. The ultrasound image clearly shows the low-scatter cylindrical "prostate" gelatin, which is surrounded by the high-scatter "pelvis" agarose. Thus, we have demonstrated our ability to construct and image a custom PET-ultrasound phantom. However, the phantom's mechanical and ultrasound properties did not have long-term stability especially at room temperature.

Custom PET-US-CT-MRI Phantom

[072] Since the custom PET-US phantom described above did not have long-term stability at room temperature, we also developed a different phantom construction process. We have constructed a multi-modality phantom using tissue mimicking mixtures of agar, gelatin, $CuCl_2$-$2H_2O$, EDTA-tetra Na Hydrate, NaCl, HCHO, Germall-Plus^{TM}, glass beads, $BaSO_4$, and deionized water (Table I). Similar agar-gelatin mixtures were proven to have long-term

mechanical, ultrasound and MRI properties for at least one year [E. L. Madsen, M. A. Hobson, S. Hairong, T. Varghese and G. R. Frank, "Tissue-mimicking agar/gelatin material for use in heterogeneous elastography phantoms," *Phys. Med. Biol.*, vol. 50, pp. 5597-5618, 2005]. These agar-gelatin-based tissue mimicking materials can be mixed with radioactive water solutions. When developing the procedures for the agar-gelatin-based phantom construction, we used non-radioactive water and short-lived ^{18}F radioactive water solutions. We can use long-lived ^{68}Ge radioactivity (271 day half-life) for phantom construction to allow repeated PET imaging of the same phantom over at least one year.

[073] We constructed a two-region PET-US-CT-MRI phantom with an inner cylindrical "prostate" within an outer rectangular "pelvis" (*i.e.*, with the same simple geometry as the PET-US phantom described above). We first filled the rectangular "pelvis" container with the "Pelvis TMM" (Table I), creating a void with a petrolatum-coated plastic rod in the center. This rod was removed once the rectangular "pelvis" hardened, then we filled the inner cylindrical "prostate" with a "Prostate TMM" (Table I) having different multi-modality properties and ^{18}F activity. The TMMs were hardened at room temperature. Figure 11a shows a photograph of the custom PET-US-CT-MRI phantom.

Table I. Dry-weight percents of the various components in the PET-US-CT-MRI custom phantom. The weight percent of the water is not shown since it makes up the remainder.

	Agar	Gelatin	$CuCl_2$-$2H_2O$	EDTA	NaCl	HCHO	Germall-Plus	Glass Beads	$BaSO_4$
Pelvis TMM	1.17	5.50	0.11	0.32	0.77	0.24	1.44	4.38	0.50
Prostate TMM	3.64	5.70	0.12	0.34	0.80	0.25	1.50	0	0

[074] Table I outlines the dry-weight percents for the "Prostate TMM" and "Pelvis TMM" used to construct the custom PET-US-CT-MRI phantom. For these tests, only the cylindrical "prostate" TMM was mixed with a ^{18}F-water solution. The primary role of each ingredient is summarized below:

- *Agar*: concentration set to achieve tissue-like US properties, such as US propagation speed. Higher agar concentration also produces shorter longitudinal (T_1) and transverse (T_2) MRI relaxation times.

- *Gelatin*: concentration set for tissue-like US properties, such as US propagation speed. Concentration must be roughly the same for "prostate" and "pelvis" regions to avoid changes in volumes due to osmosis.
- *$CuCl_2$-2H_2O* and *EDTA-tetra Na Hydrate*: EDTA forms chelate with the Cu^{2+} ions to allow Cu^{2+} to remain mobile, allowing controlled lowering of the T_1 MRI relaxation time.
- *NaCl*: anti-bacterial agent that produces tissue-like MRI coil loading.
- *HCHO* (37% formaldehyde): cross-links the gelatin, raising the melting point to 78 °C where the agar component melts.
- *Germall-Plus^{TM}*: preservative to prevent fungal and bacterial invasion.
- *Glass Beads* (20 μm average diameter): increases ultrasound attenuation and backscatter to tissue-like levels. Also lowers T_1 and T_2 MRI relaxation times.
- *$BaSO_4$*: increases radiographic attenuation for CT.
- *^{18}F*: 511 keV radioactivity for PET imaging.

[075] The expected ultrasound properties include a propagation speed of about 1535 m/s, a density of about 1.04 g/ml, and an attenuation coefficient divided by frequency of about 0.14 dB/cm/MHz for the "Prostate TMM" and 0.38 dB/cm/MHz for the "Pelvis TMM." The MRI T_1 relaxation times are expected to be about 494 ms for the "Prostate TMM" and 423 ms for the "Pelvis TMM" [E. L. Madsen, M. A. Hobson, S. Hairong, T. Varghese and G. R. Frank, "Tissue-mimicking agar/gelatin material for use in heterogeneous elastography phantoms," *Phys. Med. Biol.*, vol. 50, pp. 5597-5618, 2005].

[076] The custom PET-US-CT-MRI phantom was imaged using an EXACT HR PET scanner. PET data were acquired with a 3D emission scan followed by a 10 minute transmission scan. Iterative image reconstruction was performed with attenuation and scatter correction. Figure 11b shows a reconstructed coronal PET image of the phantom. The ^{18}F activity concentrated in the cylindrical "prostate" is clearly visible. The PET image in the "prostate" region is not uniform in this case (*e.g.*, compared to Fig. 10b) due to PET scanner hardware problems that affected the attenuation map and normalization.

[077] The custom PET-US-CT-MRI phantom was imaged by the other three modalities the following day, after the ^{18}F radioactivity decayed. The phantom was imaged with a 5MHz external Elektra ultrasound system. Figure 11c shows an ultrasound image of the phantom with a lower-scatter cylindrical "prostate" surrounded by higher-scatter "pelvis." The phantom was then

imaged with a Hawkeye CT scanner (140 keV; 2.5 mAmps) on a Millennium VG3 SPECT gantry. Reconstruction was performed with filtered backprojection using a Hann filter with a cutoff frequency of 1. Figure 11d shows a reconstructed coronal CT image of the phantom with increased radiographic attenuation in the "pelvis" due to the $BaSO_4$.

[078] The phantom was then imaged with an 1.5 T Avanto Siemens MRI scanner using a head coil with a T_1-weighted 2D spin echo pulse sequence (TE = 7.8 msec; TR = 500 msec; field of view = 220 mm x 178.8 mm x 3 mm; voxel size = 0.4 mm x 0.4 mm x 3 mm). Figure 11e shows a reconstructed T_1-weighted MRI image with a darker "prostate" representing a longer T_1 compared to the "pelvis." The glass beads (used for ultrasound imaging) shortened the T_1 in the "pelvis" to make it brighter, despite the increased agar concentration in the "prostate." The phantom was also imaged with a T_2-weighted 2D turbo spin echo pulse sequence (TE = 91 msec; TR = 4000 msec; field of view = 220 mm x 175.3 mm x 3 mm; voxel size = 0.4 mm x 0.4 mm x 3 mm). Figure 11f shows a reconstructed T_2-weighted MRI image with a darker "prostate" representing a shorter T_2 compared to the "pelvis.

[079] Finally, we removed a cylindrical section of the gel in the pelvis region, in order to allow transrectal ultrasound imaging. Transrectal ultrasound imaging was performed using a Hitachi Hi Vision 5500 system with a EUP-U533 biplane transrectal ultrasound probe. Figure 11g shows a fused PET (color) and TRUS (grayscale) coronal image of the phantom. The OsiriX software package was used for the image fusion.

[080] We plan to make a PET-TRUS prostate phantom with a more realistic geometry using ^{68}Ge water in our agar-gelatin mixture. The phantom will have structures simulating the prostate, rectum and rectal wall and urethra in a background gel with an opening for the TRUS probe (Fig. 8). The urethra is routinely simulated by filling a tube with ultrasound gel with some air bubbles. We will image this PET-TRUS prostate phantom with PET and TRUS to confirm that we have produced a phantom with the required properties. Since this PET-TRUS prostate phantom will be used only to validate image co-registration, the phantom does not have to exactly mimic the PET and TRUS properties of the prostate region.

EXAMPLE 4: CO-REGISTRATION AND PET-TRUS PROSTATE PATIENT IMAGING

[081] Dual PET-TRUS imaging will also be validated with patient studies. The patients will have prostate cancer that has been confirmed by biopsy, and most patients will be imaged prior to any treatment. The dual PET-TRUS studies will be performed at the Medical Imaging

Technology Department at LBNL in building 55 using the LBNL prostate-optimized PET scanner (or the Siemens ECAT EXACT HR PET scanner, if needed as backup) with a commercial transrectal ultrasound system (*e.g.*, Hitachi Hi Vision 5500 with a EUP-U533 bi-plane transrectal transducer probe, Accucare EXII stepper, and micro-touch stabilizer arm, or equivalent). Clinicians will administer consent, and will be available during the entire dual PET-TRUS procedure. Patients who are scheduled must meet protocol inclusion/exclusion criteria, and these will be reviewed by the attending physician prior to the procedure. During the clinician-patient conference, a short history of the present disease and an accounting of recent (48 hours) food ingestion will be recorded. The dietary information is important because choline biodistribution results might be affected by recent food ingestion.

[082] Patients will be asked to be on a light diet one day prior to this study, following a clear liquid only diet the previous day and eating nothing after midnight the night prior to the procedure. Patients will empty their bladder 30 minutes or more before the procedure, allowing for some residual liquid to be present in the bladder during the PET-TRUS scan. Patients will empty their rectum prior to the procedure, using an enema only as needed. Although enema bowel prep is common for TRUS-guided biopsy, an enema is rarely necessary for a standalone transrectal ultrasound procedure. If necessary, patients will perform a self-administered Fleets enema about 10 minutes prior to the PET-TRUS scan. (Most patients can easily self administer the enema in about 5 minutes by bending over at the waist, inserting and injecting the enema, and evacuating into the toilet.)

[083] Patients will be comfortably positioned on the patient table, lying on their back with their legs raised, for the dual PET-TRUS scan. Pillows and knee supports will be used for patient comfort. The clinician will insert the commercial transrectal probe (with condom) and position it at the prostate. A series of 2D ultrasound images will be acquired in the transverse plane from prostate base to apex (about 25 slices or less). No anesthesia will be used, in accordance with standard clinical practice. The TRUS probe tip will then be positioned axially at the center of the prostate using the stepper.

[084] Leaving the transrectal probe in place, the patient table will be moved a short distance at a slow speed to position two low-activity (<50 μCi) Ge-68 point sources near the center of the PET scanner with the aid of visible low-powered lasers (which define the major and minor axis of the PET scanner). These Ge-68 point sources are placed in a holder along the axial line of the

TRUS probe at a known distance from the TRUS probe tip. PET data from these Ge-68 point sources will be quickly acquired and analyzed to determine the current location of the TRUS probe tip (which is positioned axially at the center of the patient's prostate). These sources will expose the patient to a small dose because: they are NOT inserted into the patient; they are placed at least 2 inches from the patient; and they will be near the patient for a short time. Leaving the transrectal probe in place, the patient table will be moved a short distance at a slow speed to position the patient's prostate near the PET-center in preparation for PET imaging.

[085] A clinician will insert a small intravenous catheter and then immediately administer the PET radiopharmaceutical through the catheter. He will inject up to 10 mCi (±10%) of [^{11}C]choline per patient. PET imaging over the prostate and neighboring regions will commence immediately following injection and proceed for up to 40 minutes. No transmission scans will be performed with the LBNL prostate-optimized PET scanner. No blood sampling will be necessary (arterial or venous) for this procedure. Patients will be taken to the bathroom to urinate immediately following their dual PET-TRUS scan. The total time of the dual PET-TRUS procedure will be less than an hour, so the transrectal probe will be left in place for up to an hour.

[086] PET images will be reconstructed using a 3D iterative penalized maximum likelihood algorithm as described in in J. S. Huber, S. E. Derenzo, J. Qi, W. W. Moses, R. H. Huesman, et al., "Conceptual Design of a Compact Positron Tomograph for Prostate Imaging," *IEEE Trans Nucl Sci*, vol. NS-48, pp. 1506-1511, 2001; R. H. Huesman, G. J. Klein, W. W. Moses, J. Qi, B. W. Reutter, et al., "List mode maximum likelihood reconstruction applied to positron emission mammography with irregular sampling.," *IEEE Trans Med Imag*, vol. 19, pp. 532-537, 2000; and J. Hu, J. Qi, J. S. Huber, W. W. Moses and R. H. Huesman, "MAP image reconstruction for arbitrary geometry PET systems with application to a prostate-specific scanner." Proceedings of The International Meeting on Fully Three-Dimensional Image Reconstruction in Radiology and Nuclear Medicine, pp. 416-420, Salt Lake City, Utah, 2005, if the PET scanner used is the prostate-optimized PET scanner. The attenuation correction factors will be calculated based on body contours and a uniform attenuation coefficient. Anatomical boundaries will be obtained from the outer edges of emission sinograms acquired from transverse sections [C. Michel, A. Bol, A. G. DeVolder and A. M. Goffinet, "Online brain attenuation correction in PET: towards a fully automated data handling in a clinical environment," *Euro J Nucl Med*, vol. 15, pp. 712-718, 1989]. Similarly, attenuation correction will be made for the TRUS probe (which is left in place

at a known location during the PET scan) and the patient table. 3D anatomy contours will be identified from the TRUS images, and these TRUS contours will be superimposed onto the corresponding (resliced) PET images for anatomical localization [G. J. Klein, X. Teng, W. J. Jagust, J. L. Eberling, A. Acharya, et al., "A methodology for specifying PET VOI's using multimodality techniques," *IEEE Trans Med Imag*, vol. 16, pp. 405-415, 1997, R. H. Huesman, G. J. Klein, J. A. Kimdon, C. Kuo and S. Majumdar, "Deformable registration of multimodal data including rigid structures," *IEEE Trans Nucl Sci*, vol. 50, pp. 389-392, 2003].

[087] Since the patient is known to have prostate cancer, the [^{11}C]choline uptake in his prostate should be visible with the PET scanner within 3 minutes after injection if the patient is positioned properly. The patient positioning technique is successfully validated if the prostate has been positioned within the optimum central field of view of the PET scanner — within 3 cm from the PET-center in the transaxial plane and 1 cm from the PET-center in the axial direction — as evidenced by PET imaging. If no [^{11}C]choline uptake is seen in the field of view of the PET scanner, then there is some uncertainty. This patient may not have enhanced [^{11}C]choline uptake in his prostate or he may not have been properly positioned in the PET scanner. Further PET data will be acquired once the initial 15 minutes are complete. The patient table will be moved ±7 cm from the initial position and PET data will be acquired for 5 additional minutes at each position. If the patient has no enhanced [^{11}C]choline uptake in either of these neighboring regions, then the patient positioning will still be considered valid.

[088] The total time of the PET-TRUS study will typically be 40 minutes: 2 minutes to insert and position the TRUS probe in the patient, 3 minutes for TRUS data acquisition, 10 minutes to position the patient's prostate near the PET-center (using point sources on stepper), 15 minutes for [^{11}C]choline injection and PET data acquisition with the patient centered in the PET scanner, and 10 minutes to acquire PET data at the neighboring regions. The total time commitment for the study, including patient consent, will be approximately 2 hours.

[089] Patients will be recruited and after clinical evaluations, patients deemed appropriate for inclusion will be referred for study. Patients will have confirmed prostate cancer and will not have received treatment in the preceding four weeks, allowing time for initial healing to occur in order to minimize [^{11}C]choline accumulation in inflammatory tissue.

[090] The transrectal probe will be covered with a new condom prior to each use. Following standard clinical cleaning practices, the ultrasound equipment will be brushed with

disinfectant and washed with alcohol after each use. No follow-up visits are planned. However, the patient's prostate cancer status will be followed over a period of 3 years to provide a more accurate and thorough comparison between (a) the location of abnormal [^{11}C]choline uptake seen on the dual PET-TRUS scan and (b) the location of histologically confirmed prostate cancer. For instance, dual PET-TRUS prostate imaging could accurately detect abnormal uptake in a patient's prostate region before conventional clinical procedures (*e.g.*, biopsy) are able to detect the prostate cancer. Following the patient's prostate cancer status will allow us to evaluate discrepancies of this kind, determining if the location of abnormal radiotracer uptake accurately reflects the location of prostate cancer, so we are able to correctly evaluate our development of dual PET-TRUS prostate imaging. Hence, both current data and subsequent data relevant to the patient's prostate cancer status over a period of 3 years will be accessed in accordance with HIPAA regulations.

[091] The above examples are provided to illustrate the invention but not to limit its scope. Other variants of the invention will be readily apparent to one of ordinary skill in the art and are encompassed by the appended claims. All publications, databases, and patents cited herein are hereby incorporated by reference for all purposes.

PROPOSED CLAIMS

What is claimed is:

1. A method for accurate co-registration for dual-modality positron emission tomography (PET) and transrectal ultrasound (TRUS) imaging for prostate cancer, comprising the steps of:

a. providing a PET-TRUS system comprising a PET scanner having a patient table with a TRUS probe attached to the table through a TRUS calibrated linear stepper-arm assembly, wherein a holder with 511 keV point sources is mounted onto the TRUS stepper or probe;

b. inserting the TRUS probe inside the rectum of a patient, positioning said TRUS probe at the prostate, and fixing the stabilizer arm;

c. acquiring TRUS prostate images of the entire prostate region;

d. positioning the TRUS probe tip axially at the center of the prostate using the stepper;

e. moving the patient table so that at least two ^{68}Ge point sources are visually positioned near the PET-center with the aid of visible low-powered lasers;

f. acquiring and analyzing PET point source data, and determining the location of the point sources in PET coordinates;

g. calculating the location of the TRUS probe tip;

h. moving the patient table to position the TRUS probe tip at the PET-center;

i. injecting a 511 keV radiopharmaceutical into the patient and acquiring PET image data of the patient;

j. contouring the TRUS data two-dimensionally and reconstructing a three-dimensional TRUS image of the prostate region;

k. reconstructing three-dimensionally the PET data; and

l. accurrately superimposing the PET and TRUS images, thereby resulting in a PET-TRUS image of the patient's prostate region showing anatomical and functional detail for precise localization of any prostate cancer.

2. The method of claim 1, wherein 511 keV point sources are placed on TRUS equipment and used to determine the location of the TRUS probe relative to the PET-center.

4. A method of validating claim 1, wherein a custom PET-ultrasound phantom is constructed and imaged using a dual PET-TRUS system instead of a patient.

5. A multi-modality prostate phantom comprising a rigid container comprising a structure comprising an inner cylindrical or spherical prostate region within an outer rectangular pelvic region comprised of tissue mimicking mixtures and radioactive water.

6. The multi-modality prostate phantom of claim 5, further comprising structures simulating the rectum, rectal wall and urethra in a background gel with an opening for insertion of a TRUS probe in the rectum.

7. The multi-modality prostate phantom of claim 6, wherein the urethra is simulated by filling a tube with ultrasound gel and air bubbles.

8. The multi-modality prostate phantom of claim 5, wherein the tissue mimicking mixture comprises of agar, gelatin, $CuCl_2$-$2H_2O$, EDTA-tetra Na Hydrate, NaCl, HCHO, anti-bacterial and/or anti-fungal preservative, glass beads, $BaSO_4$, and radioactive water as set forth in Table I.

ABSTRACT OF THE DISCLOSURE

Herein are described methods and tools for acquiring accurately co-registered PET and TRUS images, as well as the construction and use of PET-TRUS prostate phantoms. Ultrasound imaging with a transrectal probe provides anatomical detail in the prostate region that can be accurately co-registered with the sensitive functional information from the PET imaging. Imaging the prostate with both PET and transrectal ultrasound (TRUS) will help determine the location of any cancer within the prostate region. This dual-modality imaging should help provide better detection and treatment of prostate cancer.

Figure 1

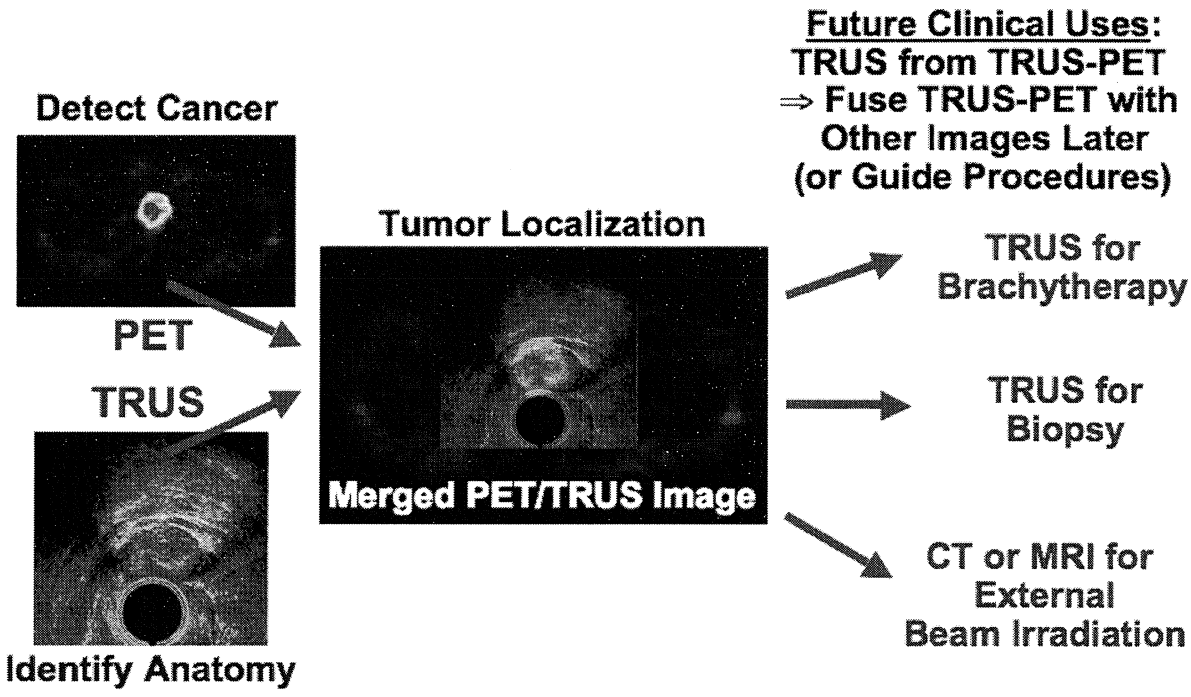
Future Clinical Uses:
TRUS from TRUS-PET
⇒ Fuse TRUS-PET with
Other Images Later
(or Guide Procedures)
Detect Cancer
PET
TRUS
Identify Anatomy
Tumor Localization
Merged PET/TRUS Image
TRUS for
Brachytherapy
TRUS for
Biopsy
CT or MRI for
External
Beam Irradiation

Figure 2

Before Therapy

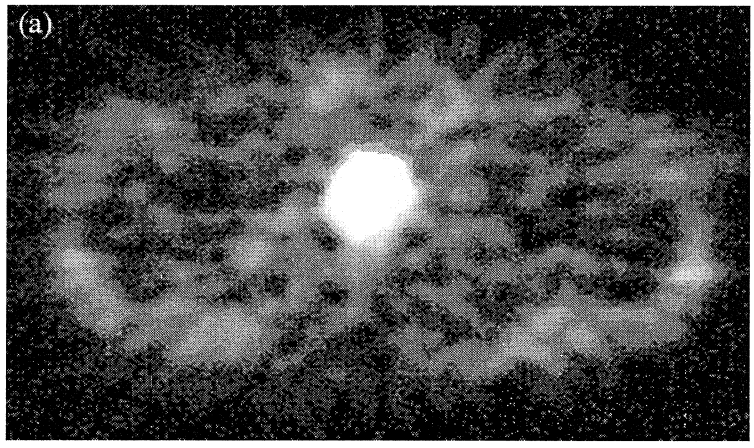

After Therapy

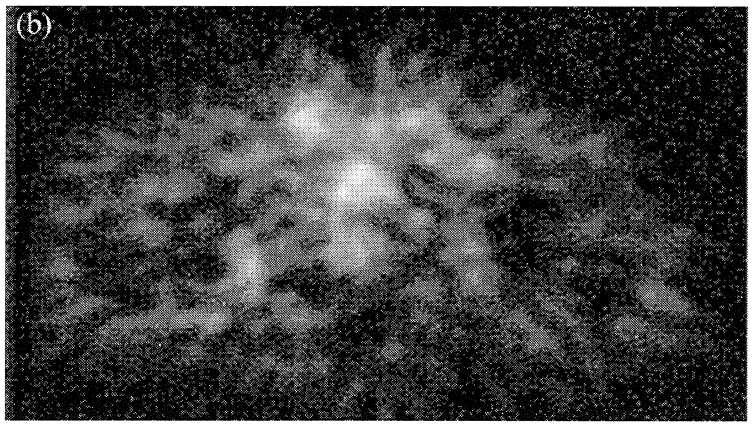

Figure 3

(a)

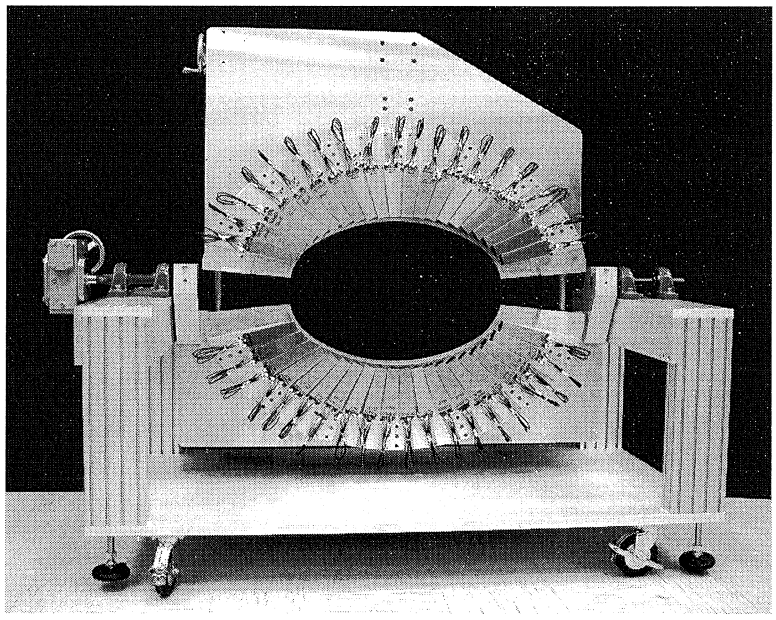

(b)

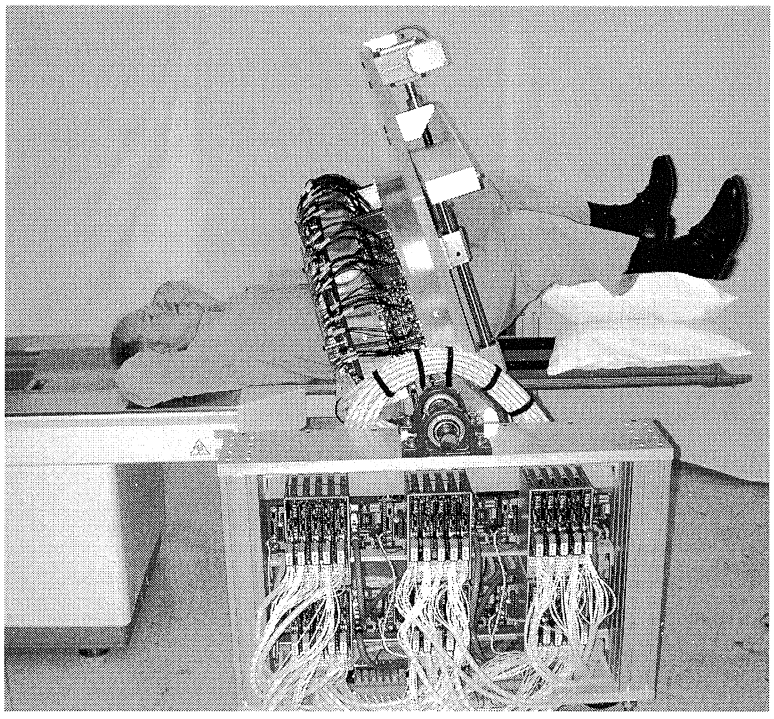

Figure 4

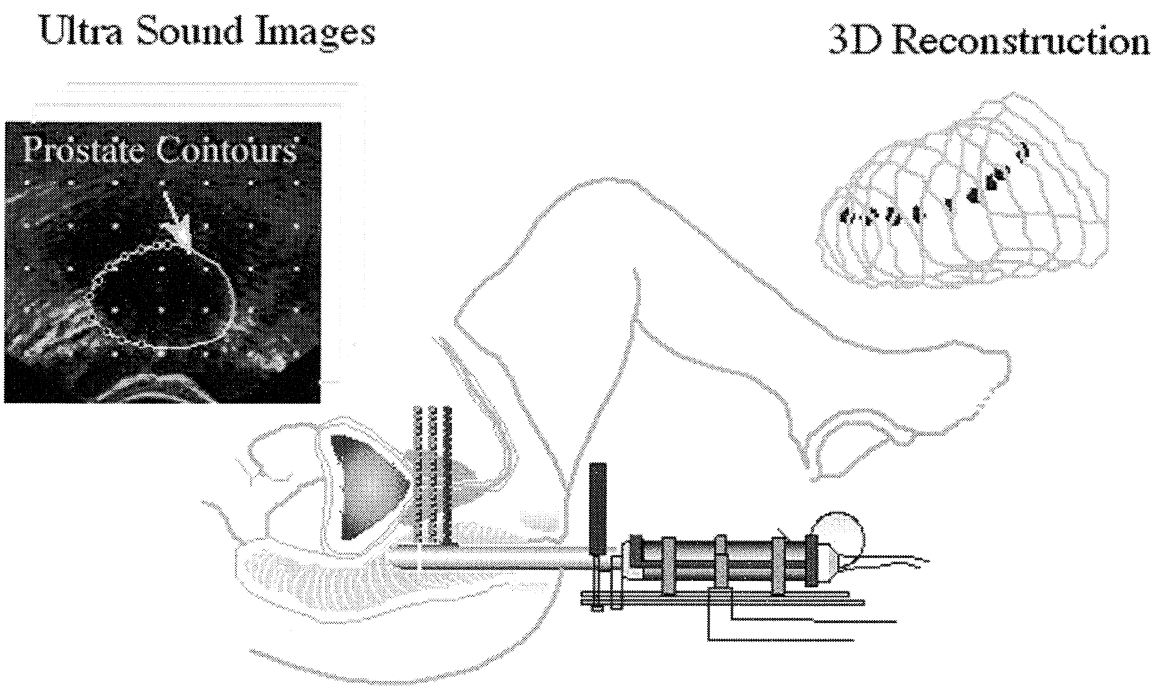

Figure 5

(a)

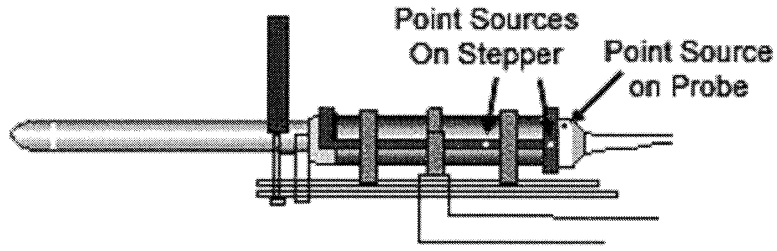
Point Sources
On Stepper
Point Source
on Probe

(b)

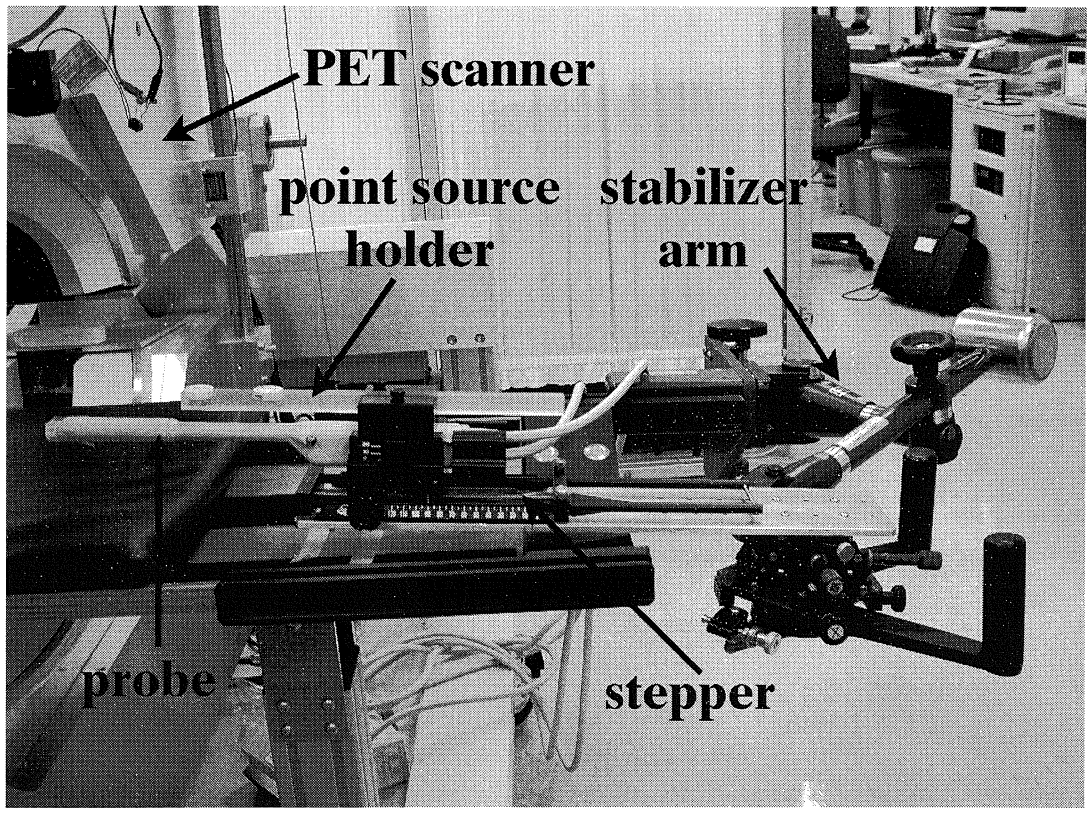
PET scanner
point source
holder
stabilizer
arm
probe
stepper

Figure 6

(a)

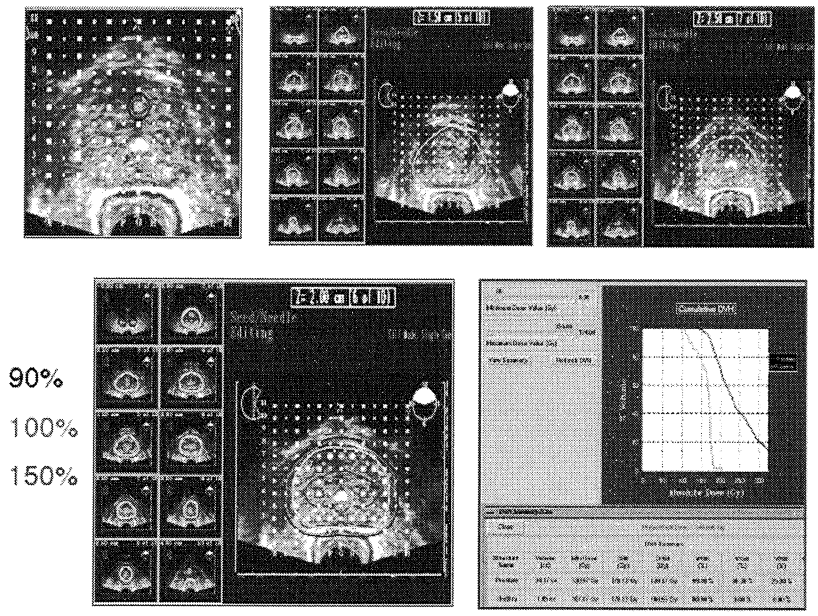
90%
100%
150%

(b)

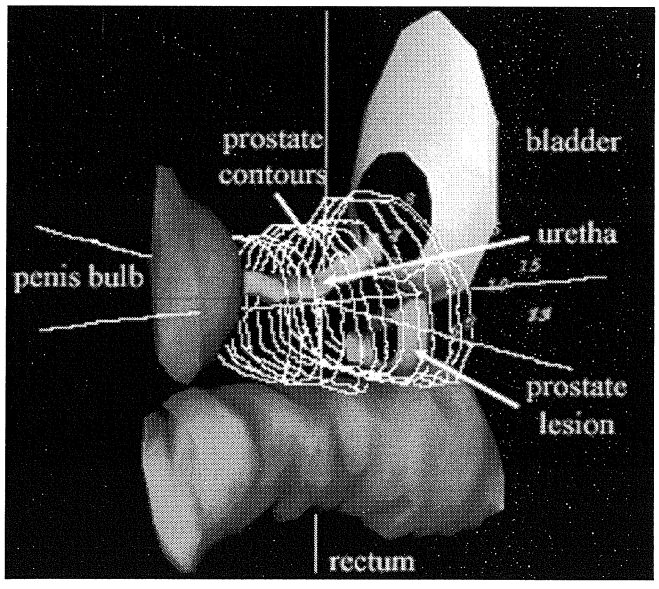
prostate contours
bladder
uretha
penis bulb
prostate lesion
rectum

Figure 7

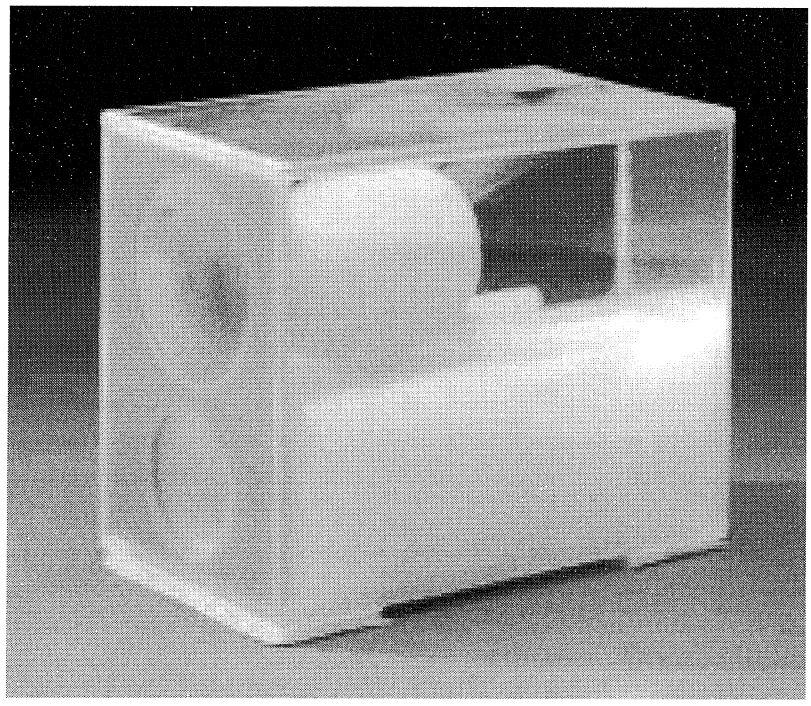

Figure 8

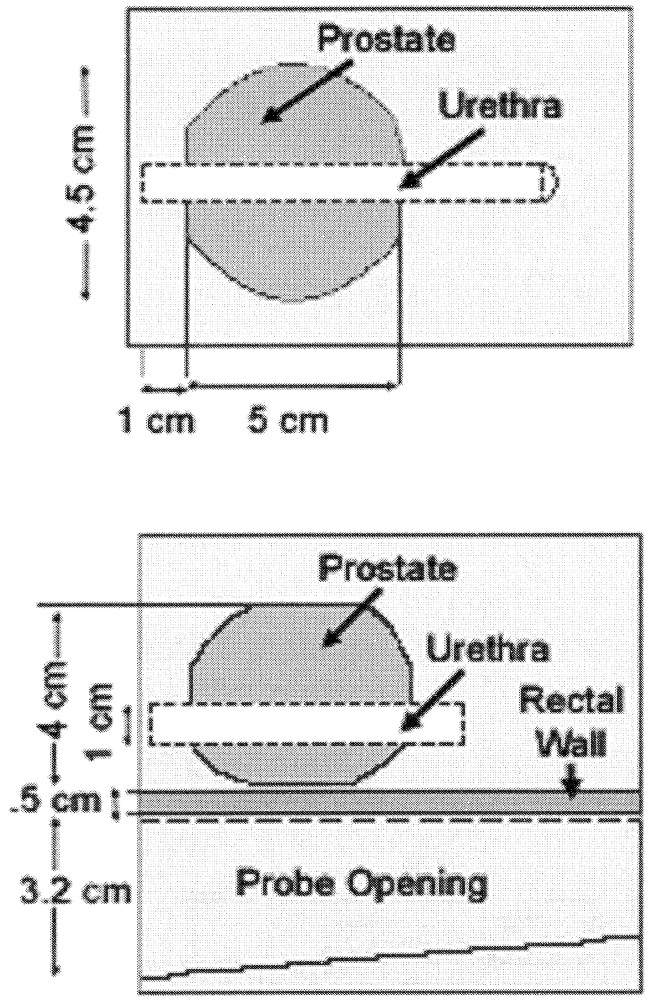
Prostate
Urethra
4.5 cm
1 cm
5 cm
Prostate
Urethra
Rectal Wall
4 cm
1 cm
.5 cm
3.2 cm
Probe Opening

Figure 9

(a)

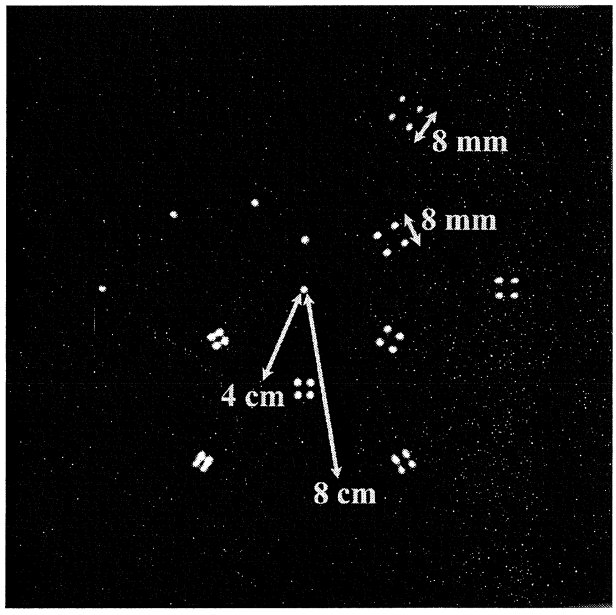

Figure 9

(b)

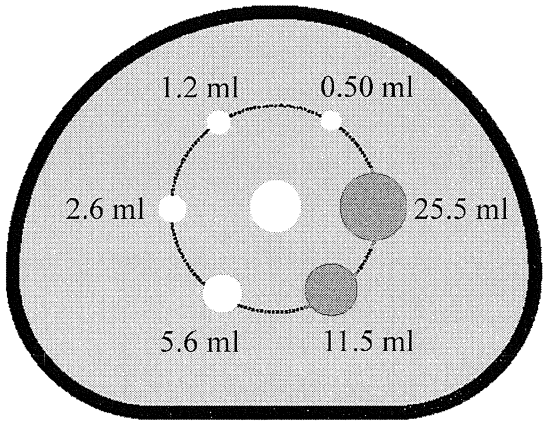

(c)

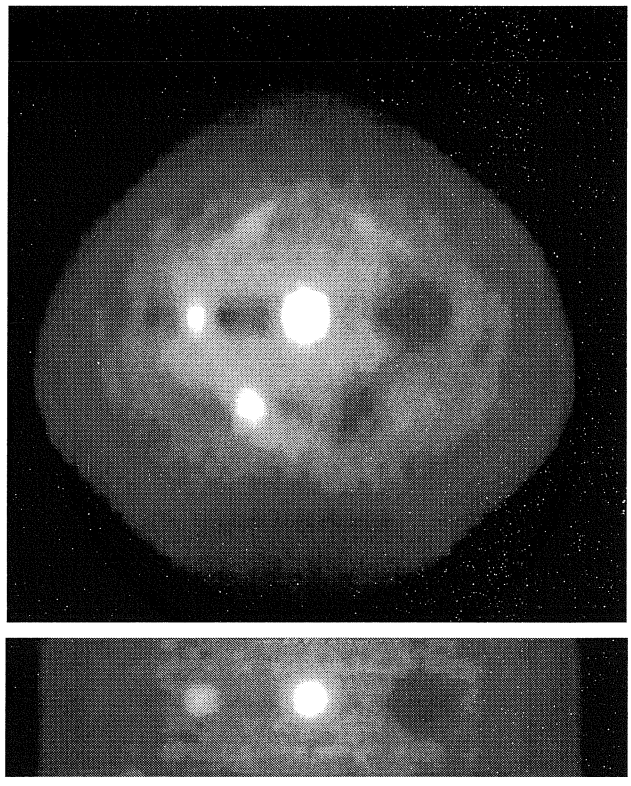

Figure 10

(a)

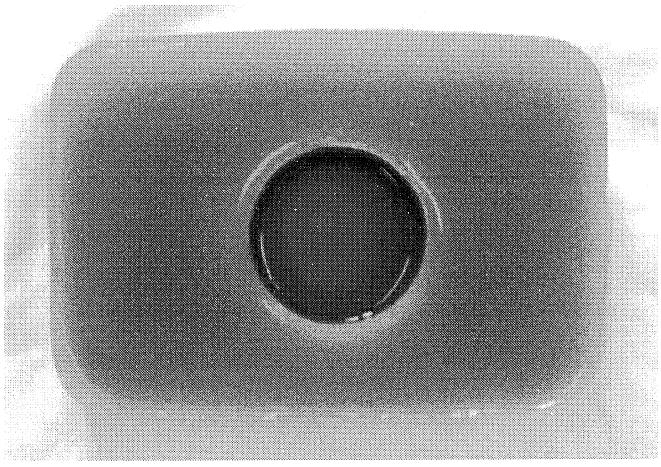

(b)

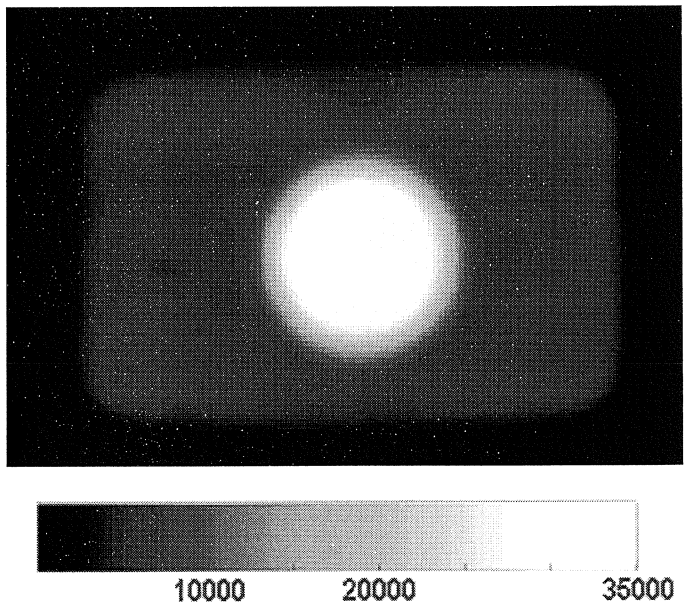

(c)

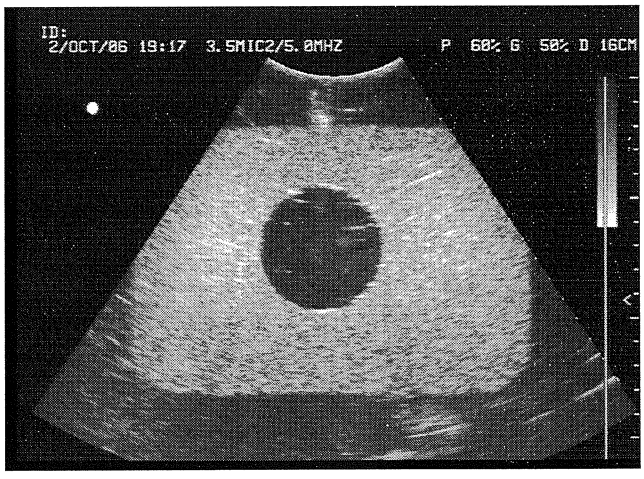

Figure 11

(a)

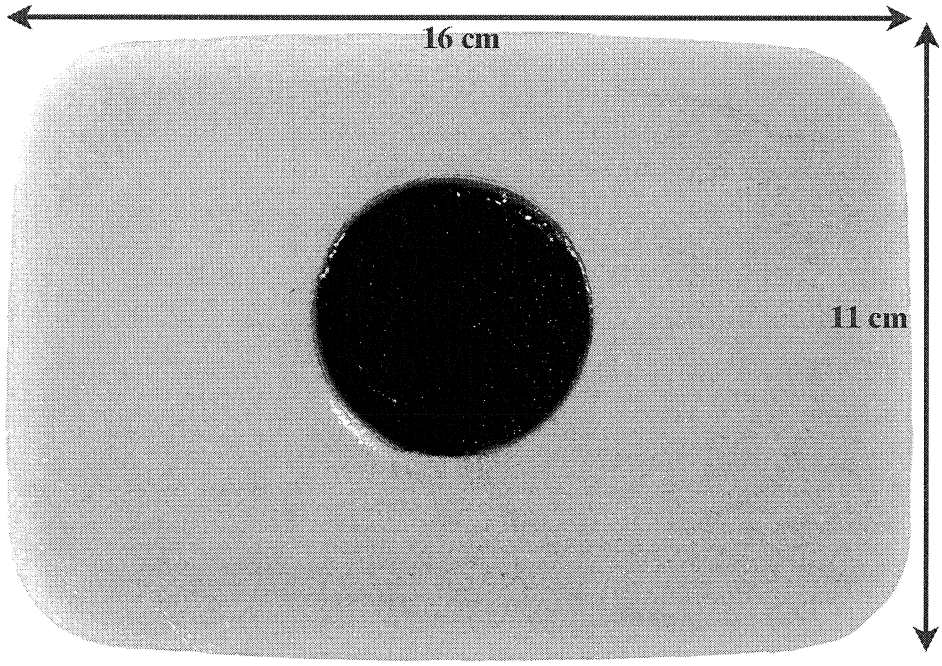

(b)

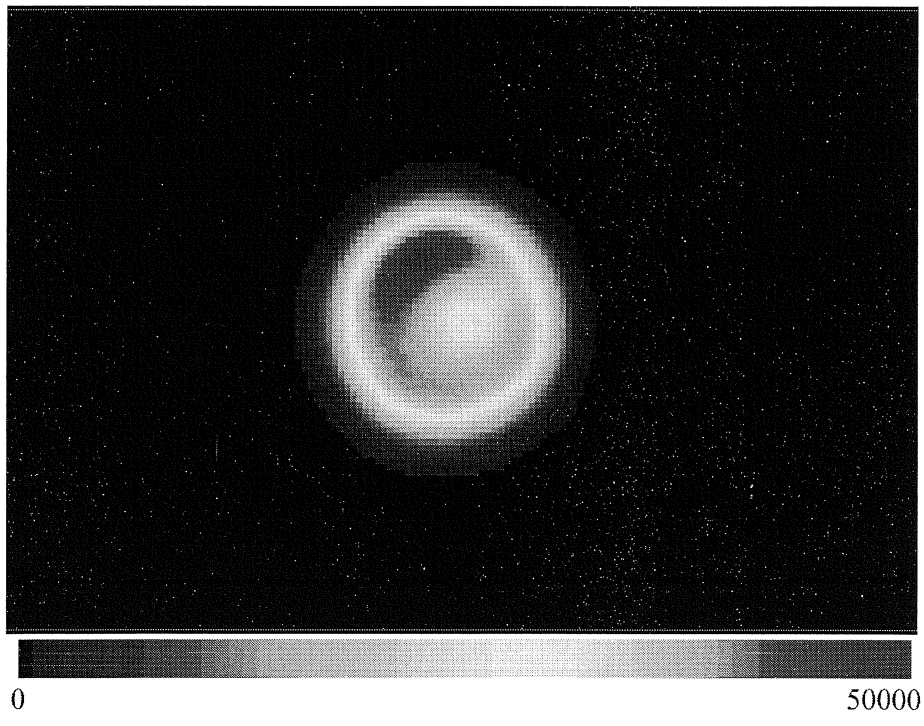

Figure 11 (c)

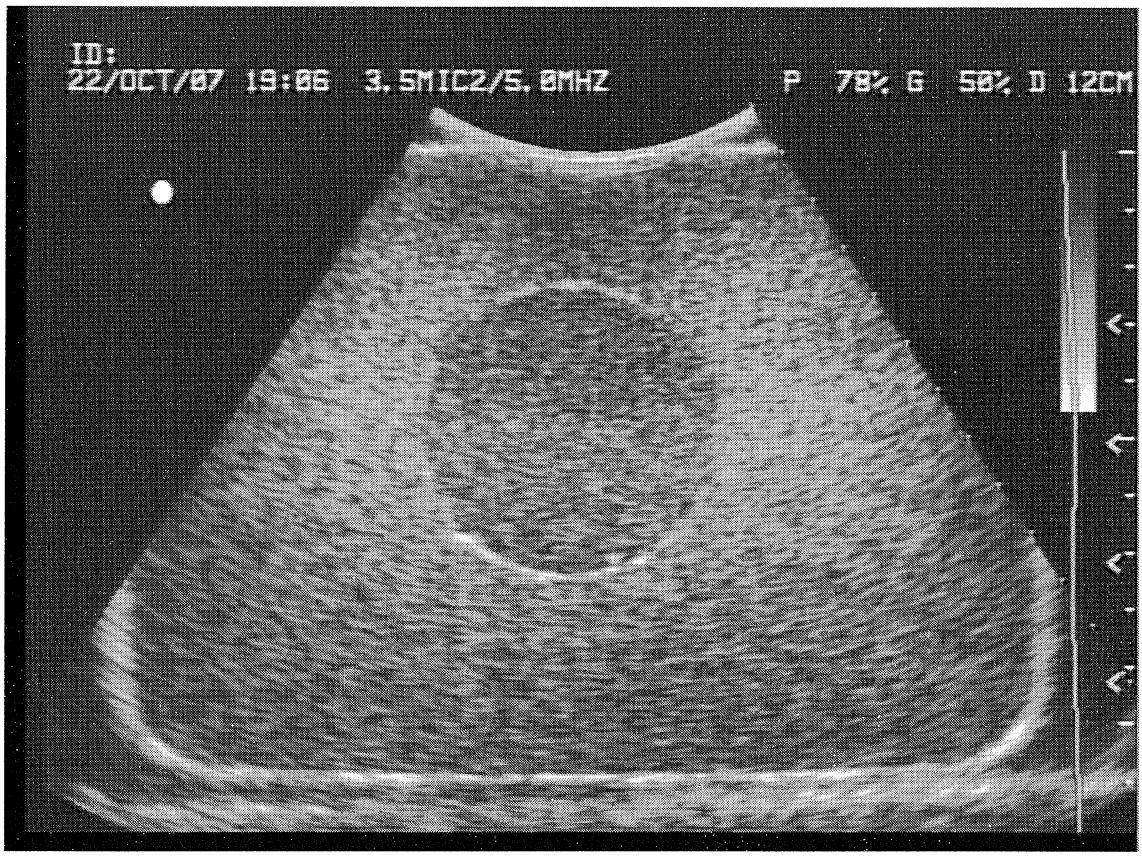

Figure 11 (d)

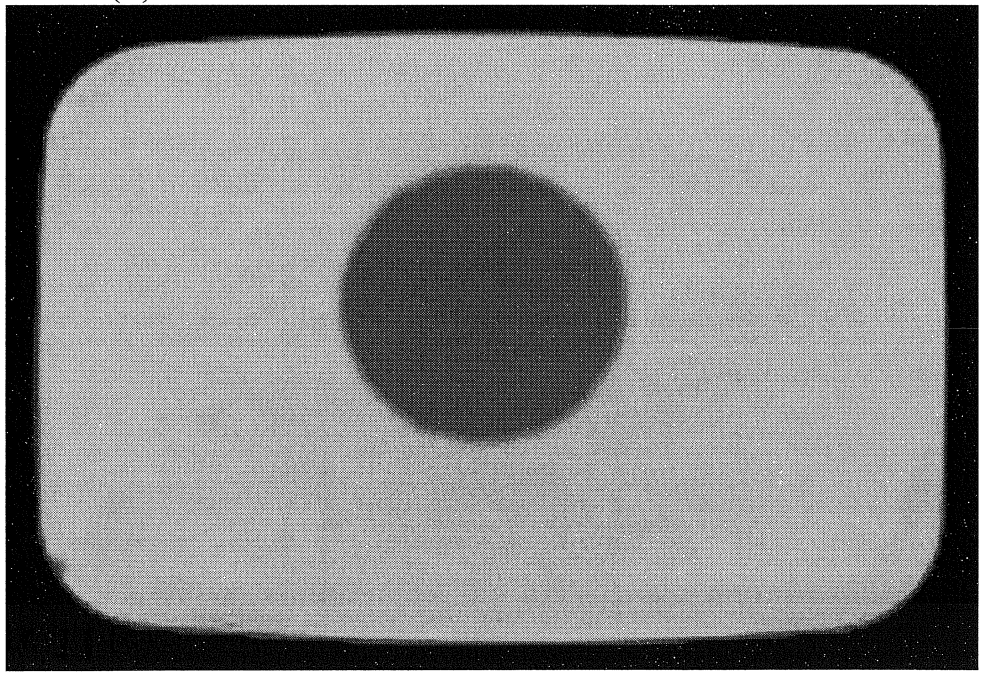

Figure 11 (e)

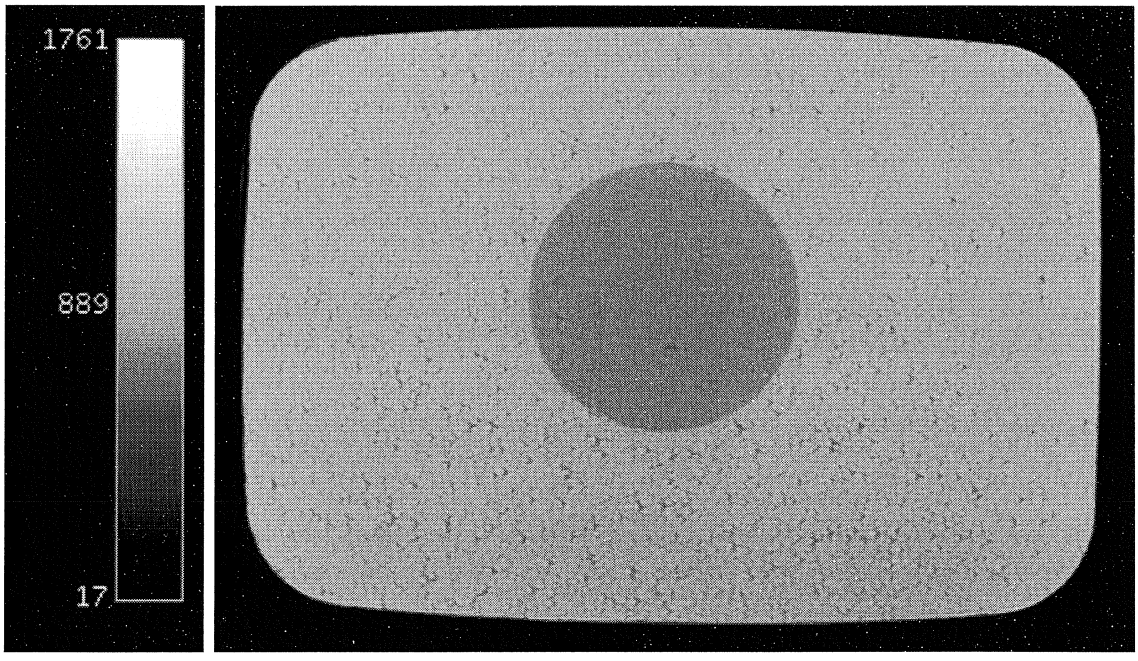

Figure 11 (f)

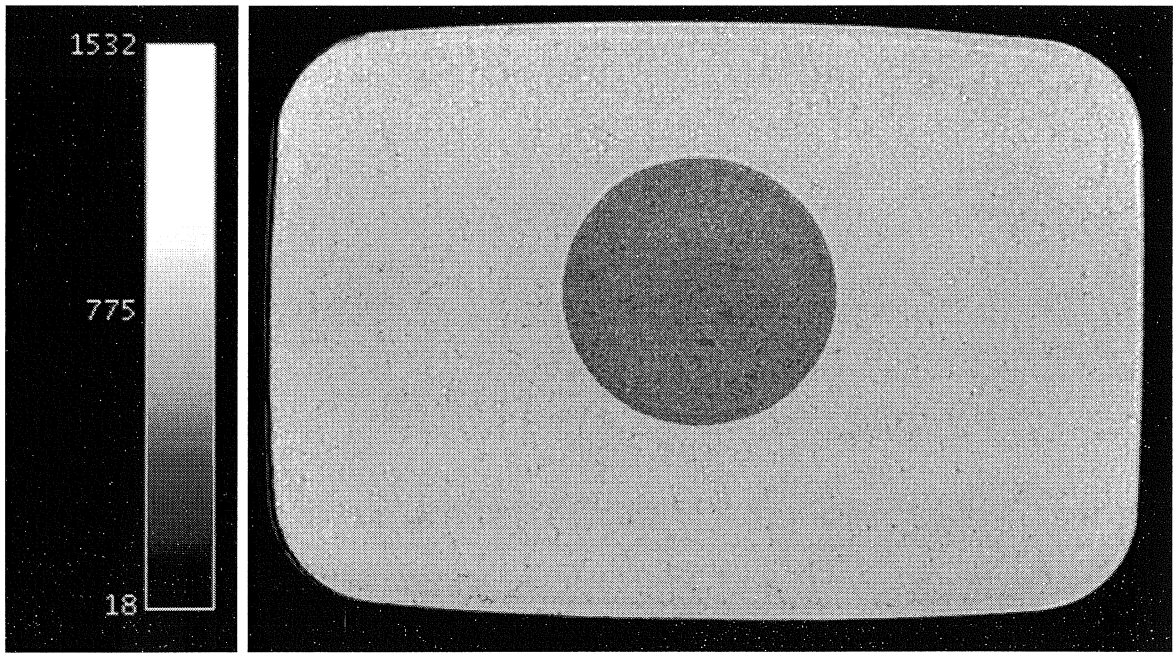

Figure 11 (g)